Reconstruction of the Stradivari Arch: A Trochoidal Curve Approach

Hwang, Il-Seok*

* *Violin Maker, H.I.S. Violin Atelier* / www.hisviolins.com / hisviolins@gmail.com

December 8, 2025

Many luthiers attempt to reconstruct the Stradivari arch, but with its constructive principles remaining unknown, they are often limited to mere imitation. This report presents a systematic method for reconstructing the Stradivari arch by employing trochoid curves. The study begins by analyzing the limitations of the Curtate Trochoid (CTD), a curve often associated with the Stradivari arch, demonstrating its inability to account for the varying degrees of *Fullness* observed in the master's work. To address this, the paper proposes a novel approach utilizing Curtate Hypotrochoid (CHT) and Curtate Epitrochoid (CET) curves, which allow for the precise adjustment of Fullness. Furthermore, for arches that fall outside the geometric limits of these trochoids, a method for generating 'Approximation Curves' is introduced. The proposed methodology is validated by reconstructing the arches of four historical models, with analysis of parameters, Fullness, and error margins confirming a high degree of accuracy and fidelity to the originals. Ultimately, this research provides a practical and scalable framework for generating a Stradivari-style arch of any specified width and height, moving beyond imitation to a principle-based reconstruction for modern instrument making.

The curve known to be most similar to the Stradivari arch is the Curtate Trochoid (CTD)[1]. However, Stradivari arches vary greatly in appearance, and most have a fuller shape than a CTD. This makes it difficult to use the CTD for reconstructing the arch. Therefore, this report aims to address the problems with the CTD curve and describe a method for systematically reconstructing the Stradivari arch. To this end, the content will be presented in the following order.

Before proceeding, it is necessary to define a key term. The degree of an arch's swell is commonly referred to as arch volume. However, since volume strictly denotes a three-dimensional quantity, it is geometrically inappropriate for the two-dimensional analysis central to this report. Therefore, this study introduces and utilizes the term *Fullness* to quantify this planar characteristic. A detailed definition of fullness is provided in Chapter 8.2.3.

First, we must define which Stradivari arch to reconstruct. For this, we will establish a reference model (the model) to be the target of reconstruction. The most rational method would be to use the average of all existing

[1] Some sources refer to it as the Curtate cycloid.

Stradivari arches as the model, but this is practically impossible. Therefore, this report uses data from a well-known book and posters as the model.

Second, this report will examine the problems with the CTD curve. It will start by explaining the definition, types, and characteristics of the Trochoid (TD) curve. Then, by comparing the previously defined model with circular arcs and CTD curves, this analysis will demonstrate how the CTD differs from the Stradivari arch and how diverse the forms of Stradivari arches are.

Third, this section will demonstrate how to reconstruct arches no. 1 through 5 using two types of TD curves: the Hypotrochoid (HTD) and the Epitrochoid (ETD).

Fourth, this section will discuss the limitations of the two aforementioned TD curves and propose a method for addressing unconstructible cases by using approximation curves.

Fifth, as the geometry of arch no. 6 is distinct from the others, its reconstruction requires a different approach. This section will outline this approach, which is based on the principles of generating approximation curves.

Sixth, this section demonstrates the practical application of the proposed methods by reconstructing the arches of four models. A subsequent analysis—covering comparative images, parameters, fullness, and errors—is then conducted to identify the characteristics of the Stradivari arch and to evaluate the reliability of the reconstruction method.

Finally, the report will conclude by considering the implications of this reconstruction method for actual instrument making.

The appendix provides a detailed analysis of contour patterns, offering insights into the arch's probable original appearance and the maker's potential intentions.

For reference, all numerical units in this text are in millimeters(mm) unless otherwise specified.

1 Definition of the Arch

The term arch is commonly used to describe a wide variety of forms, including those found in the Colosseum, bridges, and stringed instruments. Therefore, this report will first define the specific meaning of arch as used herein and the conditions it must satisfy.

1.1 Condition of the Arch

In this report, an arch refers to a curve that satisfies the following conditions.

> **Condition 1.1.** ***Conditions of the Arch***
>
> ***a***. *The slope of the tangent line must be 0 at the apex and both endpoints.*
>
> ***b***. *The curve must be monotonically increasing or decreasing.*
>
> ***c***. *It must be symmetrical with respect to the apex.*

"The slope of the tangent line" refers to the slope of a straight line that touches the curve at a specific point, as shown by the red solid line in Figure 1. In the figure, Curve A has a tangent slope of 0 (horizontal) at its apex and endpoints. For Curve B, however, the slope at the endpoints is not 0. A tangent slope of 0 indicates that the point is either the highest point (apex) or the lowest point (endpoint) of the arch. If the slope at an endpoint is not 0, as in Curve B, that point is not the lowest point of the arch and thus cannot be an endpoint. For this reason, a curve like Curve B is not defined as an arch in this report.

Furthermore, the height of an arch must continuously increase from an endpoint to the apex (monotonic increase). If a section exists where the height remains constant (horizontal) or decreases within this span, it is not considered an arch. For reference, Condition 1.1.c is not applied to the reconstruction target models.

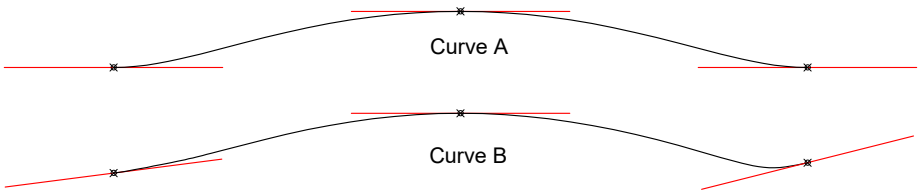

Figure 1: *Tangent slopes at the apex and endpoints of an arch*

1.2 Location of the Arches

The locations of the six arches are defined as shown in Figure 2 and Table 1. The target for reconstruction is the section from the lowest point to the highest point of each arch. Arch no. 6 is divided into an upper and a lower part, centered on its apex. However, arch no. 4 of Model D is located just below the F-hole, not at the lower corner.[2]

[2] This is presumably to prevent the arch from being interrupted by the F-hole during the CT scan.

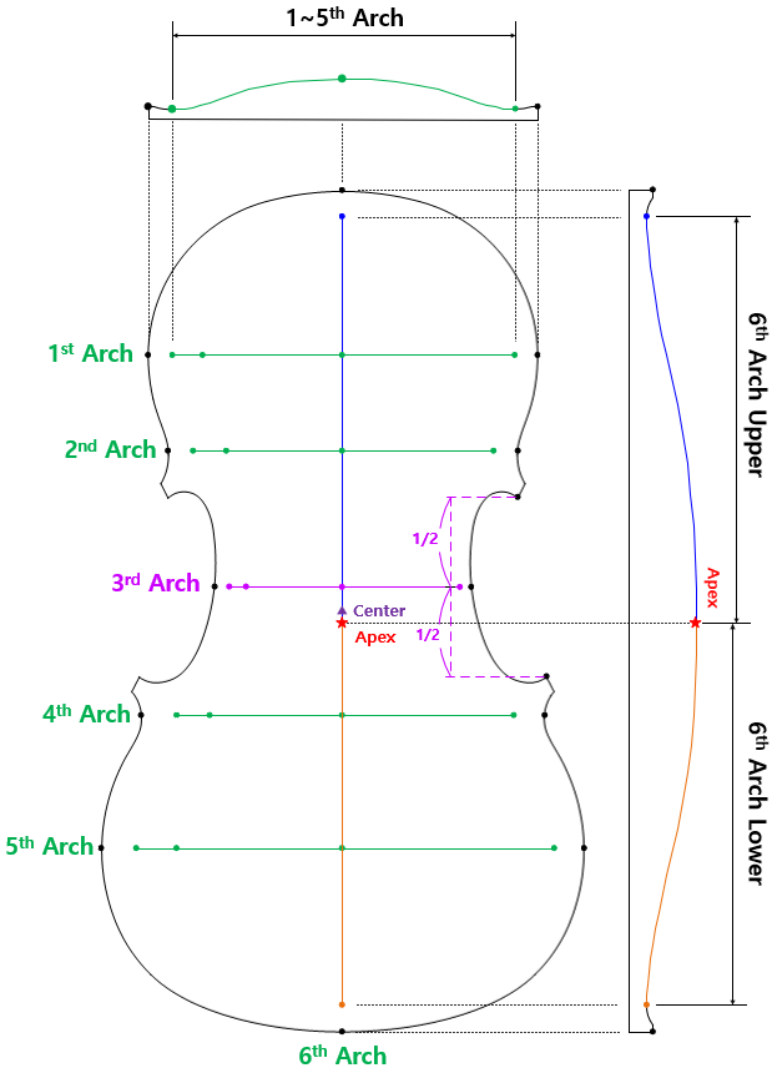

Figure 2: *Definition of the 6 arches*

Arch	Description
1st Arch	An arch running transversely across the widest part of the Upper bout.
2nd Arch	An arch running transversely across the most concave point of the upper corner.
3rd Arch	An arch running transversely across the midpoint between the upper and lower corners.
4th Arch	An arch running transversely across the most concave point of the lower corner.
5th Arch	An arch running transversely across the widest part of the Lower bout.
6th Arch Upper	The upper part of the longitudinal arch running along the center of the plate, relative to the apex.
6th Arch Lower	The lower part of the longitudinal arch running along the center of the plate, relative to the apex.

Table 1: *Definition of the 6 arches*

2 Reconstruction Target Models

This report uses a total of four instruments as models for reconstruction: two violins (Models A, D), one viola (B), and one cello (C). Since precise specifications are required to reconstruct the arches, this report performs modeling to extract the dimensions of each instrument. The drawings and numerical data from the source materials are utilized as much as possible, with any missing information extracted directly from the drawings. An important point is that the left and right arches often differ in shape due to the warping of the plates over time.

2.1 Models A, B, and C

Models A, B, and C are the violin, viola, and cello introduced in Simone F. Sacconi's book[1]. This source provides detailed data, including contour lines, in both graphical and numerical forms, making it an excellent reference for reconstruction.

However, the book does not specify which actual instruments correspond to these three models. Based on the book's content and analysis by other researchers, it is presumed that Model A is based on the Messiah (1716) or Betts (1704), Model B on the Tuscan-Medici (1690), and Model C on the Gore-Booth (1710) or Piatti (1720). It is also believed that these models incorporate the average characteristics of other instruments from the period.

The modeling method and procedure are as follows:

1. Scan the full contour line images from the source material[1] and scale them based on the longitudinal length of the plate.
2. From the scaled image, determine the width of the plate at the location of each arch.
3. Rescale the detailed arch images to match the measured widths.
4. On the detailed arch images, draw vertical lines corresponding to the position and height of the contour lines.
5. Connect the endpoints of the vertical lines with a spline curve. The spline is set so that the tangent slope is 0 at the apex and both endpoints of the arch.

Figures 3 through 8 show the arches of the three models created using the method above. The red lines represent the target arches for reconstruction, and the numbers above the arches indicate the height at each point.

The biggest challenge in modeling these three instruments is the inconsistency between the numerical data and the drawings in the source material. Strictly following the numerical data results in a curve with a bumpy surface. On the other hand, tracing the curves from the drawings yields a smooth arch, but the heights differ completely from the data values. The latter method presents an even greater problem: when the arches are combined to create overall contour lines, the result is entirely different from the contour lines in the original source. Therefore, this report adopted the former method, prioritizing the numerical data.

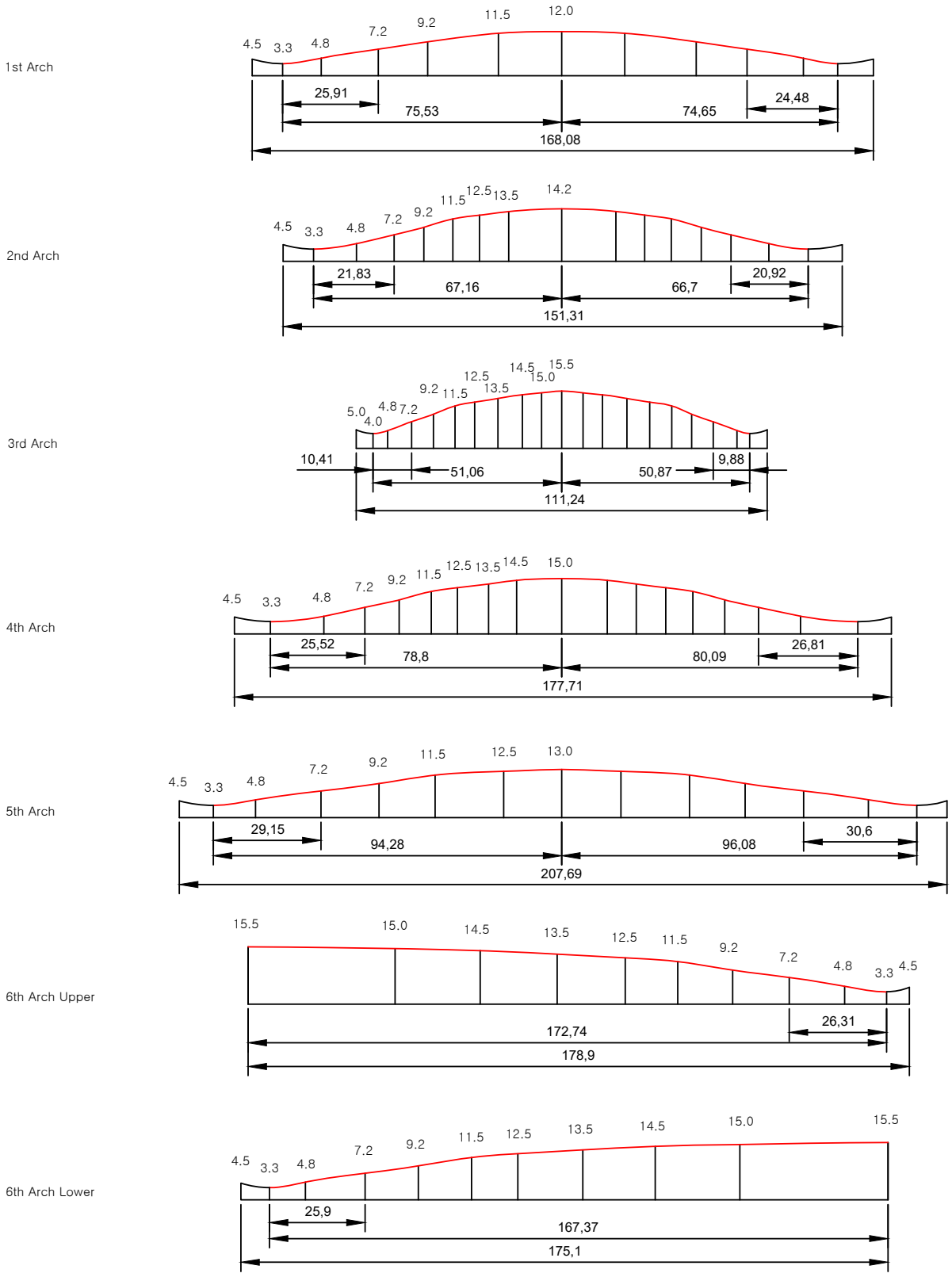

Figure 3: *Model A, Violin Front*

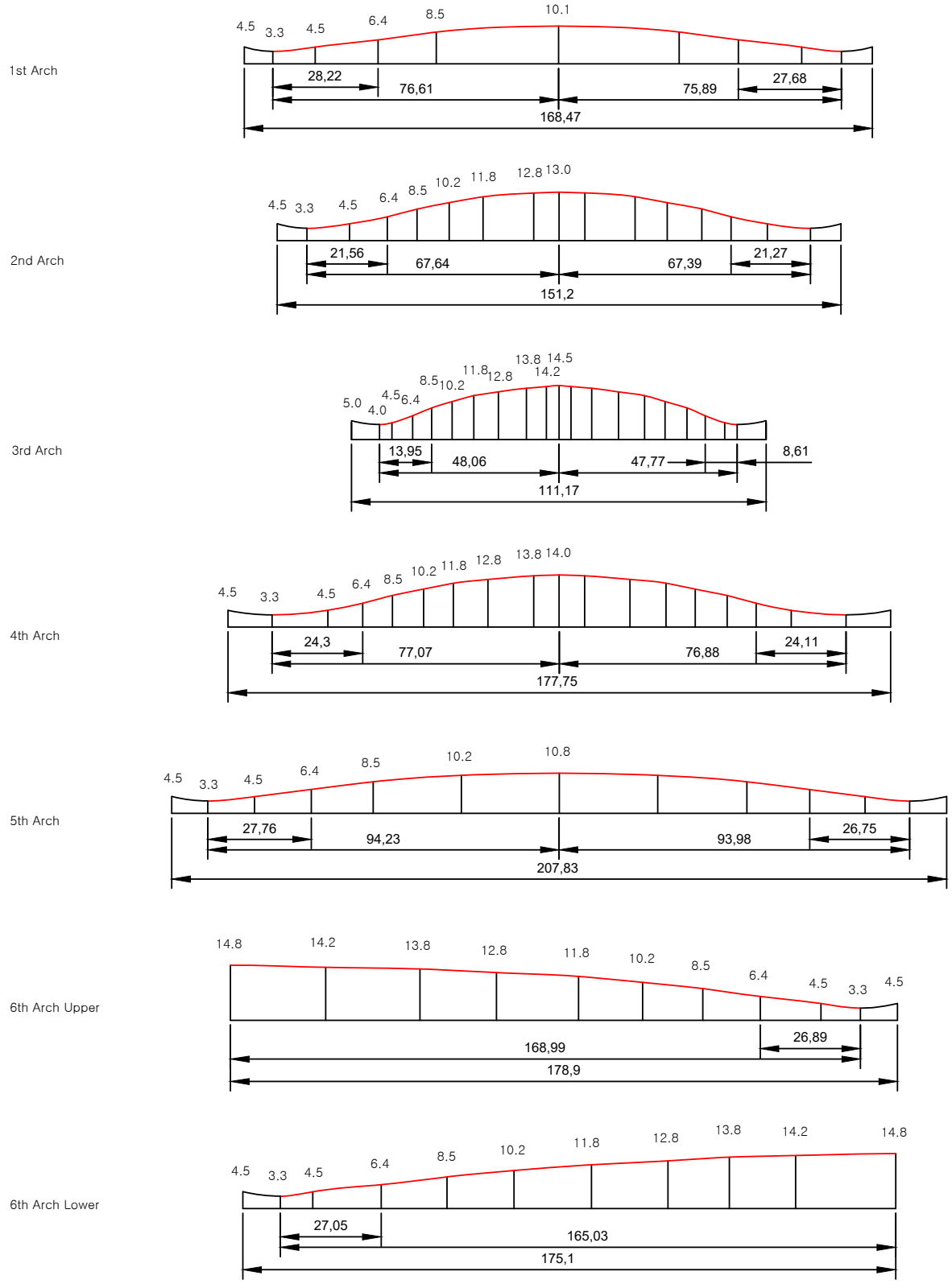

Figure 4: *Model A, Violin Back*

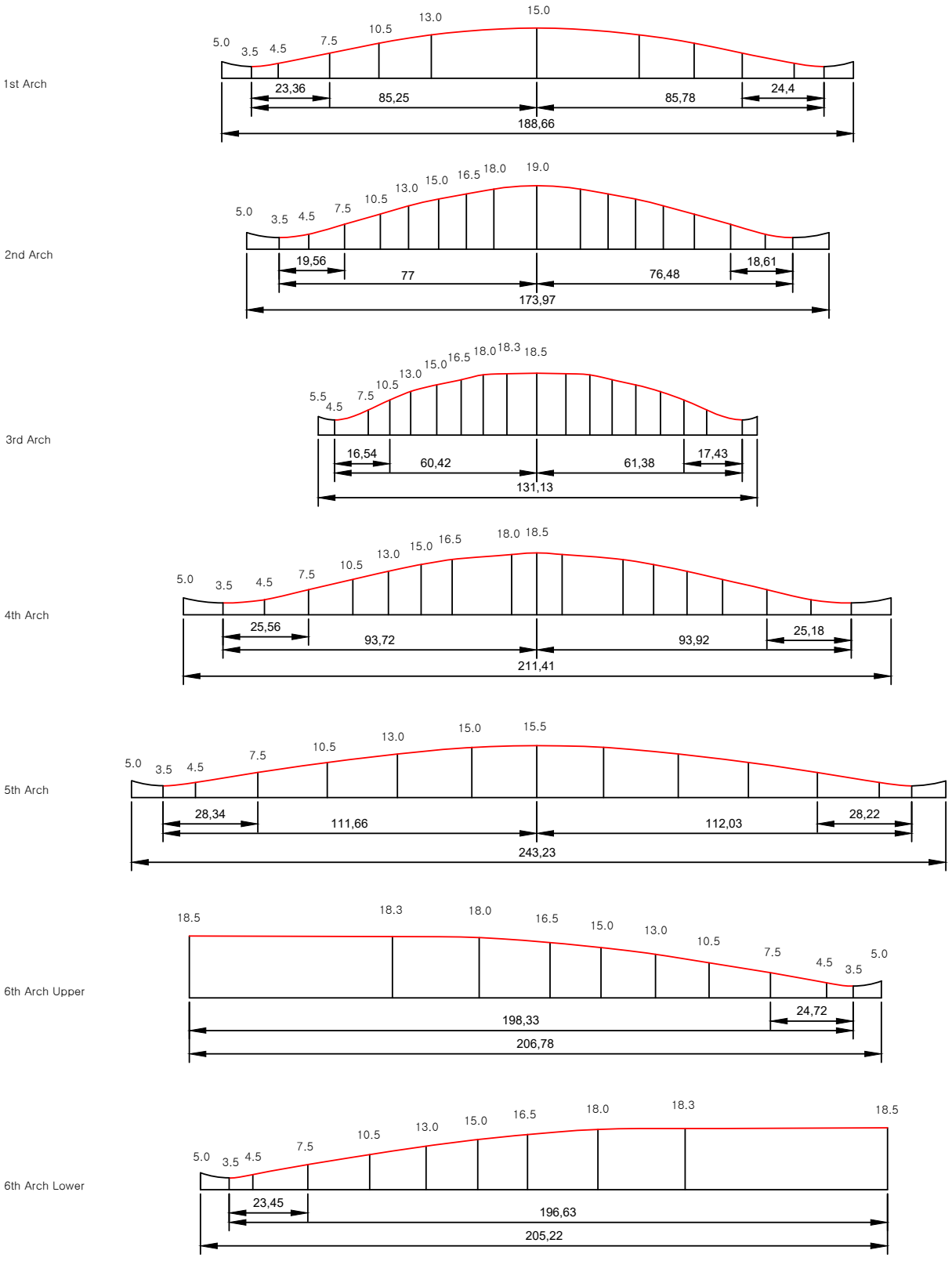

Figure 5: *Model B, Viola Front*

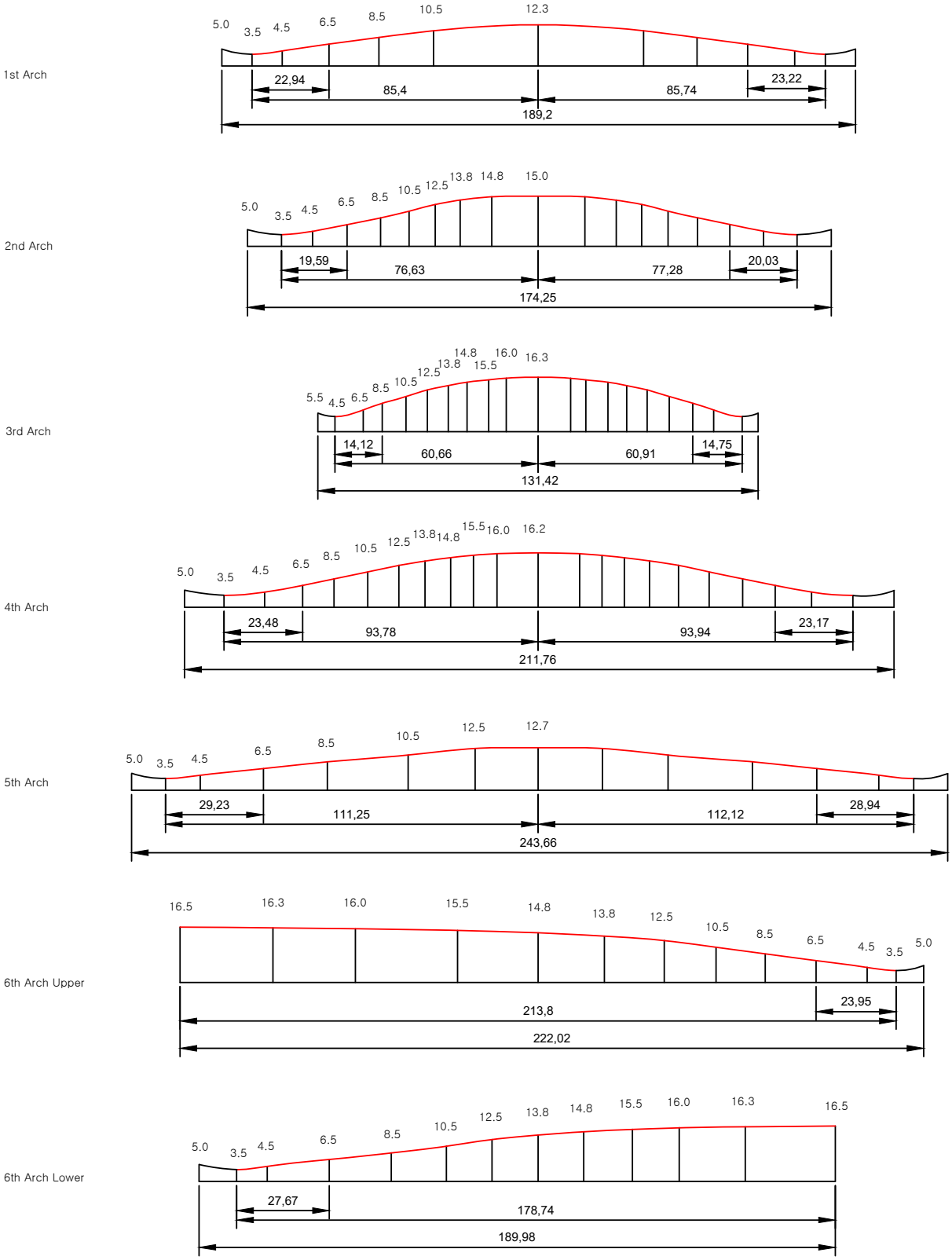

Figure 6: *Model B, Viola Back*

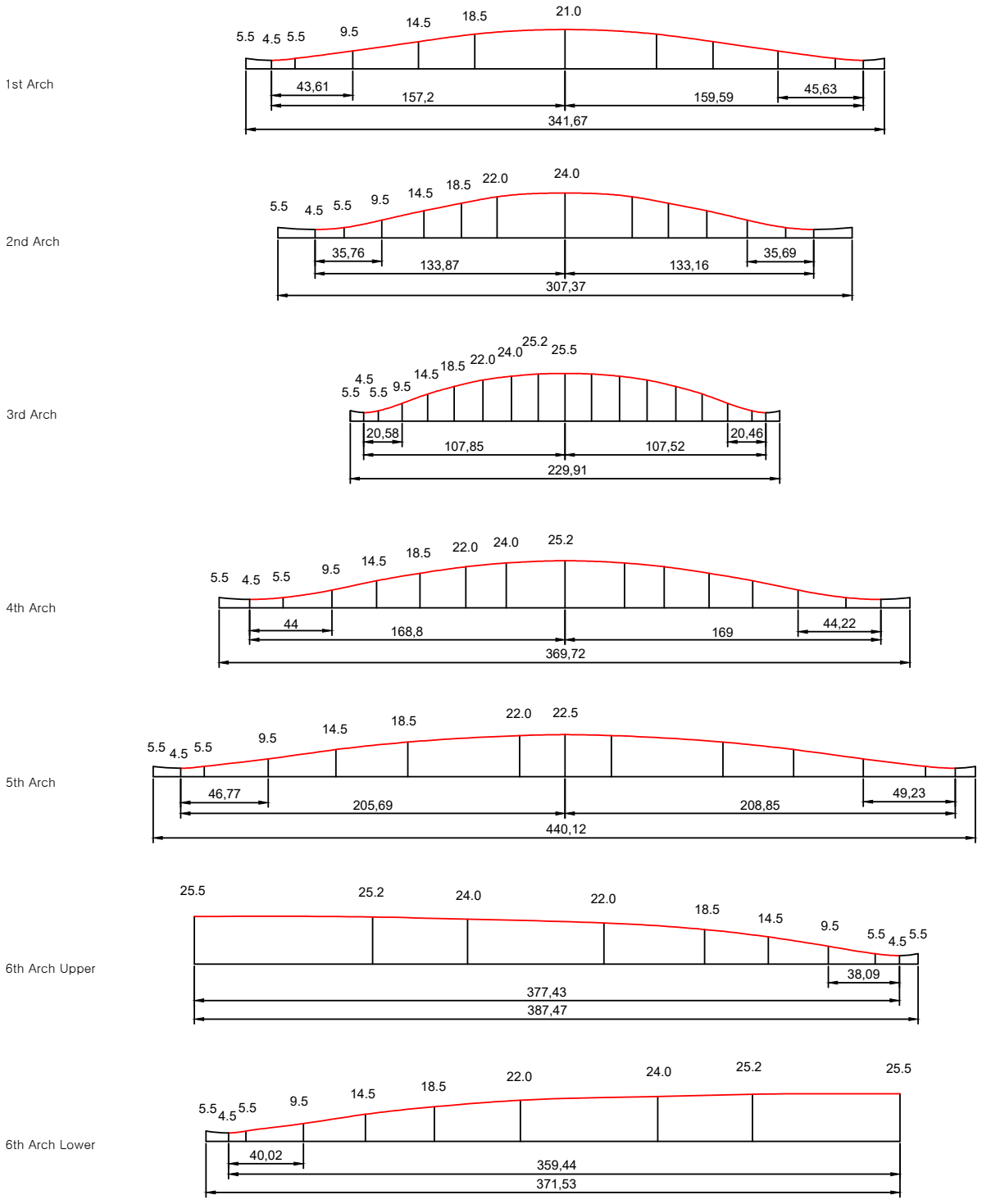

Figure 7: *Model C, Cello Front*

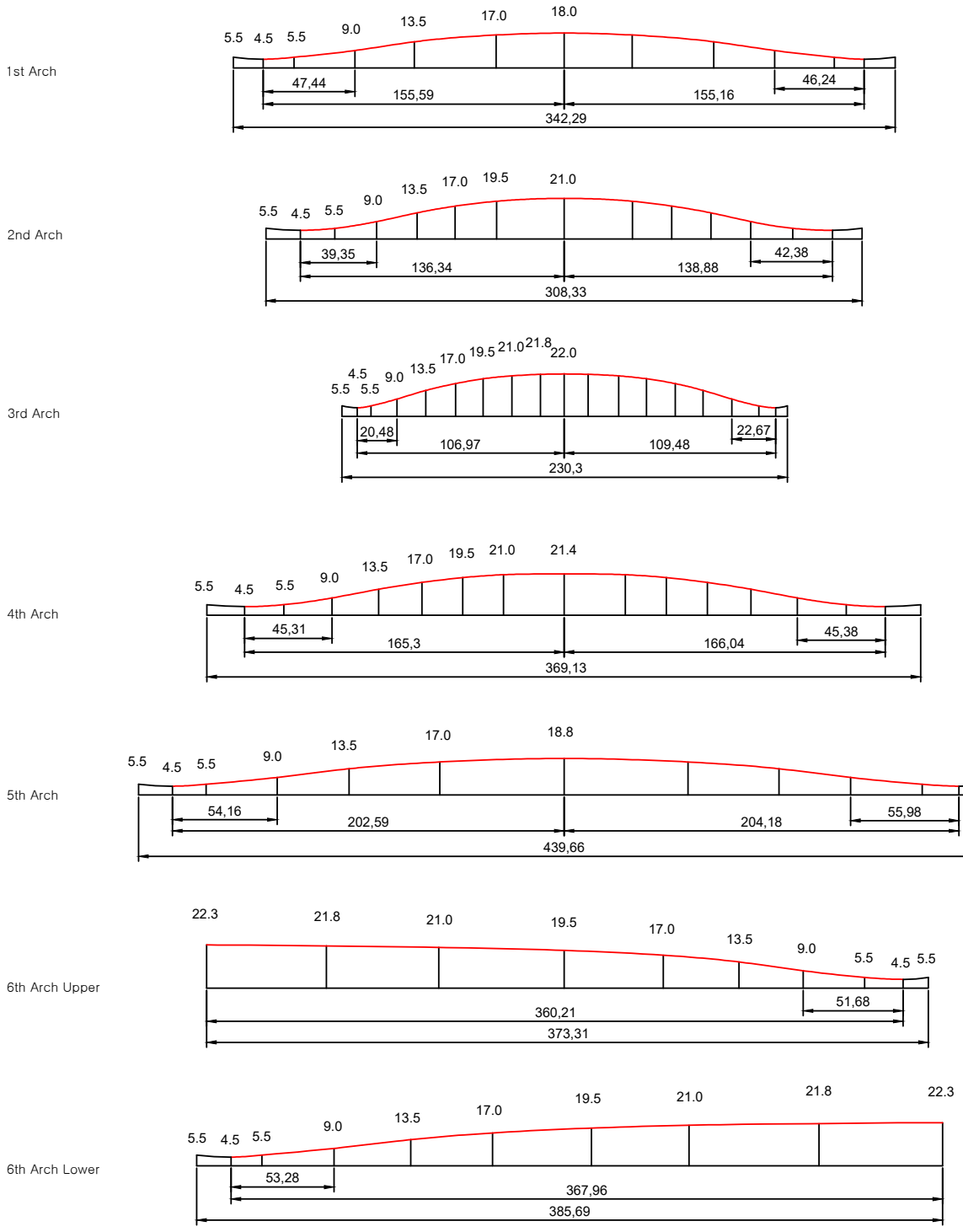

Figure 8: *Model C, Cello Back*

2.2 Model D

Model D is the violin Titian (Antonio Stradivari, 1715). For the reconstruction, this report uses poster data[2] (numerical values and arch images) from The Strad. Unlike Models A, B, and C, this data was obtained using modern CT scanning technology, so a more accurate arch shape can be expected. However, as there is no contour line data, the contours must be extracted directly from the images. The modeling method using the poster is as follows:

1. Scan the arch images from the poster.
2. Adjust the scale of the scanned images so that the arch widths match the numerical data.
3. Extract the arch curves from the scaled images using the spline function of a CAD program.
4. Divide the contour intervals evenly based on the width of the 3rd arch, and then extract the height at each point.
5. Based on the contour height values from step 4, locate and mark the contour positions for the remaining arches.

To extract the arch curves from the images, this report used a CAD program, zooming in until the lines were sufficiently thick and then creating a spline that passed through the center of the lines. To extract the contours from the 3rd arch, the width of the 3rd arch was divided into 17 equal parts, setting the odd-numbered points from the arch endpoints as the contour locations. That is, the 1st, 3rd, 5th, ..., 15th division points are set as contour locations, allowing for the creation of eight contour lines.

Figures 9 and 10 show the completed Model D. This model has several issues. First, while the arch is smooth, it is highly asymmetrical. The soundpost side, in particular, protrudes significantly. Second, the central part of the 6th arch on the Front is lower than its surroundings, making it difficult to pinpoint the apex. The location of the apex is essential for reconstructing the arch. Therefore, a minimal correction of about 0.01mm was made to raise the area near the bridge. For this reason, the apex position of the 6th arch on the Front may not be precise. Third, the apex of the 6th arch is lower than the apex of the 3rd arch, which seems to be an error from the poster production process. Finally, the upper and lower edge widths of the 6th arch on the Back are very narrow. Except for the correction to the apex of the 6th arch on the Front, the remaining issues were left as they are, using the shape from the source material without alteration.

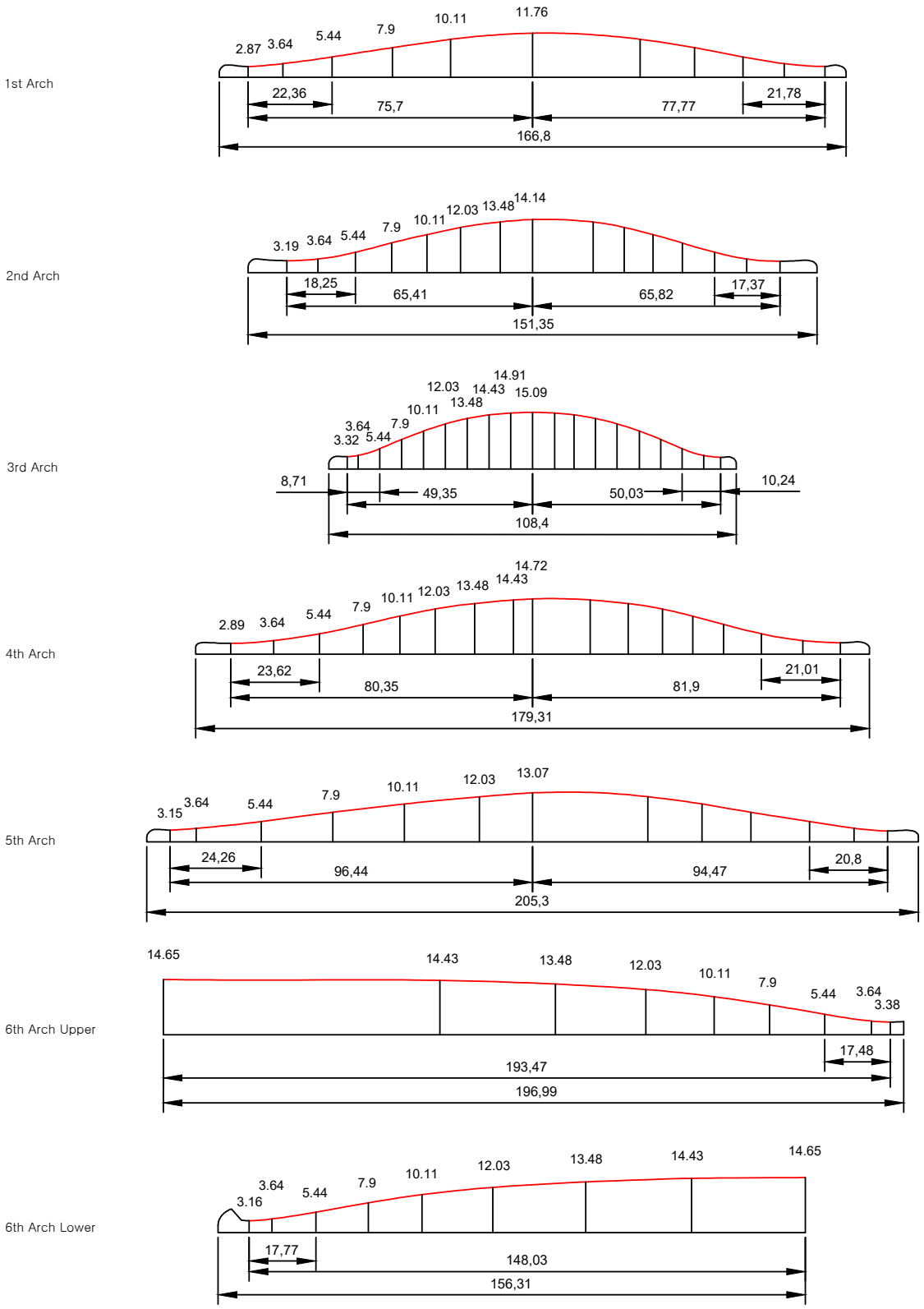

Figure 9: *Model D, Titian Front*

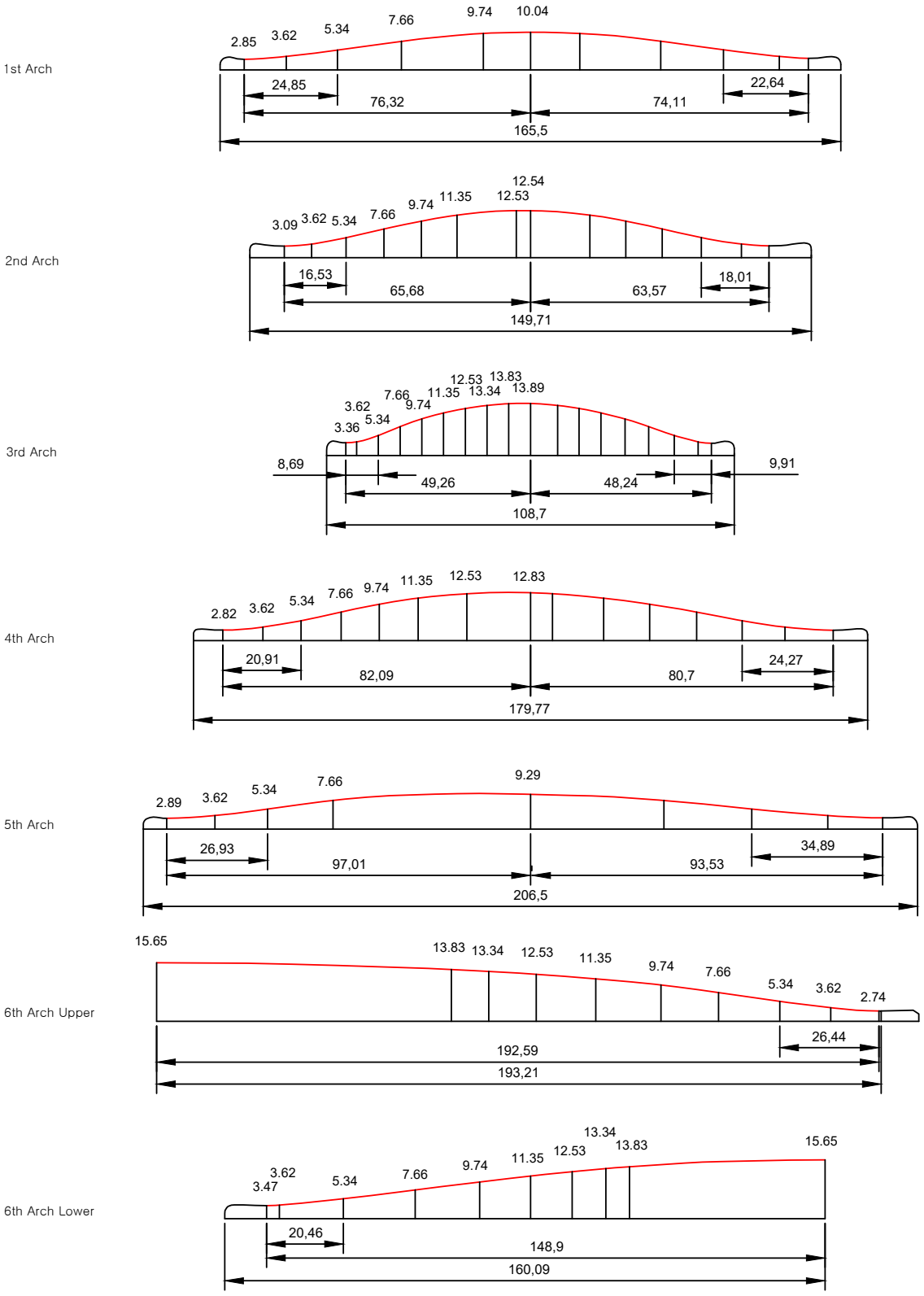

Figure 10: *Model D, Titian Back*

3 Trochoid

The Curtate Trochoid (CTD), known to be the curve most similar to the Stradivari arch, is a type of trochoid (TD). Trochoids are divided into various curves depending on their generation principle. This chapter will examine the definitions and characteristics of each type of TD and explain the problems with the CTD and their solutions.

3.1 Definition and Types of Trochoid

Definition 3.1. ***Trochoid*** **(*TD*)**
The trajectory traced by a point P, at a distance d from the center of circle A with radius r, as circle A rolls without slipping along a straight line, or along the inside (internally tangent) or outside (externally tangent) of another circle B with radius R.

According to Definition 3.1, TDs are classified into nine types of curves, as shown in the table below.

Type	Name	Base	d, r	r, R	Shape
Basic Trochoid	Curtate Trochoid	Line	$d < r$	·	Wavy
	Cycloid	Line	$d = r$	·	Pointed
	Prolate Trochoid	Line	$d > r$	·	Looped
Hypotrochoid	Curtate Hypotrochoid	Circle (inscribed)	$d < r$	$r < R$	Wavy
	Hypocycloid	Circle (inscribed)	$d = r$	$r < R$	Pointed Looped
	Prolate Hypotrochoid	Circle (inscribed)	$d > r$	$r < R$	Looped
Epitrochoid	Curtate Epitrochoid	Circle (circumscribed)	$d < r$	$r < R$	Wavy
	Epicycloid	Circle (circumscribed)	$d = r$	$r < R$	Pointed Looped
	Prolate Epitrochoid	Circle (circumscribed)	$d > r$	$r < R$	Looped

Table 2: *Types of Trochoid curves. r:radius of circle A, R:radius of circle B, d:distance from the center of circle A to the tracing point P. Wavy:violin arch shape, Looped:shape of α rotated 90 degrees.*

Trochoids are broadly divided into three types. The first, Basic Trochoid, is formed when a circle rolls along a straight line. The second, Hypotrochoid, occurs when a small circle rolls along the inside of a larger circle. The third, Epitrochoid, is when a small circle rolls along the outside of a larger circle. Additionally, the name Curtate is used when $d < r$, Cycloid when $d = r$, and Prolate when $d > r$. The prefix Hypo signifies internal rolling, and Epi signifies external rolling.

A peculiar aspect of TD terminology is that when $d = r$, the term Cycloid is used instead of Trochoid. Also, since $r > R$ is not valid by definition, such curves are not called trochoids. Therefore, the term *Curtate Cycloid*,

which is conventionally used in some literature, is mathematically not recommended; *Curtate Trochoid* is the more appropriate expression.

In the next section, this report will examine the Curtate Trochoid in more detail.

3.2 Curtate Trochoid

Here, this report will investigate what a CTD curve is and identify its problems by comparing it with the models.

3.2.1 Definition of Curtate Trochoid

A CTD is defined as follows.

> **Definition 3.2.** ***Curtate Trochoid*** (*CTD*)
> *The trajectory traced by a point P, located at a distance d from the center of circle A with radius r, as circle A rolls without slipping along a straight line.* (*where* $d < r$)

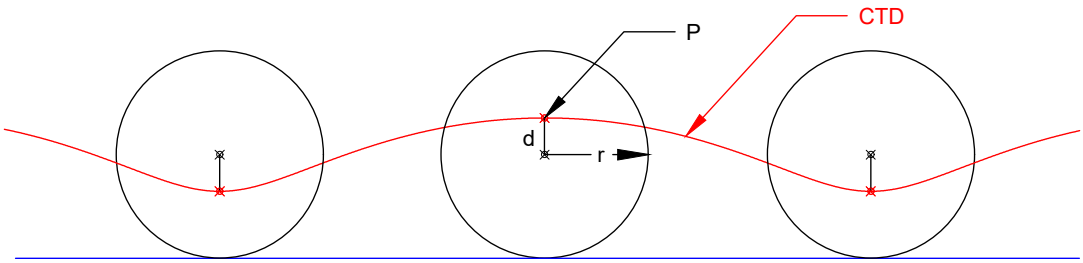

Figure 11: *Curtate Trochoid*

The CTD has a structure where the same curve pattern repeats. In this curve, the highest point reached by point P becomes the apex of the arch. The endpoints of the arch are formed when the circle rolls half a turn to the left and right from the apex, bringing point P to its lowest position.

A CTD can be expressed mathematically as follows:

$$\begin{cases} x = r\theta - d\sin(\theta) \\ y = r - d\cos(\theta) \end{cases} \tag{1}$$

r : radius of the rolling circle (wheel)

d : distance from the center of the circle to point P (where $d < r$)

θ : angle of rotation of the circle

In Figure 11, the CTD curve repeats the same pattern. This report will call a single segment of this curve, corresponding to one arch, a *Curtate Trochoid Arch* (*CTDA*).

The width W of a CTDA is equal to the circumference of the circle, and its height H is equal to twice the distance d. Therefore,

$$\begin{cases} W = 2\pi r \\ H = 2d \end{cases} \tag{2}$$

To widen the arch, one can increase the radius r, and to heighten it, one can increase d. An important fact to note here is that a CTDA has only one possible shape for a given width and height, as no other parameters can be altered. In other words,

The Fullness of a CTDA cannot be adjusted.

This is the decisive reason why it is difficult to use a CTDA for reconstructing the Stradivari arch.

3.2.2 CTDA vs. Stradivari Arch

This section will compare the CTDA with the arches of the models to identify any issues. Figures 12 through 19 compare the Front and back arches of Models A, B, C, and D with a CTDA and a circular arc. The comparison is made with the left arch of each model. For the Front, this is the bass bar side, and for the Back, it is the sound post side; for the cello, the opposite is true. In the figures, the red line represents the model arch, the blue line represents the CTDA, and the black line represents the circular arc.

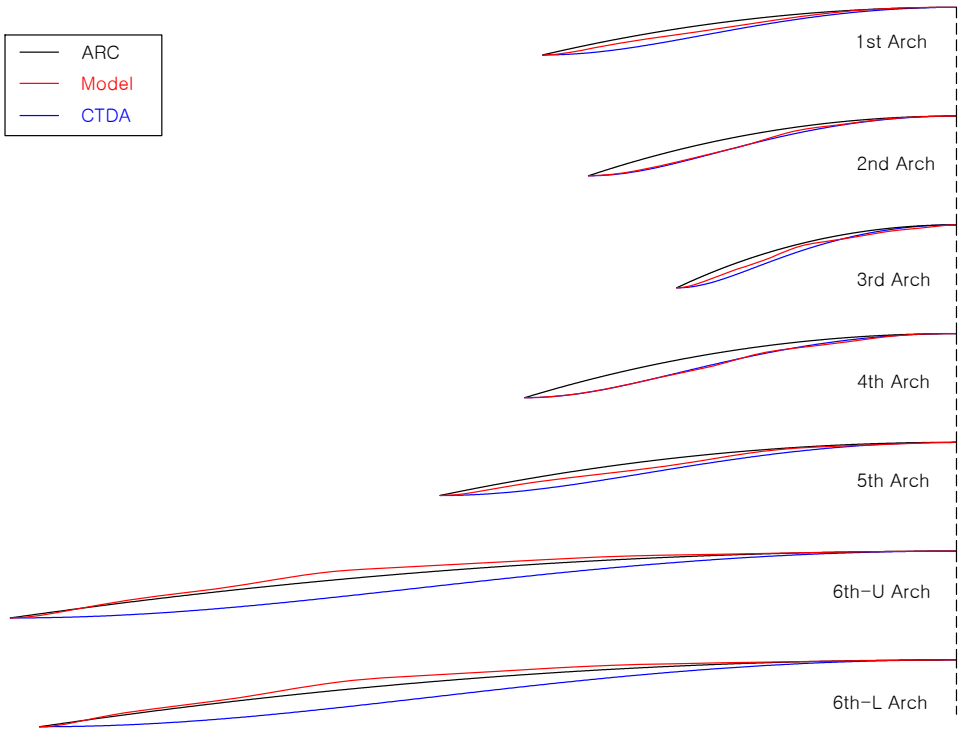

Figure 12: *Model A, Violin Front* (*Bass bar side*)

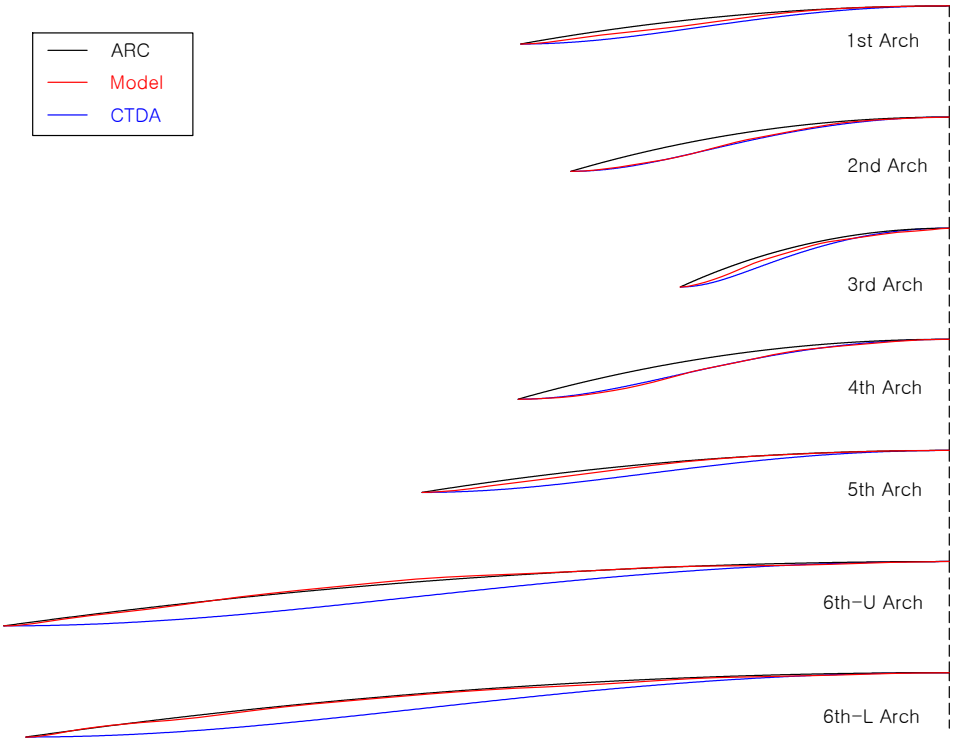

Figure 13: *Model A, Violin Back* (*Sound post side*)

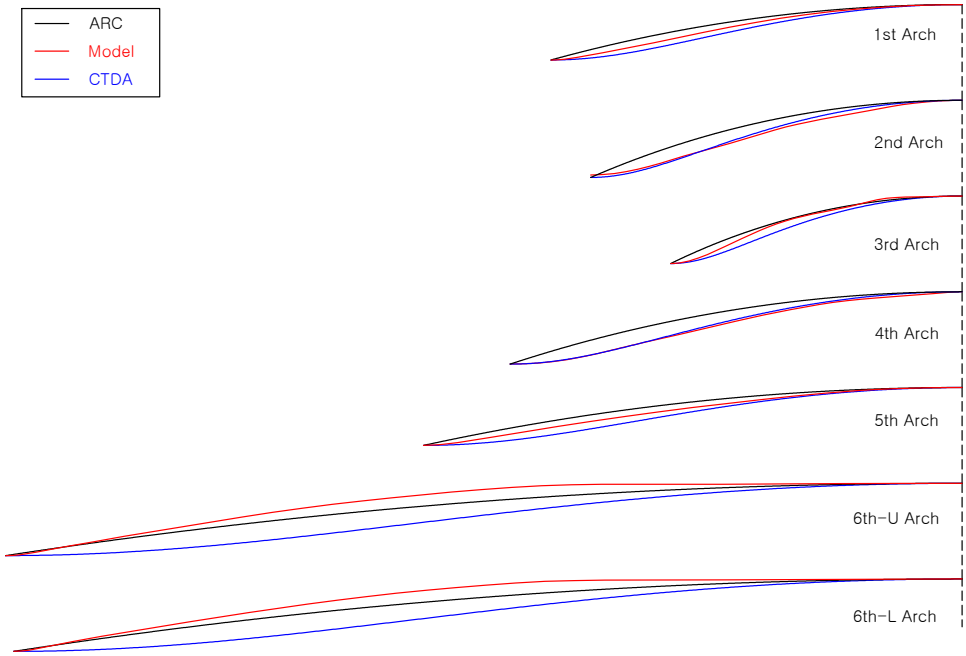

Figure 14: *Model B, Viola Front* (*Bass bar side*)

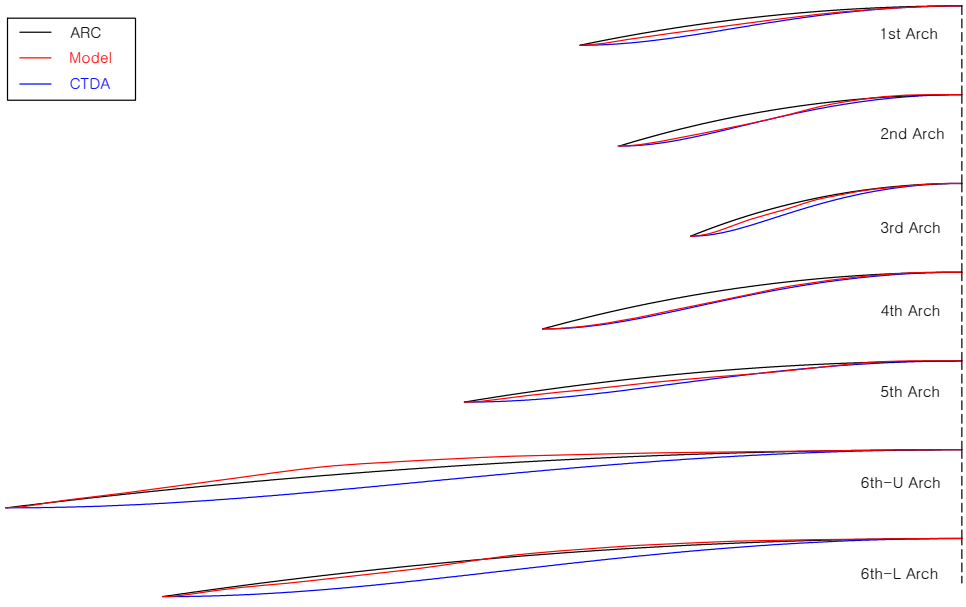

Figure 15: *Model B, Viola Back* (*Sound post side*)

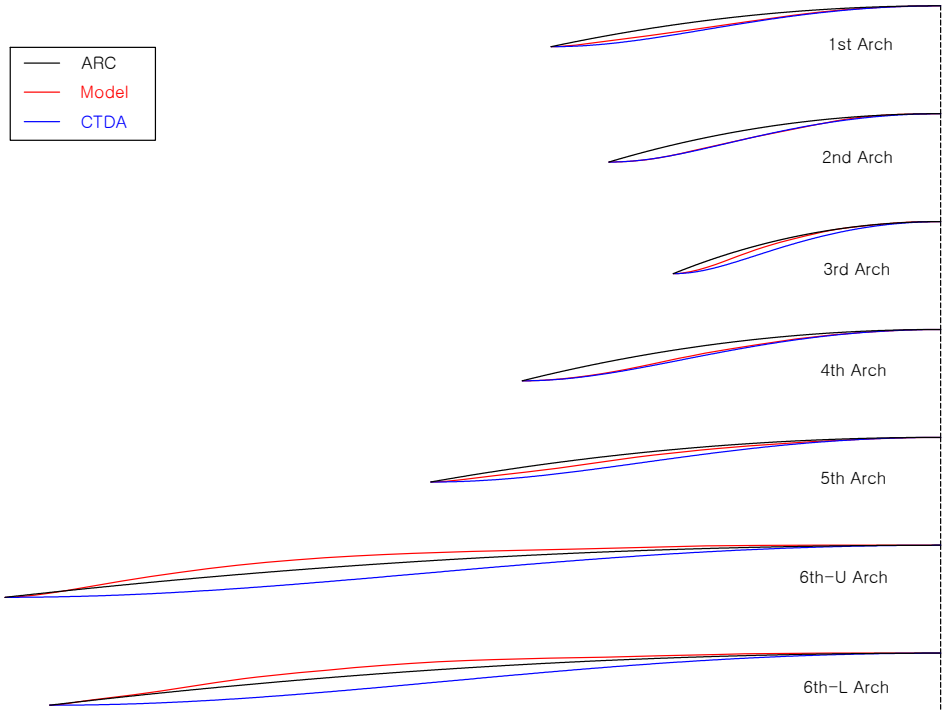

Figure 16: *Model C, Cello Front* (*Sound post side*)

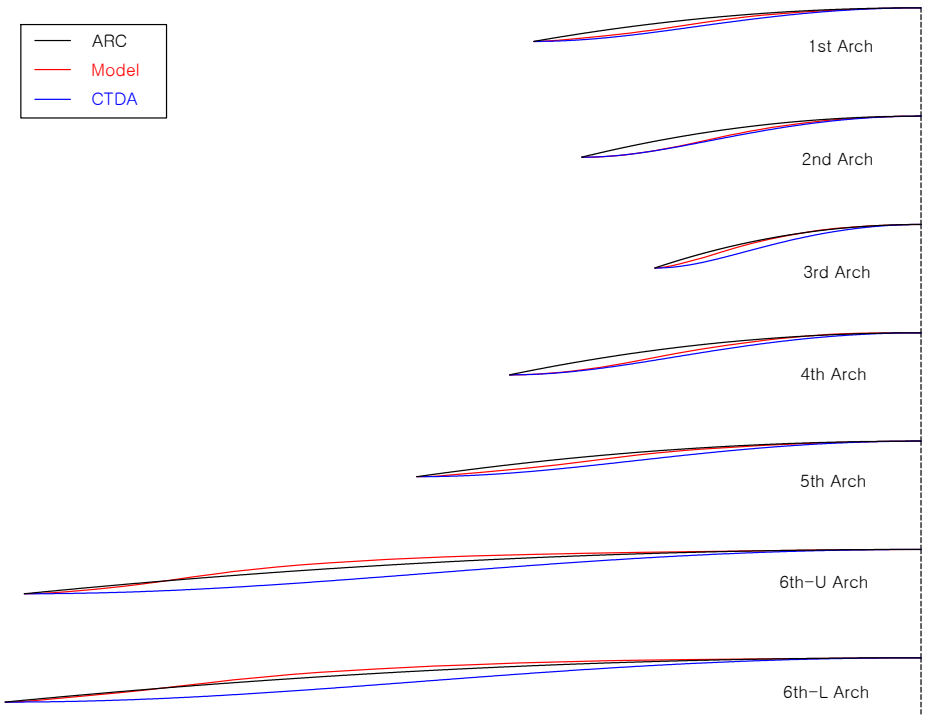

Figure 17: *Model C, Cello Back* (*Bass bar side*)

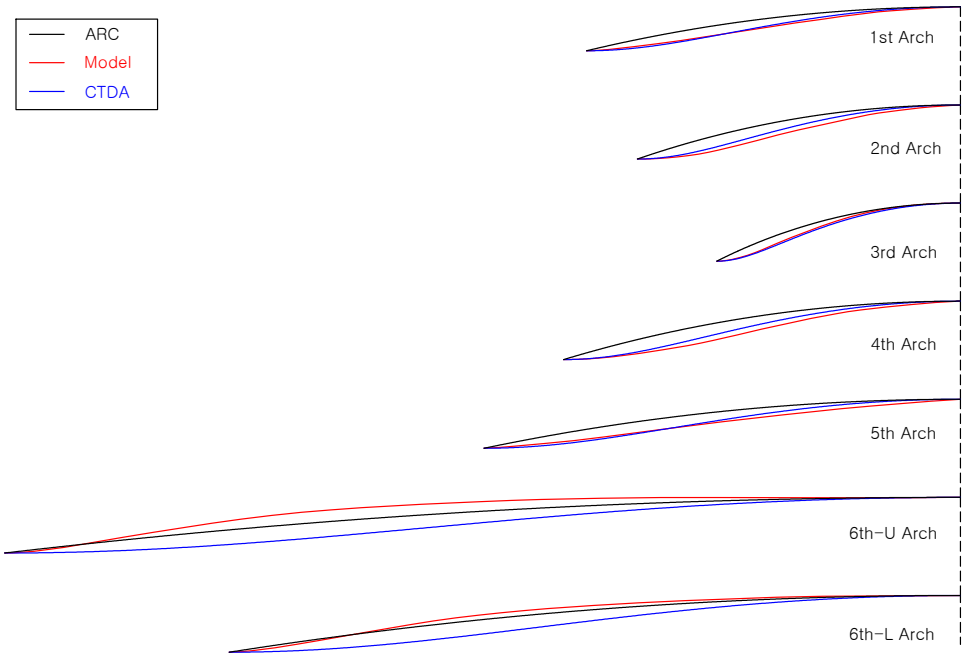

Figure 18: *Model D, Titian Front* (*Bass bar side*)

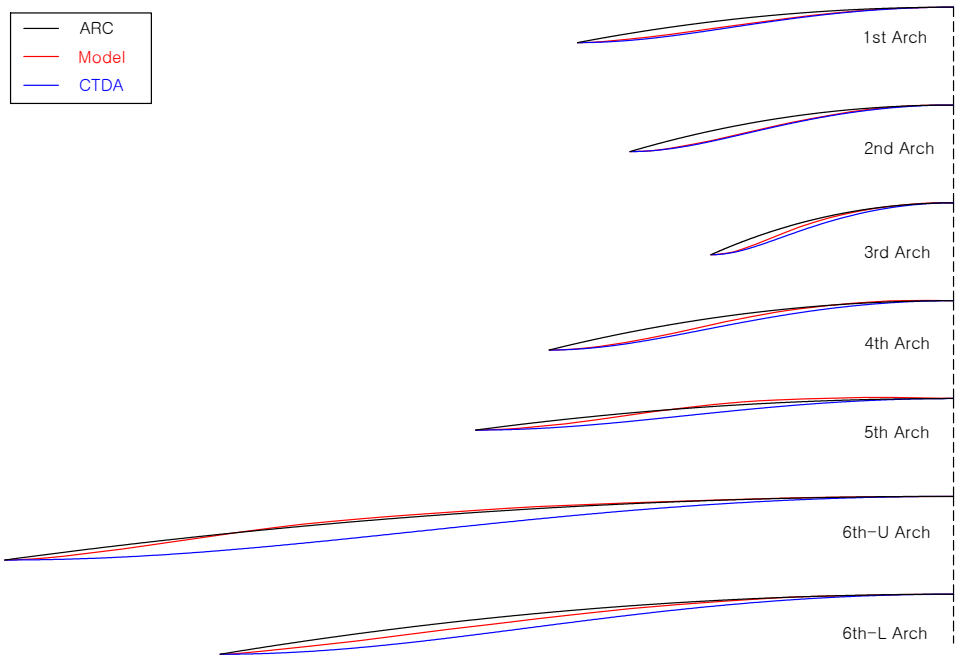

Figure 19: *Model D, Titian Back* (*Sound post side*)

An analysis of the model arches from the figures above reveals the following characteristics:

- Arches 1, 3, 5: Their shape is intermediate between a circular arc and a CTDA. They have greater fullness than a CTDA but less than a circular arc.
- Arches 2, 4: They are very similar to a CTDA, with comparable fullness.
- Arch 6: The front has greater fullness than a circular arc, while the Back is similar to or slightly fuller than a circular arc.

It can also be observed that arches 2 and 4 of Model D's (Titian) front have less fullness than a CTDA.

In summary, the CTDA generally lacks fullness compared to the Stradivari arch, although for some arches it is similar or even slightly excessive. This means that the CTDA alone cannot perfectly replicate the Stradivari arch. Therefore, to reconstruct the Stradivari arch, we reach the conclusion that:

one must be able to adjust the fullness while maintaining the width and height.

To find the solution, let us return to the definition of the CTDA.

The definition of a CTD includes the condition that "a circle rolls along a straight line". What would happen if this *straight line* were changed to a *curved line*?

Figure 20 shows the arches created when a circle rolls along a straight line versus a curved line. The top case shows a circle rolling along an upwardly curved line, the middle is a straight line (CTDA), and the bottom is a circle rolling along a downwardly curved line.

More precisely, the top case is when a circle rolls along the inside of another circle (internal rolling), and the bottom case is when it rolls along the outside (external rolling). To accurately compare the fullness of the three arches, all arches must have the same width and height, so the parameter values (R, r, d) have been appropriately adjusted. Figure 21 below shows the three arches superimposed for easier comparison.

Figures 20 and 21 illustrate the core concept of this report.

- The arch created when a circle rolls along an upwardly curved line has greater fullness than a CTDA.
- The arch created when a circle rolls along a downwardly curved line has less fullness than a CTDA.

From this, we can conclude that:

by replacing the straight baseline in a CTD with a curved line, one can adjust the fullness of the arch.

Here, as the radius (R) of the upwardly/downwardly curved line (circle) approaches infinity, it becomes a straight line, and the resulting arch becomes nearly identical to a CTDA. Conversely, as the radius is decreased, the fullness increases for internal rolling and decreases for external rolling.

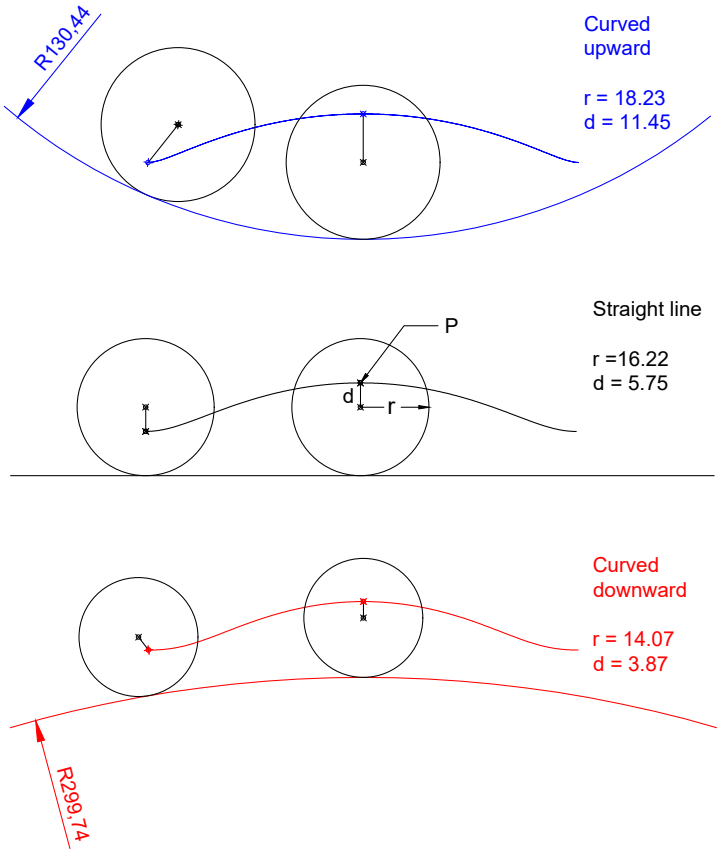

Figure 20: *Arches created by a circle rolling on a curve vs. a CTDA*

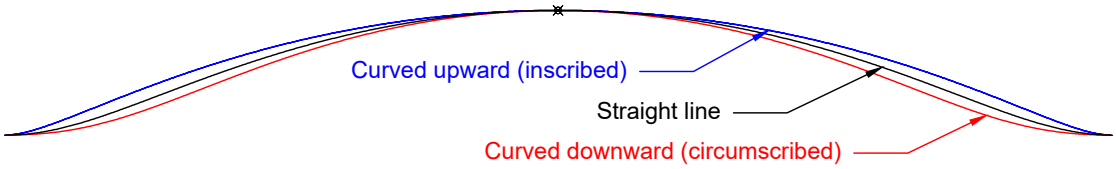

Figure 21: *Comparison of arches created by a circle rolling on a curve and a CTDA*

As explained in Table 2 earlier, the curves generated when a circle rolls on another circle are the hypotrochoid and the epitrochoid. The blue arch in the figure is a *Curtate Hypotrochoid* (*CHT*), and the red arch is a *Curtate Epitrochoid* (*CET*). In other words, by using CHT and CET, one can freely adjust the fullness of the arch while maintaining its width and height. However, to obtain an arch-shaped curve, the conditions $d < r$ and $r < R$ must be met. If $d = r$, the ends become pointed, violating the basic conditions of an arch. If $r > R$, a completely different curve shape is produced.

3.3 Curtate Hypotrochoid

3.3.1 Definition of Curtate Hypotrochoid

A CHT is defined as follows.

Definition 3.3. ***Curtate Hypotrochoid*** **(*CHT*)**
The trajectory traced by a point P, at a distance d from the center of a small circle A with radius r, as circle A rolls without slipping along the inside of a large circle B with radius R. (*where $d < r, r < R$*)

The main difference between a CHT and a CTD is that the circle rolls along the inside of another circle, not a straight line.

Its mathematical expression is as follows:

$$\begin{cases} x(\theta) = (R-r)\cos(\theta) + d \cdot \cos(\frac{R-r}{r}\theta) \\ y(\theta) = (R-r)\sin(\theta) - d \cdot \sin(\frac{R-r}{r}\theta) \end{cases} \tag{3}$$

R : radius of the outer circle B

r : radius of the inner circle A (where $r < R$)

d : distance from the center of inner circle A to point P (where $d < r$)

θ : angle of rotation of the inner circle

Figure 22 is an example of a CHT. A CHT is a continuous curve created as the small circle rotates. Therefore, to analyze the width, height, and fullness of an arch, one segment must be extracted from this continuous curve. This report will call the arch extracted from a CHT the *CHTA* (*Curtate Hypotrochoid Arch*). To extract the arch accurately, we need to know the positions of the apex and endpoints, which are defined as follows.

Definition 3.4. ***Apex of a Curtate Hypotrochoid***
A point on the trajectory that is closest to the center of the large circle B.

Definition 3.5. ***Endpoints of a Curtate Hypotrochoid***
Two points on the trajectory where a line perpendicular to the line connecting the center of the large circle B and the apex becomes tangent. These two points are located symmetrically with respect to the apex.

Finding the apex is simple, but finding the endpoints is difficult. This is because a CHT repeats its pattern while rotating overall, so it is highly unlikely that the desired arch segment is perfectly horizontal. The method for extracting an arch from a CHT is as follows.

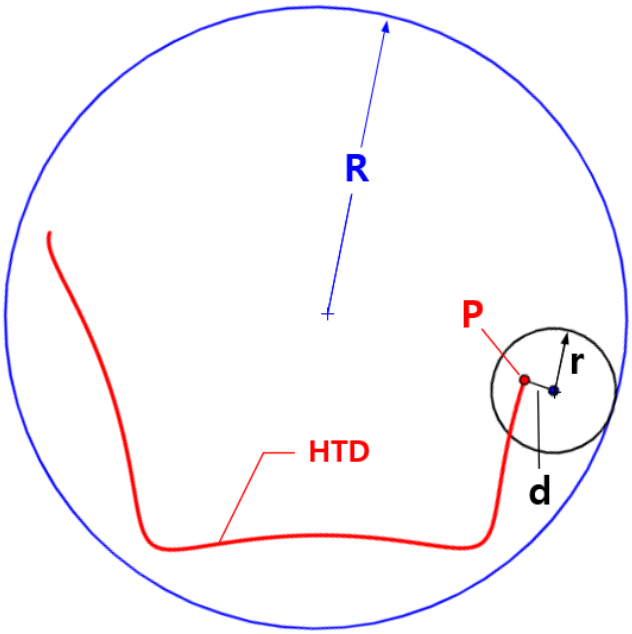

Figure 22: *Hypotrochoid*

3.3.2 Extracting an Arch from a Curtate Hypotrochoid

A CHT is a curve with a repeating pattern. To extract an arch from it, the apex and endpoints must be precisely located. The extraction process is as follows:

1. Draw the CHT curve. - Figure 23.(a) -
2. Among adjacent points, select the two points farthest from the center of the large circle B (red dots) as temporary endpoints. - (a) -
3. Extract the segment between the two temporary endpoints to create a temporary arch. - (b) -
4. Rotate the entire curve so that the endpoints of the temporary arch are horizontal. - (b) -
5. On the rotated temporary arch, find the points where the tangent slope is 0; these are the actual endpoints of the arch (green dots). - (b) -
6. Extract the segment between the two identified actual endpoints (green dots) as the final arch. - (c) -

Once the CHTA is extracted in this way, we can finally determine its width, height, and fullness. However, while width and height can be easily measured, a separate standard is needed to evaluate the fullness.

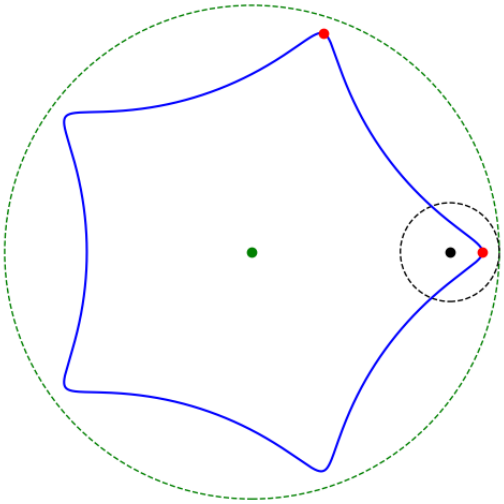

(a) *The entire CHT curve*

(b) *Extraction and rotation of the temporary arch*

(c) *Finding endpoints and re-extraction of the arch*

Figure 23: *Process of extracting an arch from a CHT*

3.3.3 Fullness of the Curtate Hypotrochoid Arch

To determine the fullness of a CHTA, a reference point is needed. This report will call this reference point the *Fullness control point* Z. The fullness control point Z is an arbitrary point on the arch, selected at a distance of about 1/8 to 1/6 of the arch width from the endpoint in the x-direction. This section is chosen because it is where the displacement is greatest when the arch's fullness changes, making it easier to see changes in fullness.

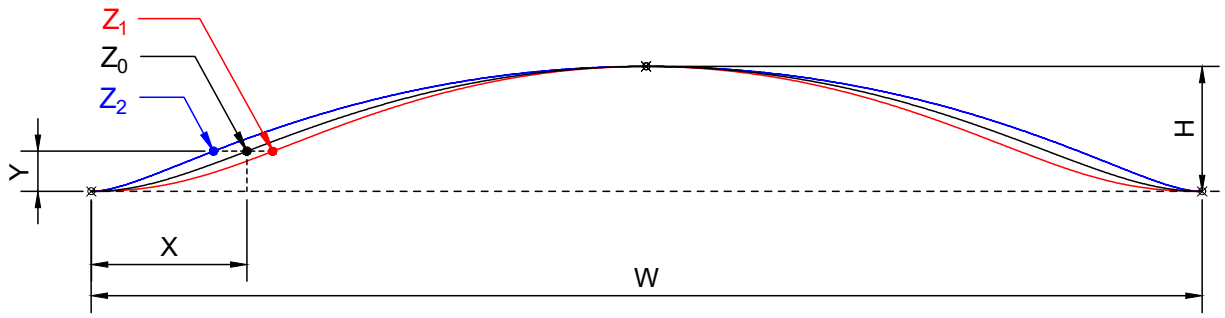

Figure 24: *Fullness control point* Z

Figure 24 shows the fullness control points (Z_0, Z_1, Z_2) for three arches to compare their fullness. All three control points have the same height on the y-axis but different positions on the x-axis. Compared to the reference point Z_0 (black arch), Z_1 (red arch) is located inside the arch (to the right), so its fullness is judged to be smaller. In contrast, Z_2 (blue arch) is outside the arch (to the left), so its fullness can be considered greater.

To adjust the fullness of a CHTA using this principle, one must first specify the target position of the fullness control point. Then, one must find the CHT parameters (R, r, d) that make the arch pass through that point. Finding the parameters that satisfy all three conditions—width, height, and fullness—for a CHTA is a very complex process. The following section will explain why this is the case and how to create a CHTA that meets all three conditions.

3.3.4 Characteristics of the Curtate Hypotrochoid Arch

To create a CHTA with the desired width, height, and fullness, one must understand how the arch's shape changes with variations in the parameters (R, r, d).

Figure 25 shows how the arch changes when $R, r,$ and d are altered individually. A decrease in R reduces both width and height. An increase in r increases the width but decreases the height. An increase in d increases both width and height. It is important to note that from this figure alone, one cannot judge the change in fullness, because the width and height have also changed. (However, as previously confirmed, if the width and height are kept constant, the fullness increases as R decreases.)

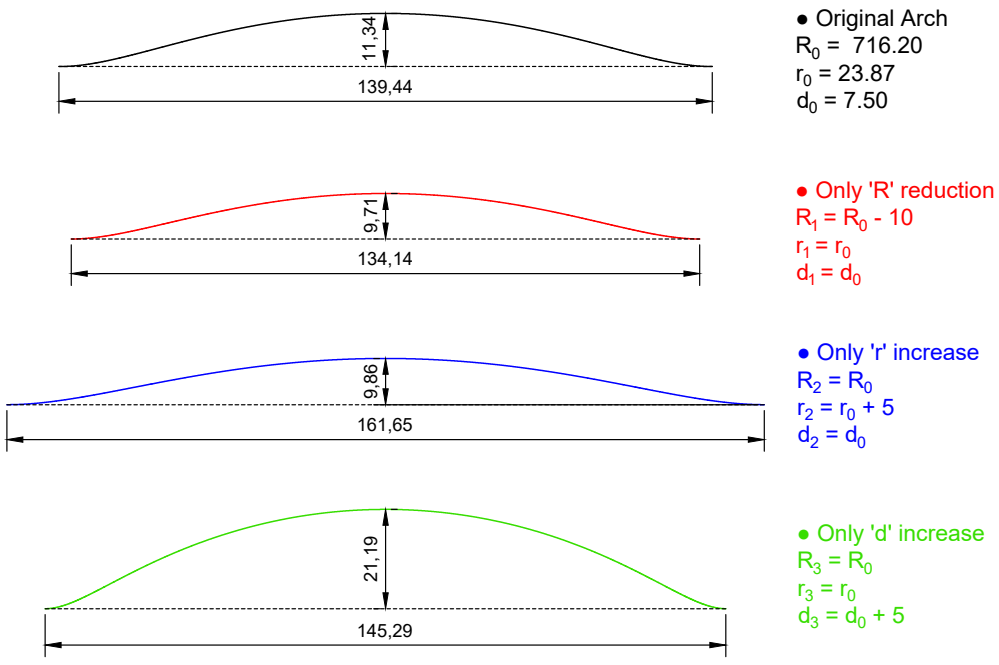

Figure 25: *Change in CHTA shape according to parameter variation*

As seen, unlike a CTDA, a CHTA has complex characteristics, making it difficult to obtain a desired arch. This requires numerous iterative calculations using a computer. The characteristics of a CHTA for each parameter are summarized in the table below. In Table 3, Width and Height show the results of changing only a single

parameter, while Fullness shows the result when width and height are kept constant.

Parameter	Width	Height	Fullness
R −	−	−	−
r +	+	−	·
d +	+	+	·

Table 3: *Changes in CHTA according to parameter variation. +:increase, −:decrease*

● Why fullness increases as R decreases

Figure 26 illustrates why the fullness of the arch increases when the radius (R) of the base circle is reduced for a circle rolling internally. (For reference, the straight baseline of a CTDA can be considered a circle with an infinite radius.)

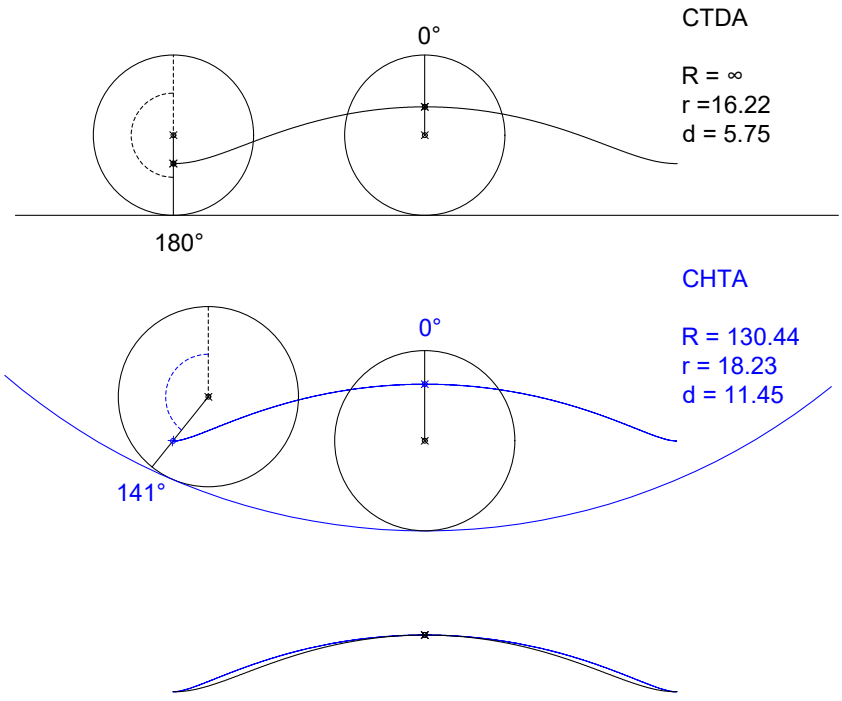

Figure 26: *Change in CHTA according to the value of R*

The figure shows that for a CTDA, the rolling circle must rotate 180° from the apex to reach the endpoint. In contrast, for a CHTA, it only needs to rotate 141° to reach the endpoint. This difference in the angle of rotation creates the change in fullness. As the required angle of rotation to reach the endpoint decreases, the end part of the arch becomes proportionally closer to the apex. This shortens the flat section at the ends of the arch, resulting in greater fullness.

Conversely, when aiming to reduce fullness, the opposite principle applies, which will be explained in detail in the next chapter.

3.4 Curtate Epitrochoid

3.4.1 Definition of Curtate Epitrochoid

A CET is defined as follows.

Definition 3.6. ***Curtate Epitrochoid*** **(*CET*)**
The trajectory traced by a point P, at a distance d from the center of a small circle A with radius r, as circle A rolls without slipping along the outside of a large circle B with radius R. (where $d < r, r < R$)

The main difference between a CET and a CHT is that the rolling circle moves along the outside of the large base circle B, not the inside.

Its mathematical expression is as follows:

$$\begin{cases} x(\theta) = (R+r)\cos(\theta) - d \cdot \cos\left(\frac{R+r}{r}\theta\right) \\ y(\theta) = (R+r)\sin(\theta) - d \cdot \sin\left(\frac{R+r}{r}\theta\right) \end{cases} \tag{4}$$

R : radius of the large circle B

r : radius of the small circle A (where $r < R$)

d : distance from the center of small circle A to point P (where $d < r$)

θ : angle of rotation of the small circle

Figure 27 is an example of a CET. Like a CHT, a CET also generates a continuous curve. To use it as an arch, a necessary segment must be extracted. This report will call the arch extracted from a CET the *CETA* (*Curtate Epitrochoid Arch*), and its apex and endpoints are defined as follows.

Definition 3.7. ***Apex of a CETA***
A point on the trajectory that is farthest from the center of the large circle B.

Definition 3.8. ***Endpoints of a CETA***
Two points on the trajectory where a line perpendicular to the line connecting the center of the large circle B and the apex becomes tangent. These two points are located symmetrically with respect to the apex.

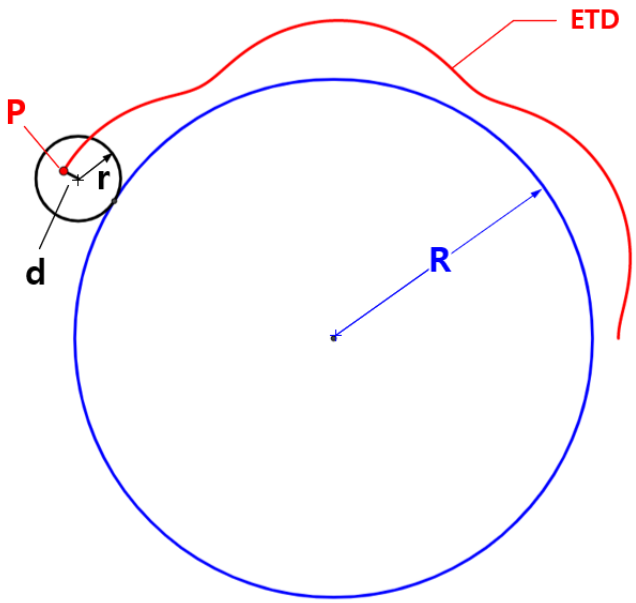

Figure 27: *Epitrochoid*

The method for extracting an arch from a CET is slightly different from that for a CHT, and the process is as follows:

3.4.2 Extracting an Arch from a Curtate Epitrochoid

1. Draw the CET curve.
2. Of the three adjacent points farthest from the center of the large circle B, select the two outer points as temporary endpoints.[3]
3. Extract the segment between the two temporary endpoints to create a temporary arch.
4. Rotate the temporary arch so that its endpoints are horizontal.
5. On the rotated temporary arch, find the points where the tangent slope is 0; these are the actual endpoints of the arch.
6. Re-extract the segment between the arch endpoints.

3.4.3 Fullness of the Curtate Epitrochoid Arch

The explanation regarding fullness is the same as for the CHTA described earlier. (See Chapter 3.3.3)

3.4.4 Characteristics of the Curtate Epitrochoid Arch

Figure 28 shows how the shape of the arch changes when the values of $R, r,$ and d are altered. A decrease in R increases both width and height; a decrease in r reduces both; and a decrease in d increases the width and decreases the height. Also, as with the CHTA, one cannot determine the change in fullness from this figure alone.

[3] The middle point is the apex of the arch.

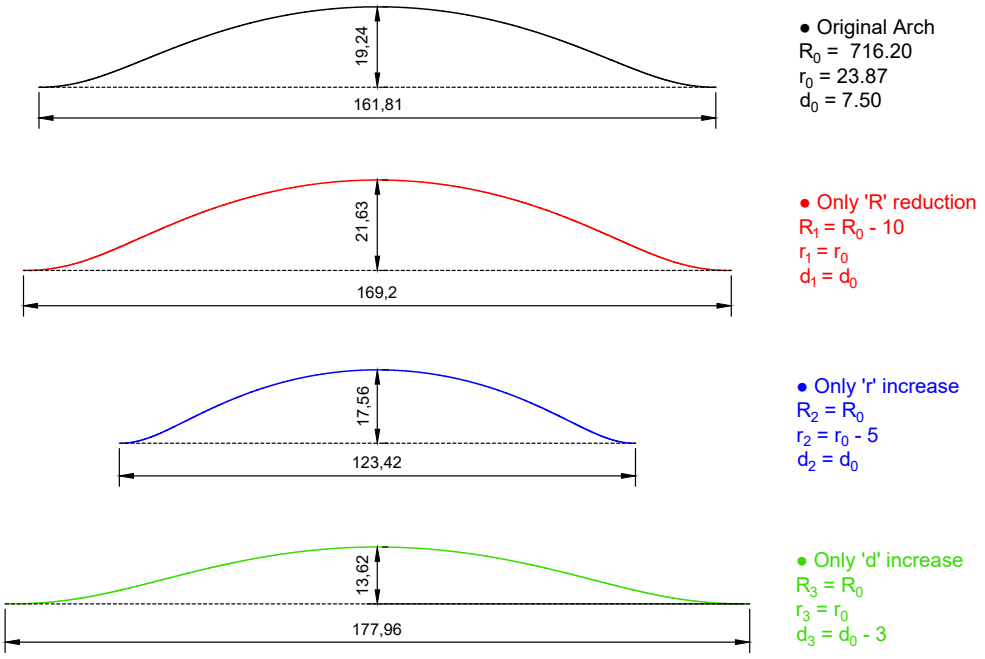

Figure 28: *Change in CETA shape according to parameter variation*

The characteristics of a CETA are summarized in Table 4. Similar to the CHTA, the width and height in the table are the results of changing a single parameter, while the fullness is the result when the width and height are kept constant.

Parameter	Width	Height	Fullness
R −	+	+	−
r −	−	−	·
d −	+	−	·

Table 4: *Changes in CETA according to parameter variation. + increase, −:decrease*

● Why fullness decreases as R decreases

Figure 29 illustrates why the fullness of the arch decreases when the radius (R) of the base circle is reduced for a circle rolling externally. (For reference, the straight baseline of a CTDA can be considered a circle with an infinite radius.)

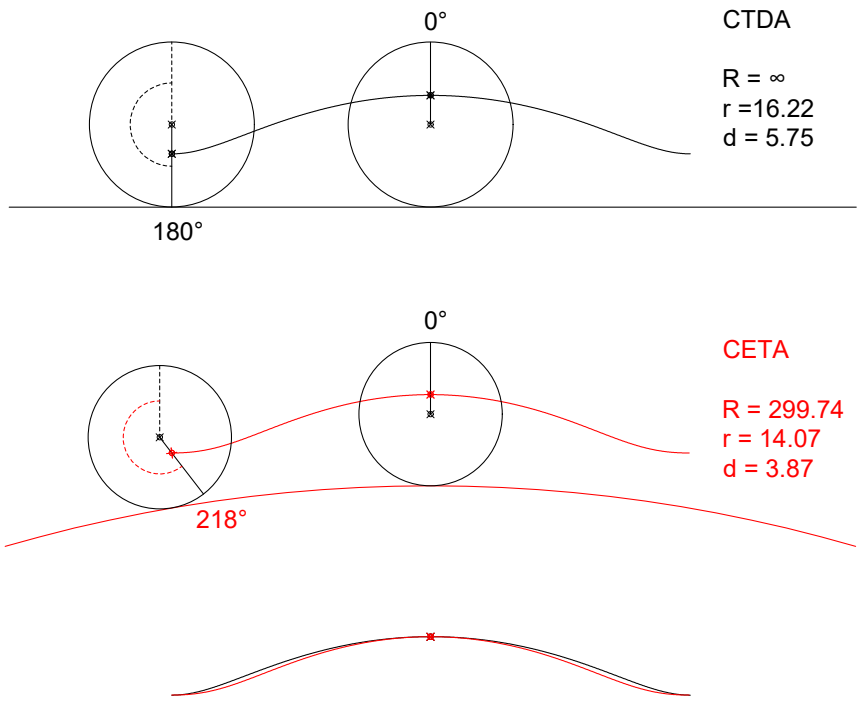

Figure 29: *Change in CETA according to the value of R*

The figure shows that for a CTDA, the rolling circle must rotate 180° from the apex to reach the endpoint. In contrast, for a CETA, it must rotate 218°. As the required angle of rotation to reach the endpoint increases, the end part of the arch becomes proportionally farther from the apex. This lengthens the flat section at the ends of the arch, resulting in reduced fullness.

4 Creating Trochoid Arches

If the fullness of the target arch is greater than that of a CTDA with the same width and height, a CHTA is created. If it is smaller, a CETA is created. If the fullness is the same (which is statistically very rare), a CTDA is created.

4.1 Creating a Curtate Trochoid Arch

As explained in Chapter 3.2.1, the generation principle of a CTDA is simple. Therefore, it can be created immediately if the width and height of the desired arch are known.

For example, let's assume we are creating a CTDA with a width of 100 and a height of 15. After calculating the values of r and d according to Equation 3, we can obtain the curve by substituting these values into the formula.

$$\begin{cases} r = W/2\pi = 100/(2 * 3.14) = 15.92 \\ d = H/2 = 15/2 = 7.5 \end{cases} \tag{5}$$

4.2 Creating a Curtate Hypotrochoid Arch

A CHTA is used to create an arch with greater fullness than a CTDA. The creation process begins with a CTDA. Since a CTDA is equivalent to a state where the radius (R) of the large base circle is infinite (a straight line), the desired arch is found by gradually decreasing this value of R. The detailed method is as follows:

1. Determine if the fullness of the target arch is greater or smaller than that of a CTDA. If it is greater, create a CHTA.
2. Decide the initial value of R.[4] Since the R value of most completed CHTAs does not exceed $400r$, it is advisable to start from around $500r$ (500 times the value of r).
3. From the set initial value of R, iteratively calculate by slightly increasing r and d until the arch's width and height reach the target values.
4. Once the width and height match the target values, check the fullness. If the fullness is insufficient, decrease the value of R.
5. With the reduced value of R, repeat the calculation by increasing r and d until the width and height reach the target values again.
6. Repeat steps 4 and 5 until the width, height, and fullness all satisfy the target values.

The method above is a simplified summary of the calculation process. In reality, much more complex operations are required due to issues like digital quantization errors and computation time. The reason for decreasing the value of R during these calculations is to gradually increase the fullness. As R decreases, the width and height of

[4] Instead of starting from infinity, we start from a specific value. Using an infinitely large number would make the calculation time infinitely long.

the arch also decrease. To bring them back to the target values, r and d are continuously adjusted upwards. Here, increasing d increases both width and height, but increasing r actually decreases the height. This difference is used to appropriately adjust r and d to match the width and height.

4.3 Creating a Curtate Epitrochoid Arch

A CETA is used to create an arch with less fullness than a CTDA. The generation principle is similar to that of a CHTA, starting from a CTDA. In other words, we start from a state where the radius (R) of the base circle is infinite and gradually decrease the value of R to find the desired arch. The detailed method is as follows:

1. Determine if the fullness of the target arch is greater or smaller than that of a CTDA. If it is smaller, create a CETA.
2. Decide the initial value of R. (Generally, the R value for a CETA is slightly larger than for a CHTA.)
3. From the set initial value of R, iteratively calculate by slightly decreasing r and d until the arch's width and height reach the target values.
4. Once the width and height match the target values, check the fullness. If the fullness is excessive, decrease the value of R.
5. With the reduced value of R, repeat the calculation by decreasing r and d until the width and height reach the target values again.
6. Repeat steps 4 and 5 until the width, height, and fullness all satisfy the target values.

The reason for decreasing the value of R during these calculations is to gradually reduce the fullness. For a CETA, as R decreases, the width and height actually increase. Therefore, to bring them back to the target values, r and d are continuously adjusted downwards.

4.4 Trochoid Arches That Cannot Be Created

There are limits to the fullness that can be adjusted with a CHTA and CETA. This can result in cases where the desired arch cannot be created. These limitations can be broadly divided into two types. In both cases, an approximation curve is used as an alternative.

4.4.1 Cases Where the Arch Does Not Exist

This refers to cases where the CHT or CET curve itself is generated, but an arch shape (CHTA, CETA) cannot be extracted from it. For example, if the value of R is reduced too much in an attempt to excessively increase fullness, a CHT curve is formed, but the segment that satisfies the basic conditions of an arch disappears.

The fullness of a CHTA and CETA cannot be increased or decreased indefinitely. Beyond a certain limit, the curve no longer meets the basic conditions of an arch. As shown in Figure 30, if the value of R is reduced too much, the generated CHT curve no longer contains a segment that can be defined as an arch.

For a fixed width and height, let's call the arch with the maximum possible fullness that can be made with a trochoid *maxCHTA*, and the one with the minimum fullness *minCETA*. In fact, the 5th arch of the Back of Models A, B, and C often has a fullness greater than even the maxCHTA. To reconstruct arches that exceed the limits of trochoids, the approximation curves discussed in the next chapter are necessary.

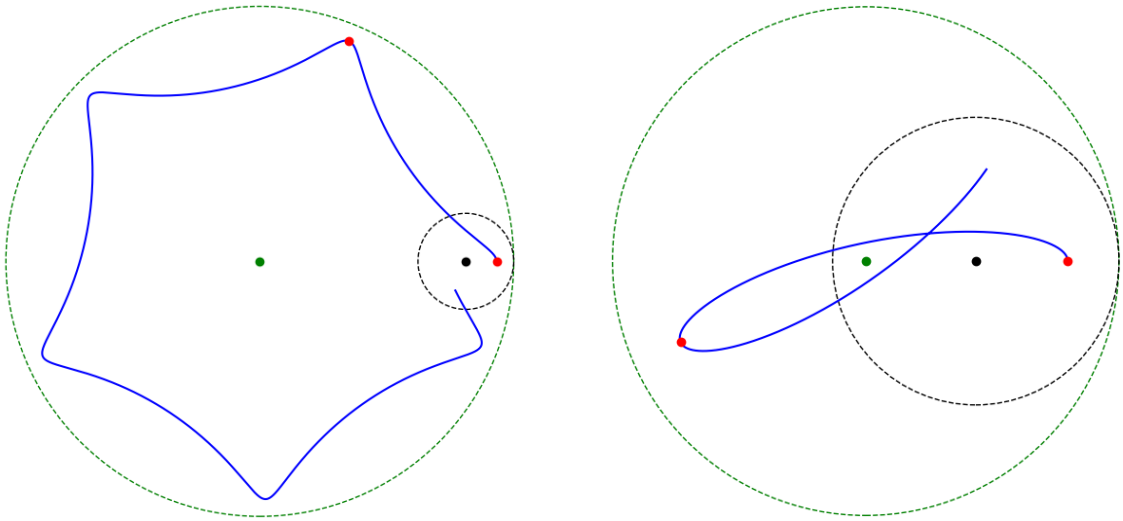

(a) *Case where a CHTA exists (R=6r)* **(b)** *Case where a CHTA does not exist (R=2.5r)*

Figure 30: *Existence of an arch segment in a CHT curve*

4.4.2 Cases Where the Arch Exists but Cannot Be Created

This refers to cases where a CHTA or CETA theoretically exists but cannot be created due to computational limitations. This means failing to find an exact solution due to errors arising from the digital calculation process, such as precision issues and optimization failures.

Although a TD curve is inherently a continuous line, a computer represents it as a set of numerous points (discrete values). If the exact solution we are looking for lies between these points, the computer may fail to find it, causing the calculation to fail.

Due to this issue of digital quantization, appropriate compromises are necessary in the calculation process. If the compromise point is set incorrectly, the calculation can fail or the time required can increase exponentially. Therefore, in such cases, using an approximation curve is more efficient.

5 Trochoid Approximation Curve

When the fullness of the target arch falls outside the expressible range of a CHTA or CETA, or when it cannot be created due to computational issues, we must create and use a similar arch instead.

For example, if the maximum achievable fullness is 10 but an arch with a fullness of 12 is desired, we first create an arch with a fullness of 10 and then transform it to have a fullness of 12. As another example, if the calculation for an arch with a fullness of 7 fails, we create an arch with a fullness of 6.9 instead and transform it to become 7. As shown in Figure 31, the principle is that if a curve passing through the target points Z_1 or Z_2 cannot be created for any reason, a creatable curve passing through Z_0 is generated first and then transformed to pass through Z_1 or Z_2.

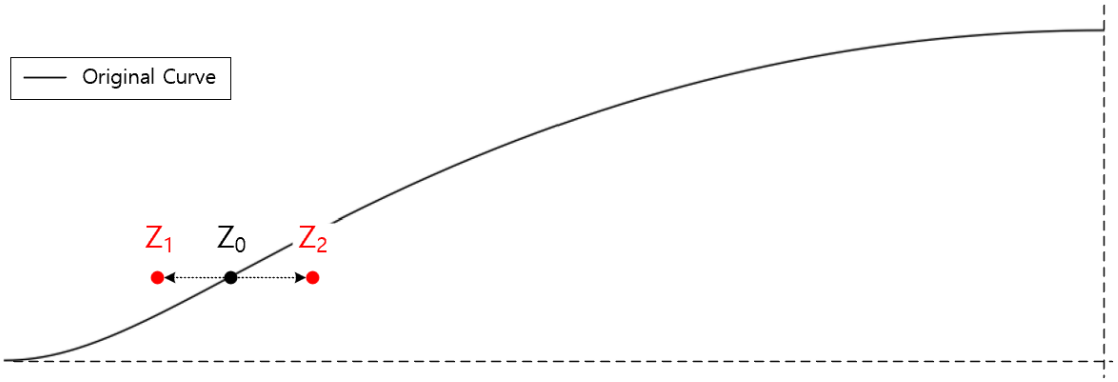

Figure 31: *Concept of the approximation curve*

Thus, when the target arch cannot be directly created, the curve obtained by first creating an achievable arch and then transforming it will be called an *Approximated Arch* or *Approximation Curve*. Below, this report will examine the principles and creation method of the approximation curve.

For reference, the concept of an approximation curve only applies to arches no. 1 through 5. The method for creating arch no. 6 is similar, but it is not called an approximation because the goal is not to resemble a CHTA or CETA.

Strictly speaking, the curve created when the target curve theoretically does not exist (e.g., when fullness exceeds maxCHTA) is closer to *generation* than approximation. On the other hand, the result when the curve exists but cannot be created for computational reasons can be called an approximation. However, for convenience in this report, both cases will be collectively referred to as approximation curves.

5.1 Basic Principle of the Approximation Curve

The approximation curve is created by adjusting the fullness of an original CHTA or CETA. The principle is to horizontally shift the numerous points that make up the original curve. During this process, the gentle S-shape

of the original curve must be maintained, and the tangent slope must be 0 at the endpoints and the apex. To achieve this, different shift amounts must be applied to each point on the curve.

For example, the apex and endpoints of the arch must not move. The shift amount must increase towards the middle and decrease towards the ends to maintain the overall arch shape. A consistent rule, or pattern, is needed to determine the horizontal shift for each point.

Figure 32 explains the horizontal shift pattern of the points. (a) is the case of increasing fullness, and (b) is the case of decreasing fullness.

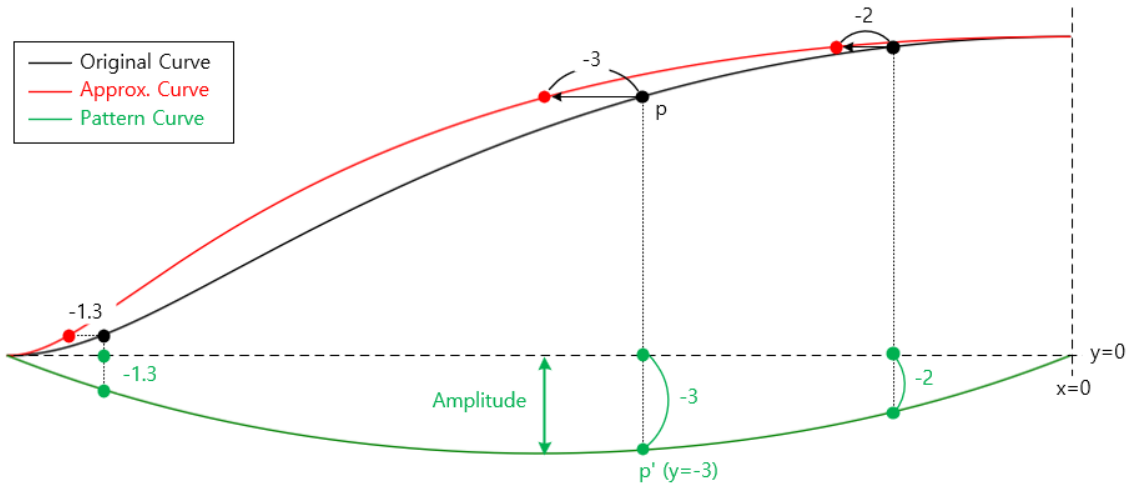

(a) *Case of increasing fullness*

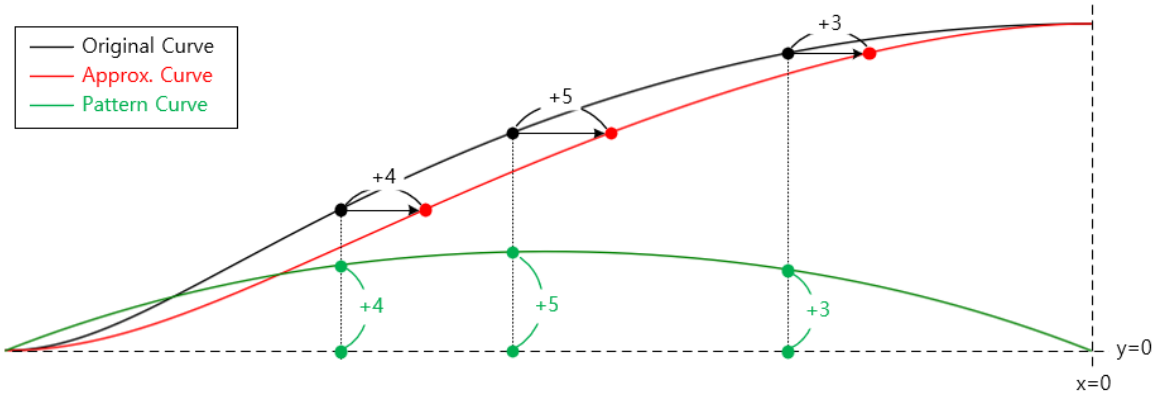

(b) *Case of decreasing fullness*

Figure 32: *Principle of creating an approximation curve using a pattern curve*

The apex and endpoints of the original arch (black) must be fixed, while only the central part should be shifted. The shift amount should increase towards the center and decrease towards the ends. The pattern representing this rule should have the form of a smooth curve. Also, the ends of this pattern curve must have the same x-

coordinates as the apex and endpoints of the original arch, and their y-values must be 0.

This report will call the curve representing this shift pattern a *Transformation pattern curve*, or *Pattern curve* for short. The shape of the pattern curve determines the final shape of the approximation curve, and its amplitude (height) determines the amount of change in fullness. That is, the larger the amplitude, the larger the shift of each point, resulting in a greater change in fullness.

The pattern curve indicates how much to horizontally shift each point of the original arch. For example, in figure (a), to know how much to shift a point p on the original arch, find the point p' on the pattern curve with the same x-coordinate as p. If the y-value of p' is -3, then point p should be shifted by -3 in the x-direction, that is, 3 units to the left. By shifting all points of the original arch horizontally according to the y-values of the pattern curve, a new approximation curve is created.

Whether the pattern curve is convex upwards or downwards determines whether the arch's fullness increases or decreases. The figure above uses the left half of the arch as an example. In this case, shifting points to the left increases fullness, and shifting them to the right decreases it. Therefore, if the pattern curve is convex downwards (negative y-value), fullness increases, and if it is convex upwards (positive y-value), fullness decreases. For the right half of the arch, this direction is reversed.

So, which curve should be used as the pattern curve? The purpose of the approximation curve is to change only the fullness while maintaining the shape of the original trochoid arch as much as possible. Therefore, if an approximation curve created with a certain pattern curve perfectly matches a real trochoid arch with the same target fullness, that pattern curve can be considered ideal.

Various curves such as circular arcs, ellipses, and catenaries can be considered as candidates for the pattern curve. After testing several curves, this report found only minor differences and could not find an ideal curve. Among them, the Catenary curve yielded the best results. However, it was difficult to obtain a satisfactory approximation curve with the catenary curve alone, so this report decided to make slight modifications to it to create the final pattern curve.

For convenience, from now on, an approximation curve created from a CHTA will be denoted as nCHTAce, from a CETA as nCETAice, and from a CTDA as CTDAce or CTDAice (see appendix for abbreviations).

5.2 Creating the Pattern Curve

The catenary curve is used as the pattern curve. The optimal pattern is found by observing the approximation curve created while slightly modifying the shape of this curve.

First, under the condition that the width and height of the arch are the same, the following four curves are compared.

- Original curve A: CTDA
- Target curve B: CHTA passing through the target fullness control point Z
- Pattern curve C: Catenary curve used to create approximation curve D
- Approximation curve D: The resulting curve created by transforming original curve A with pattern curve C to pass through the fullness control point Z

This process verifies how similar the approximation curve (D) is to the target curve (B). If B and D completely overlap, the pattern curve used for the transformation can be considered ideal. If they do not match, we can see the difference and determine how to modify the pattern curve. Figure 33 shows these four curves together.

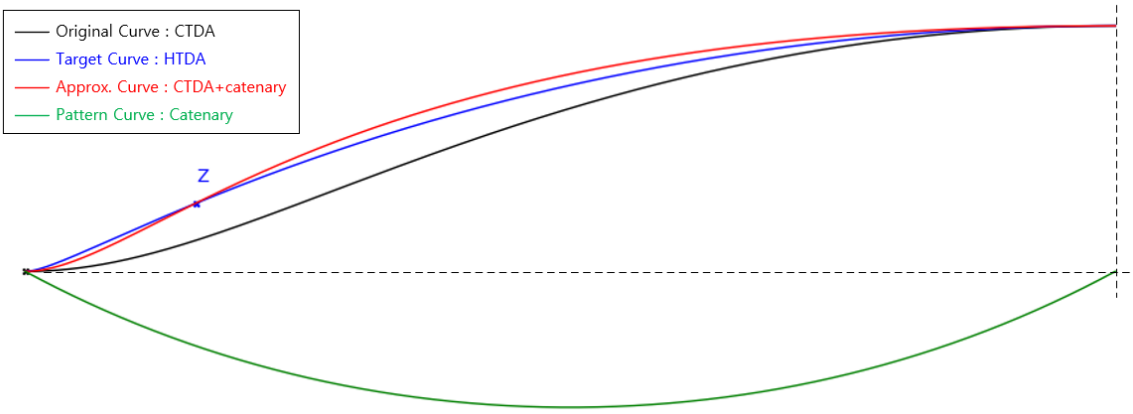

Figure 33: *Approximation curve using a catenary curve*

In the figure, the approximation curve (red) shows insufficient fullness towards the arch endpoint and excessive fullness towards the apex, relative to the fullness control point Z. This means that the pattern curve (green) does not provide enough transformation near the arch endpoint and provides too much transformation near the apex. To solve this problem, the apex of the currently downwardly convex catenary curve must be shifted towards the arch endpoint. Such an apex shift is equivalent to concentrating the curve to one side and can be implemented by applying an exponential function to the catenary curve. A positive exponent value concentrates the curve to the left, while a negative value concentrates it to the right.

The method for applying an exponential function to the catenary curve is as follows. First, the x-axis itself is distorted (stretched or compressed) by applying an exponential function. Then, the original catenary curve is

drawn on the distorted x-axis. Finally, the x-axis is restored to its original state. (-Figure 34-)

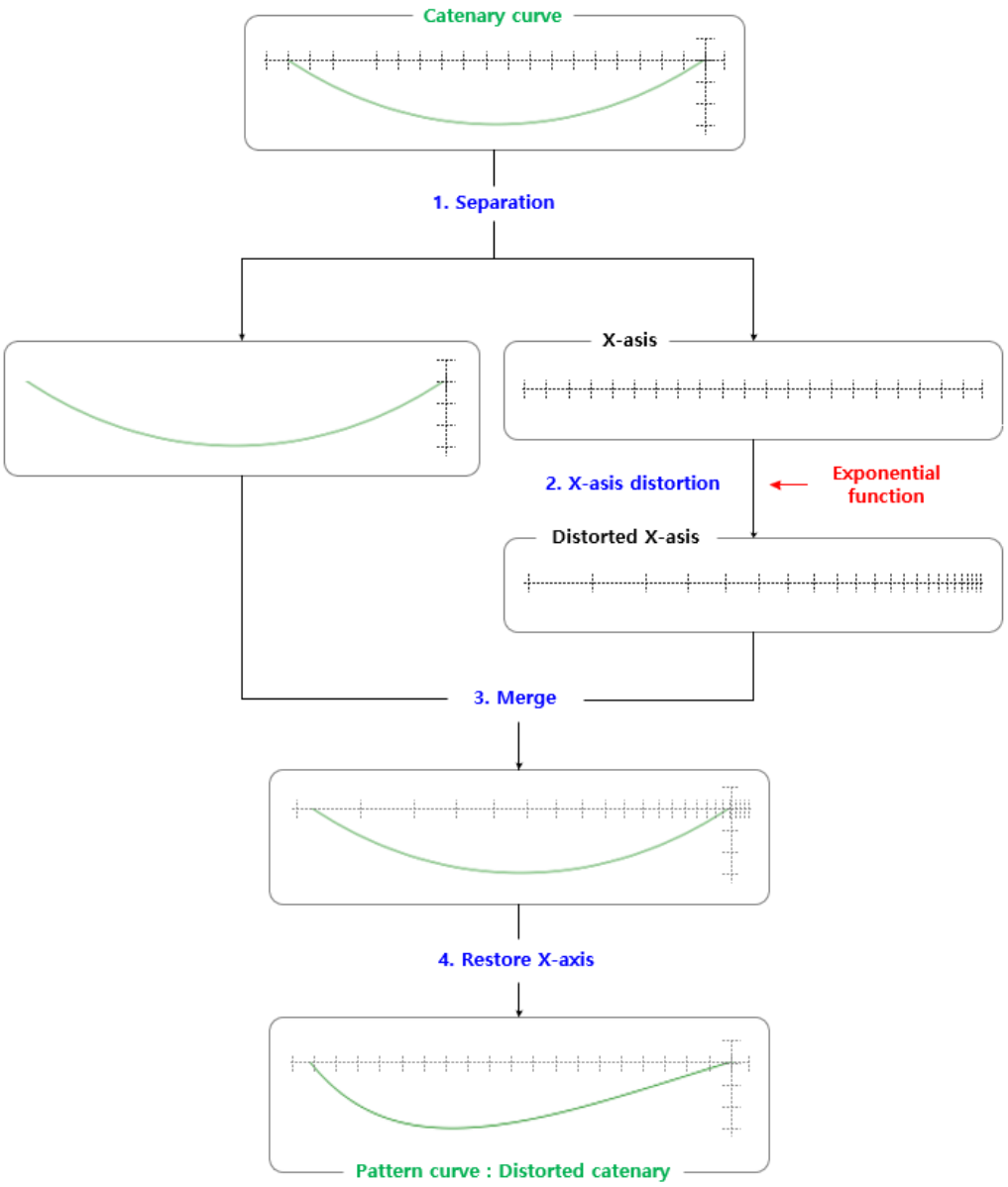

Figure 34: *Method of applying an exponential function to a catenary curve*

The approximation curve created by shifting the apex position of the catenary curve (concentrating it to one side) using the method above changes as shown in Figure 35.

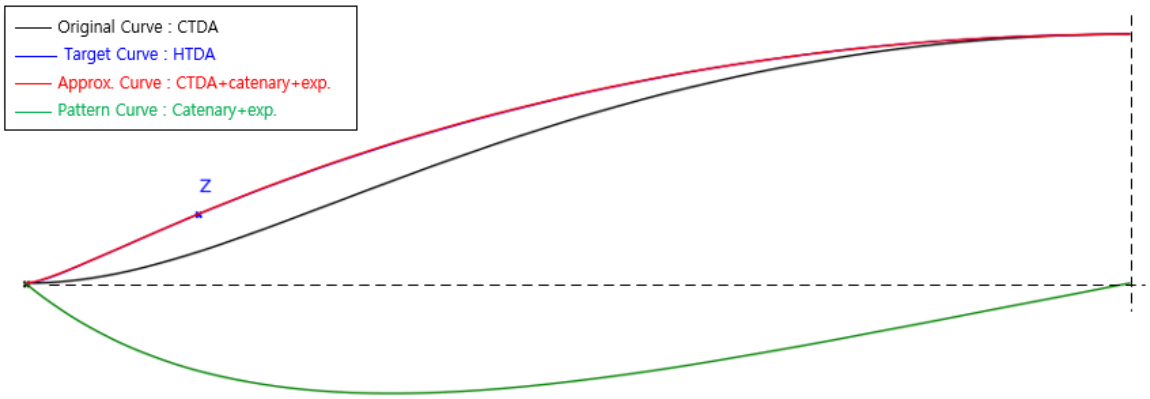

Figure 35: *Approximation curve using an exponentially distorted catenary curve*

The figure shows that the target curve (blue) and the approximation curve (red) are nearly identical. The exponent value used here is the most suitable for the current arch's width and height. If the width and height of the arch are the same, this optimal exponent value can be used consistently, regardless of the magnitude of the fullness. However, this value is only applicable when increasing the fullness. When decreasing the fullness, the direction of the pattern curve's apex shift is opposite, so a different optimal exponent value with a different sign and magnitude must be found separately.

Finding the optimal exponent value is done through iterative computer calculations. The difference between the approximation curve and the target curve is calculated as an error area, and the exponent value that minimizes this area is selected.

Below is the mathematical explanation for this process.

The definition and general equation of a catenary curve are as follows.

> **Definition 5.1.** ***Catenary curve***
> *The curve formed by a flexible, inextensible, and uniformly dense chain or rope suspended from two points and hanging under its own weight.*

$$y = a \cosh\left(\frac{x}{a}\right) \tag{6}$$

Here, a is a constant representing the distance from the lowest point of the curve to the x-axis, which determines the width and shape of the curve. In this report, to fix the shift amount at both ends of a specific interval (x_s, x_e) to 0 and to control the amplitude (A), the equation is modified and used as follows.

$$y = A\left[\cosh\left(\frac{x' - x_c}{w}\right) - \cosh(1)\right] \tag{7}$$

Here, x_c is the center of the curve, w determines the width, and x' is the final coordinate input to the function.

To make the curve asymmetrical, the input coordinate x' is generated by distorting the original x-coordinate x_o with an exponential function. This process is applied after normalizing x_o to the range $[0, 1]$.

$$x' = \left(\frac{e^{\left(\frac{x_o - x_s}{L}\right)\cdot \text{expo}} - 1}{e^{\text{expo}} - 1}\right) \cdot L + x_s \quad \text{, where } L = x_e - x_s \tag{8}$$

The final exponentially distorted catenary function, which combines the above equations, is as follows.

$$y(x_o) = A \cdot \left(\cosh\left(\frac{x' - x_c}{w}\right) - \cosh(1)\right) \tag{9}$$

x_o : original X coordinate

A : coefficient determining the overall amplitude of the curve

x' : final coordinate input to the function

x_s, x_e : x-axis range of the curve

expo : coefficient determining the strength and direction of the exponential distortion

x_c, w : center and width coefficients of the catenary curve $(x_c = \frac{x_s + x_e}{2}, w = \frac{L}{2})$

6 Creating Trochoid Approximation Curves

Approximation curves are created by dividing the process into two cases. The first is when the target arch theoretically does not exist, and the second is when it exists but cannot be created due to computational issues.

6.1 Case Where the Arch Does Not Exist

The creation sequence is as follows:

1. Generate a CTDA and a maxCHTA (or minCETA), each with the same width and height as the target arch.
2. Adjust the exponent value and amplitude of the pattern curve to find the optimal exponent value at which the approximation curve, transformed from the CTDA, most closely resembles the maxCHTA (or minCETA).
3. Apply the optimal exponent value found previously to the pattern curve. Then, readjust the amplitude to transform the maxCHTA (or minCETA), thereby completing the final approximation curve, nCHTAce (or nCETAice).

(※ To reduce the error of the approximation curve, the following should be noted. When determining the exponent value, calculate the area of the closed curve formed by the two curves (error area) and select the exponent value that minimizes this area. However, even if the error area is small, the overall shape of the curves may differ. Therefore, the standard deviation should also be compared, and a value that provides a good balance of low error area and low standard deviation should be chosen.)

6.2 Case Where the Arch Exists but Cannot Be Created for Computational Reasons

The creation sequence is as follows:

1. Generate a CTDA and a maxCHTA (or minCETA), each with the same width and height as the target arch.
2. Adjust the exponent value of the pattern curve to find the optimal exponent value at which the approximation curve, transformed from the CTDA, most closely resembles the maxCHTA (or minCETA).
3. Generate the calculable nCHTA (or nCETA) that is closest in fullness to the target curve as the original curve.
4. Apply the optimal exponent value found previously to the pattern curve. Then, adjust the amplitude so that the approximation curve, transformed from the original curve (nCHTA) created in step 3, passes through the target fullness control point.
5. Using the exponent value and amplitude found in the previous step, transform the nCHTA (or nCETA) to complete the final approximation curve, nCHTAce (or nCETAice).

If the target curve is very similar to a CTDA, the parameter R can become very large, putting a heavy load on the computation (in terms of time, precision, etc.). Therefore, using an approximation curve is also efficient in this case. Here, a CTDA is used as the original curve instead of an nCHTA (or nCETA), and the generated approximation curve is denoted as CTDAce (or CTDAice).

(※ To reduce the error of the approximation curve, the following points should be noted. First, when finding the exponent value of the pattern curve, the case with the largest displacement should be used as the basis. That is, the original curve should be set to a CTDA and the target curve to a maxCHTA (or minCETA) for the calculation. Second, when creating the final approximation curve, the calculable CHTA (or CETA) closest to the target fullness control point should be used as the original arch. Third, the optimal exponent value should be selected by considering both the error area and the standard deviation.)

7 The 6th Arch

While the widths of arches no. 1-5 are mainly determined by the width of the plate, their heights are determined by the shape of the 6th arch. Therefore, the 6th arch can be considered the most important step in the reconstruction process.

The 6th arch has greater fullness than the other arches, and its shape features a long, flat section near the apex. Due to these characteristics, it cannot be reconstructed with a standard CHTA. Therefore, it must be created by transforming a CTDA using a separate pattern curve.

7.1 Principle of Creating the 6th Arch

Since the 6th arch has a different shape from the others, additional reference points are needed to define its form. While arches no. 1-5 were defined by a total of three points (apex, endpoints, and fullness control point), the 6th arch requires at least two more reference points. Also, while arches no. 1-5 are symmetrical, the 6th arch is asymmetrical, so it must be created by dividing it into upper and lower parts based on the apex.[5]

As additional reference points to determine the shape of the 6th arch, the first and fourth points representing the contour line positions are used. The reconstruction curve must pass through the fullness control point Z. However, the partial fullness on the endpoint side and the apex side, relative to Z, can vary depending on the shape of the pattern curve. Therefore, the first and fourth contour points are used as additional reference points to check and adjust the fullness of these two parts.

Ideally, the reconstruction curve should pass through all contour points and the positions of arches no. 1-5. However, as seen earlier, the contour point positions of the models contain errors, resulting in an uneven surface. Therefore, it is reasonable to select a few of the most suitably located points as reference points. Since the fullness control point (the second contour point) must be passed through, one reference point is placed on each side of it. The first contour point is selected on the arch endpoint side, and the fourth contour point, which reacts most sensitively to changes in the pattern curve's shape, is selected on the apex side.

The reconstruction curve will always pass through the arch endpoint, point Z, and the arch apex. With this condition, we check if it also passes through the first and fourth contour points. If the curve passes above a contour point, the fullness is excessive; if it passes below, it is insufficient. Based on this result, the shape of the pattern curve is adjusted so that the reconstruction curve also passes through these two contour points.

This report will call these two additional reference points, used to determine the shape of the 6th arch, *Shape control points*. The one on the arch endpoint side relative to the fullness control point is defined as the Shape control point-bottom, and the one on the apex side is the Shape control point-top. Therefore, the shape control

[5] Since the arches of the models are not symmetrical, this report reconstructs the left and right sides of arches no. 1-5 separately.

point-bottom is the first contour point, and the shape control point-top is the fourth contour point. However, like the fullness control point, using contour points as shape control points is merely for convenience. Any point on the target arch can be used as a control point. They were chosen simply because the position values of the contour points are already known; using the fifth or sixth contour point instead of the fourth as the shape control point-top would also be acceptable.

The pattern curve for the 6th arch is created by blending a *cubic polynomial curve*, an *exponential curve*, and a *catenary curve*. The catenary curve adjusts the overall fullness, making the reconstruction curve pass through the fullness control point. The cubic polynomial curve adjusts the overall shape of the arch, and the exponential curve serves to fine-tune the shape. Therefore, when reconstructing the arch, the parameters (amplitude, exponent value, etc.) of these three curves must be appropriately combined.

7.2 Creating the Pattern Curve

A cubic polynomial curve is similar to a catenary curve but has an asymmetrical shape that is flatter on one side. It resembles a spoon, with one side concave (the bowl part) and the other extending long (the handle part). The length and position (left/right) of this handle, as well as the amplitude of the curve, determine the appearance of the reconstructed arch. For example, when creating the left half of an arch, if the handle is on the left, the reconstructed arch will have less fullness at the endpoint and increasing fullness towards the apex (a steepening slope effect). The length of the handle is controlled by applying an exponential function to the cubic polynomial curve, which means concentrating the curve to the left or right. A positive exponent value concentrates it to the left, and a negative value to the right. Generally, the handle is placed on the left, but in some cases, it may be placed on the right.

Below is an explanation of the cubic polynomial curve.

> **Definition 7.1.** ***Cubic polynomial curve***
> *A curve defined by the form $y=ax^3 + bx^2 + cx + d$, where the highest power of the variable x is 3 (x^3). It can have up to two extrema, allowing it to create more complex S-shaped smooth curves than a simple parabola.*

The basic form of the cubic polynomial curve used in this report is defined by the following equation:

$$y = x^2(x - 1) \tag{10}$$

The final pattern curve is created by adding an exponentially distorted cubic polynomial curve and a catenary curve (Figure 36). First, a catenary curve and a cubic polynomial curve are prepared separately. Then, the x-axis of the cubic polynomial curve is distorted with an exponential function to transform its shape (adjusting the handle length). This transformed cubic polynomial curve is then added to the prepared catenary curve to complete the final pattern curve. (For the method of applying an exponential function to the cubic polynomial

curve, refer to Figure 34)

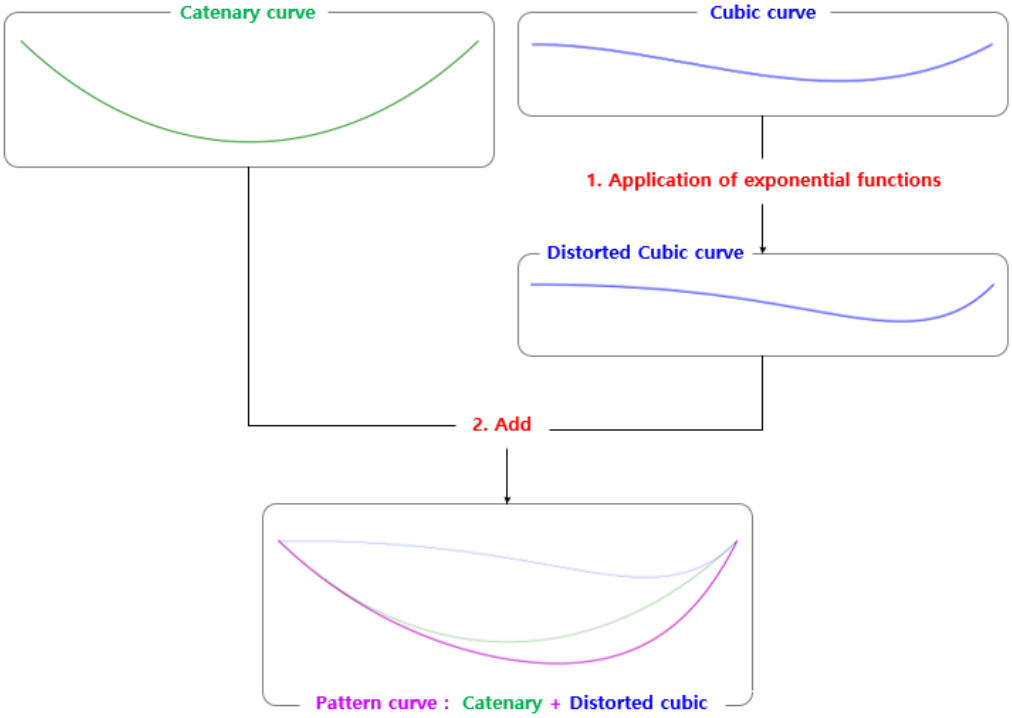

Figure 36: *Final pattern curve combining an exponentially distorted cubic polynomial curve and a catenary curve*

Figure 37 shows how the reconstruction curve changes each time a component is applied to the pattern curve. (※ Since these are example figures, each parameter has been set arbitrarily.)

Relative to the fullness control point Z, (a) shows excessive fullness towards the endpoint and insufficient fullness towards the apex, while (b) shows the opposite. (c) is slightly closer to the target curve than (a). While combining the three functions allows for free adjustment of the reconstruction curve's shape, finding the optimal parameters is not easy. First, the amplitude of the catenary curve is found through iterative calculations until the reconstruction curve passes through the fullness control point Z. Then, the amplitude of the cubic polynomial curve and the exponent of the exponential function must be found through iterative calculations by changing their values until the reconstruction curve passes through both the first and fourth contour points.

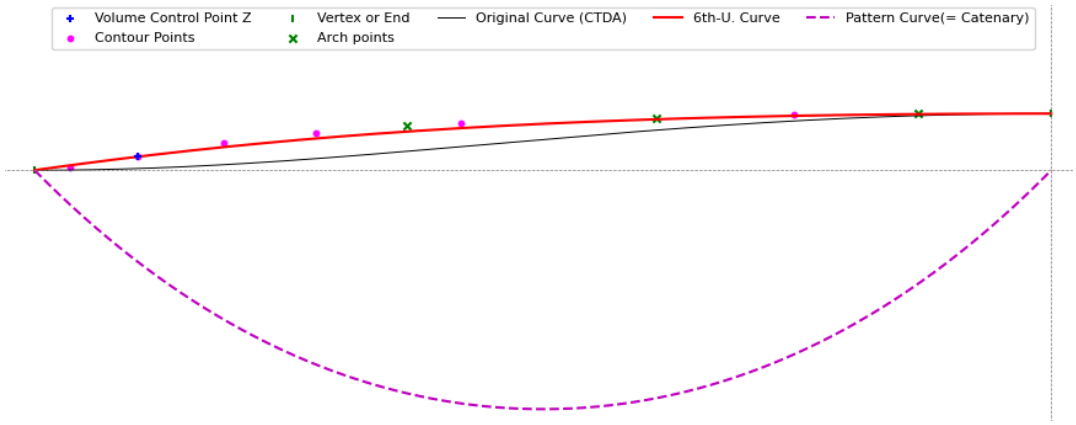

(a) *Result of using only a catenary curve as the pattern curve*

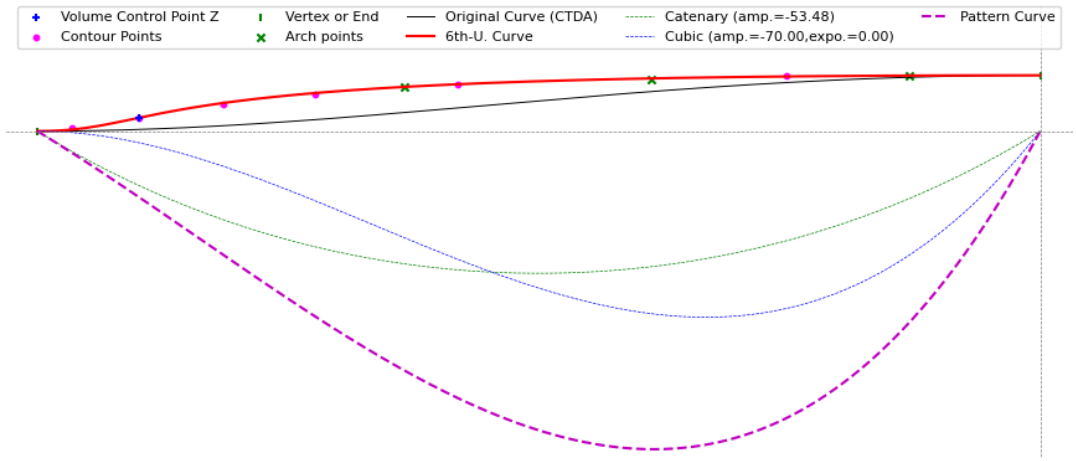

(b) *Result of adding a cubic polynomial curve to (a)*

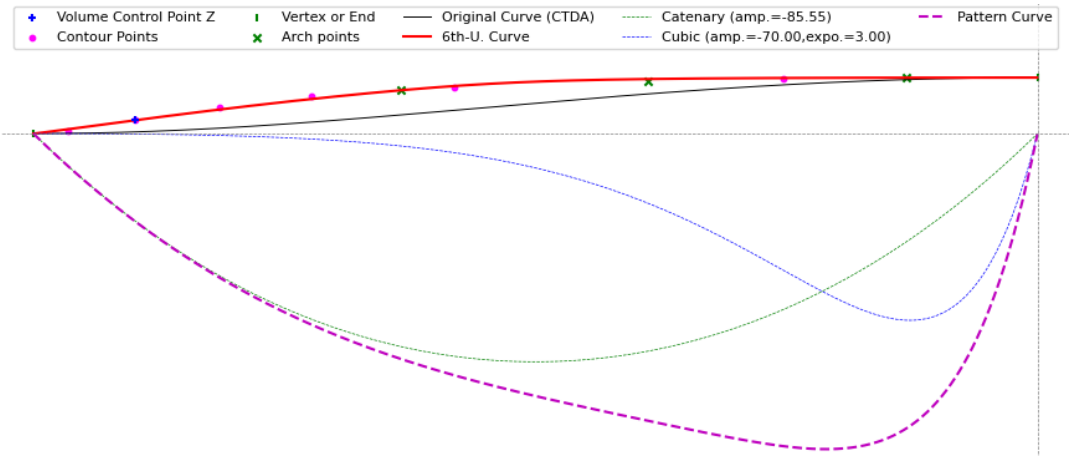

(c) *Result of applying an exponential function to the cubic polynomial curve in (b)*

Figure 37: *Change in the reconstruction curve according to the combination of pattern curve elements*

Figure 38 is the final result after finding and applying the optimal parameters through the iterative calculations described above. Compared to the previous example figures, it can be seen that the reconstruction curve matches the positions of the contour points very well.

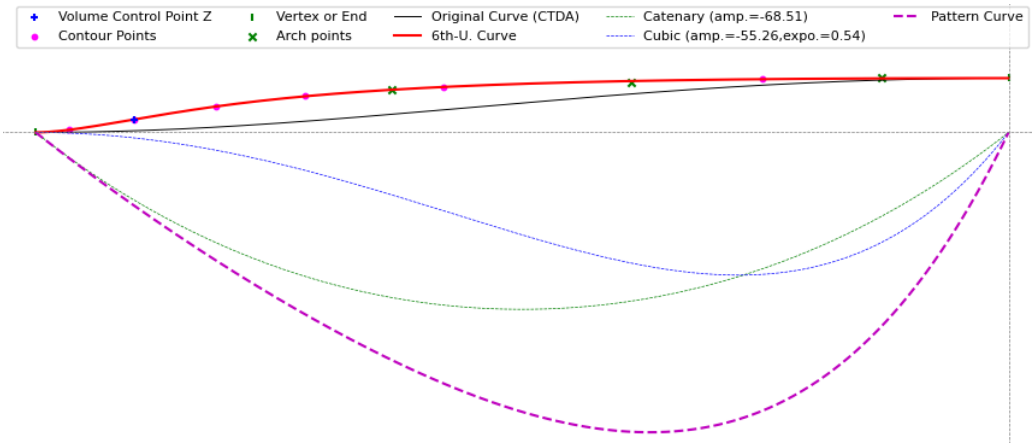

Figure 38: *Final pattern curve combining an exponentially distorted cubic polynomial curve and a catenary curve (Optimized)*

By appropriately specifying the positions of the shape and fullness control points and adjusting the pattern curve so that the reconstruction curve passes through all these points, various forms of arches can be created with precision.

7.3 Sequence for Creating the 6th Arch

The sequence for reconstructing the 6th arch is as follows:

1. Specify the positions of the fullness control point Z and the upper/lower shape control points.
2. Generate a CTDA with the same width and height as the arch to be reconstructed, to serve as the original curve.
3. Prepare the catenary curve and the cubic polynomial curve to be used for the pattern curve.
4. Find the optimal values by gradually increasing from 0 the exponent to be applied to the cubic polynomial curve and the amplitudes of each curve (cubic polynomial, catenary), so that the reconstruction curve passes through the fullness control point and both the upper and lower shape control points.
5. Complete the final pattern curve by applying the found exponent value and the two amplitude values.
6. Generate the final arch by transforming the CTDA created in step 2 using the completed pattern curve.

8 Reconstruction of the Stradivari Arch

Using the methods described so far, this report will now reconstruct the arches of Models A, B, C, and D. However, due to its unique characteristics, the 6th arch is presented separately. The subsequent tables, from Table 6 to 5, summarize all relevant information, including the parameter values and arch types used in the reconstruction.

Arches no. 1-5 are reconstructed by dividing them into front and back plates, and then into left (bass bar side) and right (sound post side) halves. Reconstruction is first attempted using a CHTA or CETA. Only if this is impossible is an approximation curve (nCHTAce, nCETAice, etc.) created using a pattern curve. The position of the fullness control point Z was standardized to the second contour line for all cases.

The 6th arch is reconstructed by dividing it into upper and lower parts based on the apex and is created by transforming a CTDA with a pattern curve (CTDAcec). The fullness control point Z was standardized to the second contour line, and the bottom shape control point to the first contour line. For the top shape control point, the most suitable point among the 5th, 6th, and 7th contour lines was chosen for Models A, B, and C, while the 4th contour line was used for Model D.

The greatest difficulty in reconstructing the 6th arch is creating a curve that passes through all three control points (the fullness control point and the upper/lower shape control points). If these points are scattered and do not lie on a smooth curve, it is impossible to create a smooth reconstruction curve that passes through all of them. For example, a single shape control point might protrude significantly. If the positions of the reference points are uneven like this, a smooth arch passing through all points cannot exist. Even if a curve is forced to pass through all points, it will not be a smooth arch but a distorted shape.

Particularly for Models A, B, and C, as confirmed earlier, the arch surfaces are uneven. In this state, simply designating the first, second, and fourth contour lines as the respective control points makes reconstruction nearly impossible. Therefore, some adjustment is necessary when the original curve is not smooth.

In such cases, the position of the fullness control point (second contour line) is assumed to be accurate. Instead, the two shape control points must be chosen carefully so that the reconstruction curve matches the original as closely as possible. The top shape control point is selected from among the 3rd to 7th contour lines to find the one that produces the most natural curve. For the bottom shape control point, an attempt is first made with the first contour line. If curve generation is impossible, its height must be adjusted little by little to find the optimal position where a curve can be created.

Figures 39 through 42 show the reconstructed 6th arches along with the relevant points. Let's take the upper part of Model A's front as an example (Figure 39). This arch was reconstructed based on the second contour line (fullness control point), the first contour line (bottom shape control point), and the sixth contour line (top shape control point). The figure shows that, compared to the reconstructed curve, the fourth contour line and

the first arch position point are raised. Visually, the positions of these two points do not seem logical. If the raised fourth contour line had been used as the top shape control point instead of the sixth, the upper part of the reconstruction curve would have been bloated overall, increasing the difference from the original.

The lower part of Model B's back arch is also a good example (Figure 40). Initially, the 2nd, 1st, and 7th contour lines were used as the control points, but the curve generation failed because the position of the first contour line was too high. Therefore, after iteratively lowering the height of the bottom shape control point, a curve could finally be created only after a reduction of 0.4mm. The figure shows that the reconstruction curve passes below the first contour line. At the same time, the third and fourth contour lines are well below the reconstruction curve. This implies that either the position of the fullness control point is incorrect, or the positions of the 3rd and 4th contour lines might be incorrect. However, since it is currently impossible to know which is correct, the reconstruction proceeded according to the principle that the fullness control point is the second contour line.

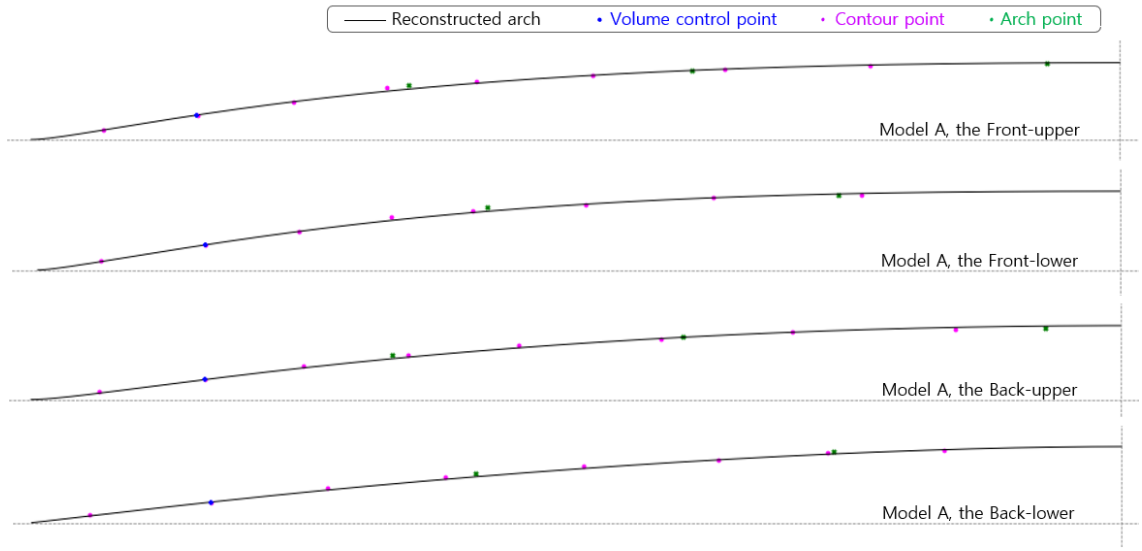

Figure 39: *Model A, 6th Arch: Model points and reconstruction curve (Front/Back, Upper/Lower parts)*

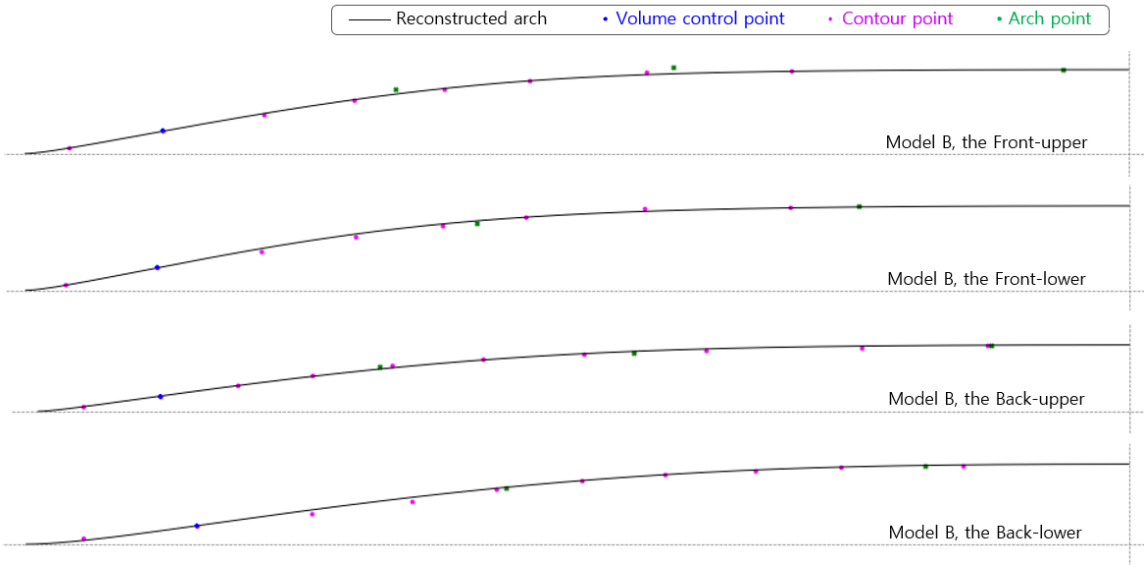

Figure 40: *Model B, 6th Arch: Model points and reconstruction curve (Front/Back, Upper/Lower parts)*

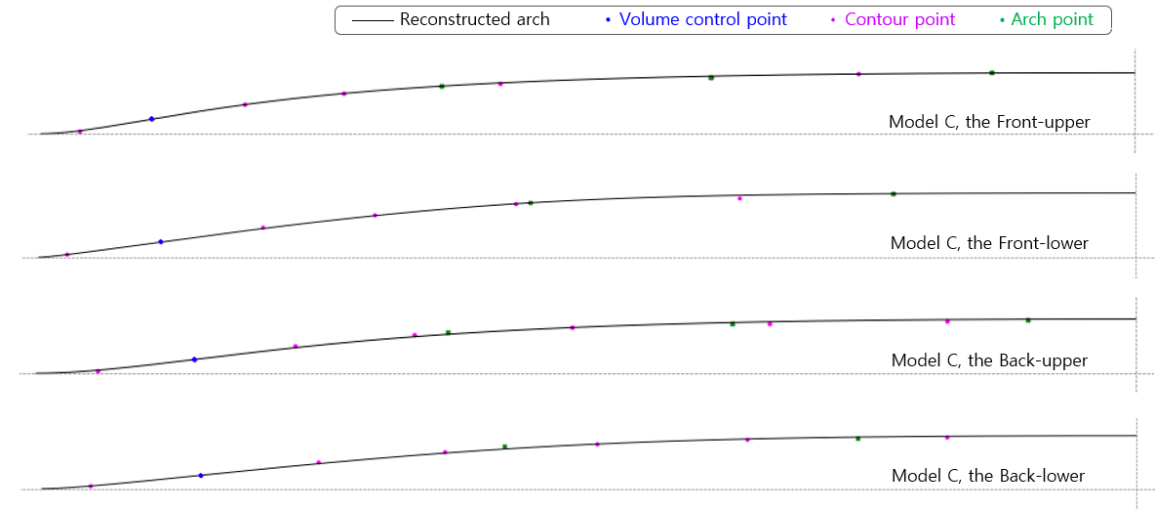

Figure 41: *Model C, 6th Arch: Model points and reconstruction curve (Front/Back, Upper/Lower parts)*

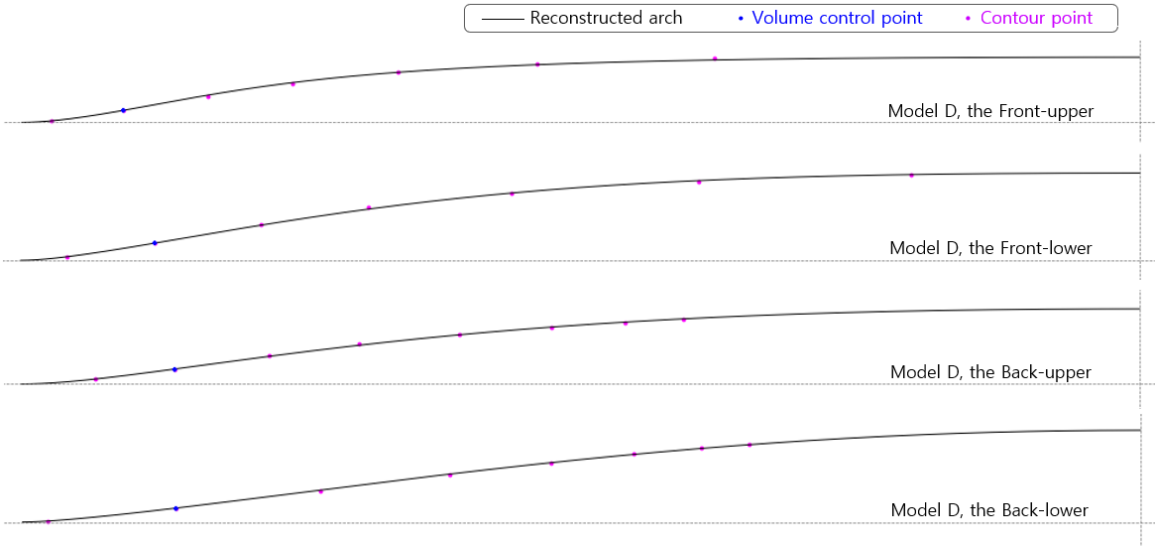

Figure 42: *Model D, 6th Arch: Model points and reconstruction curve (Front/Back, Upper/Lower parts)*

8.1 Reconstruction Results

Figures 43 through 54 show the final reconstruction results for all model arches.

Figure 43: *Model A, Front arches no. 1-5 reconstruction results* (*Left/Right*)

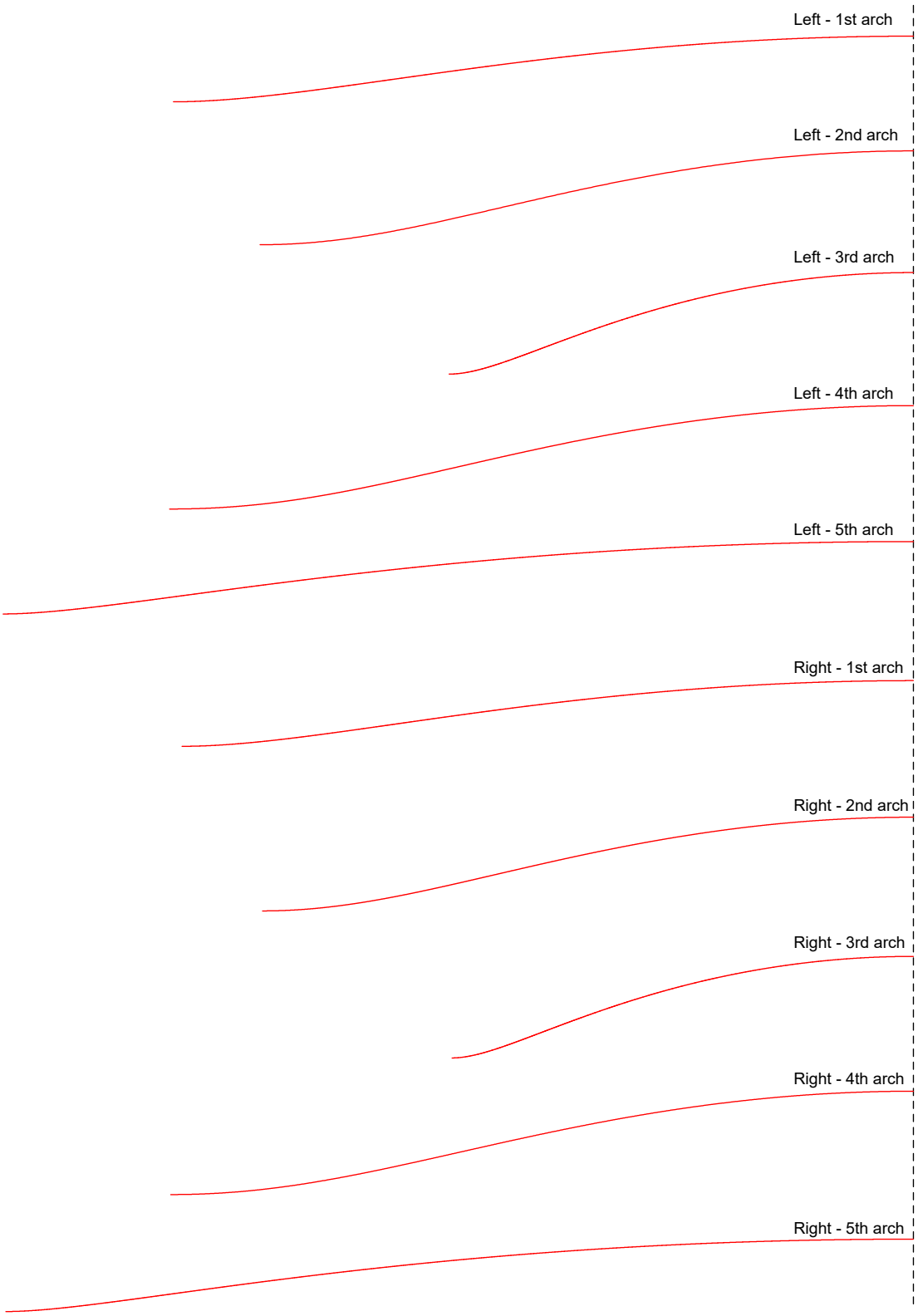

Figure 44: *Model A, Back arches no. 1-5 reconstruction results (Left/Right)*

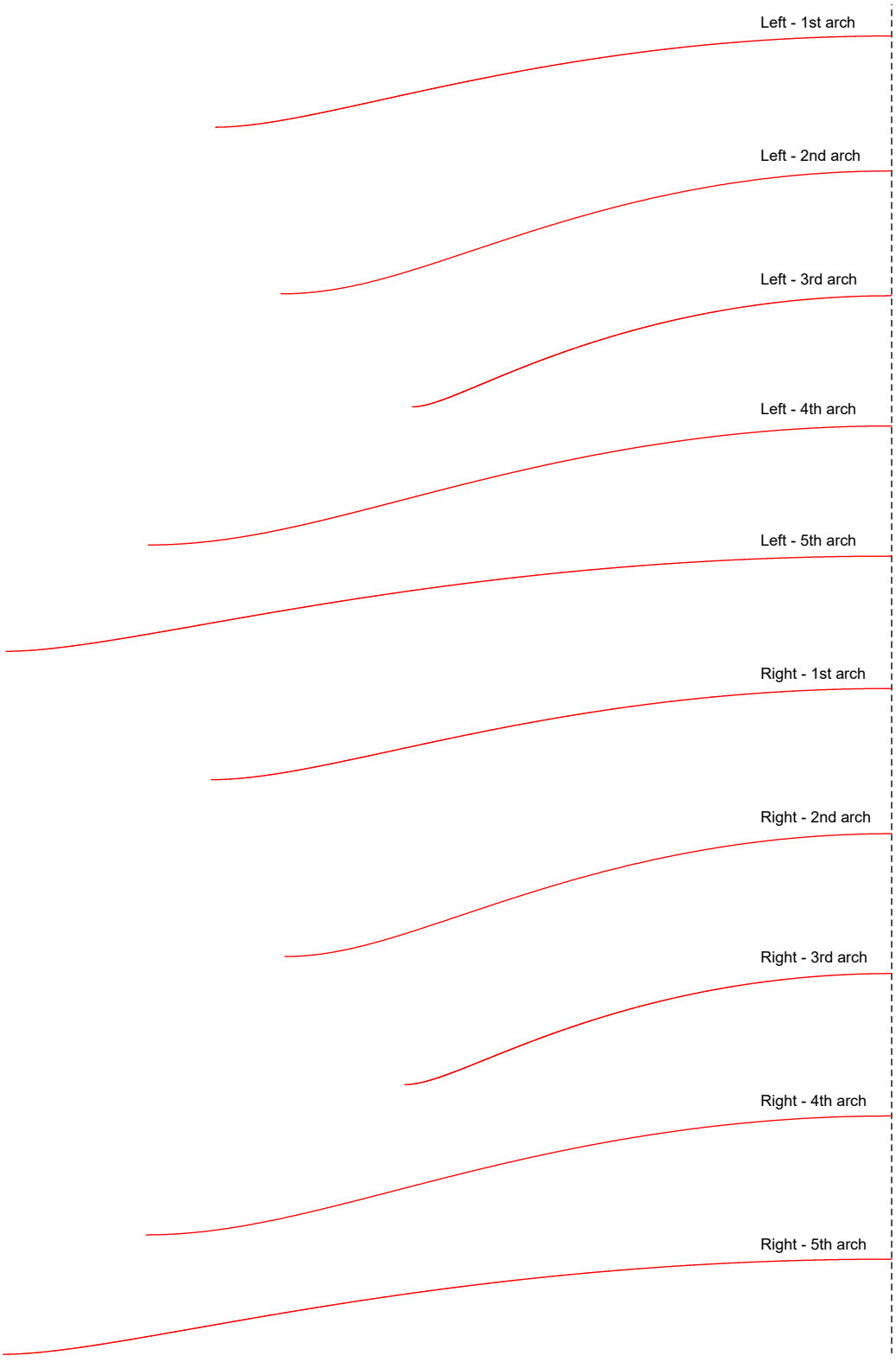

Figure 45: *Model B, Front arches no. 1-5 reconstruction results* (*Left/Right*)

Figure 46: *Model B, Back arches no. 1-5 reconstruction results (Left/Right)*

Figure 47: *Model C, Front arches no. 1-5 reconstruction results* (*Left/Right*)

Figure 48: *Model C, Back arches no. 1-5 reconstruction results* (*Left/Right*)

Figure 49: *Model D, Front arches no. 1-5 reconstruction results* (*Left/Right*)

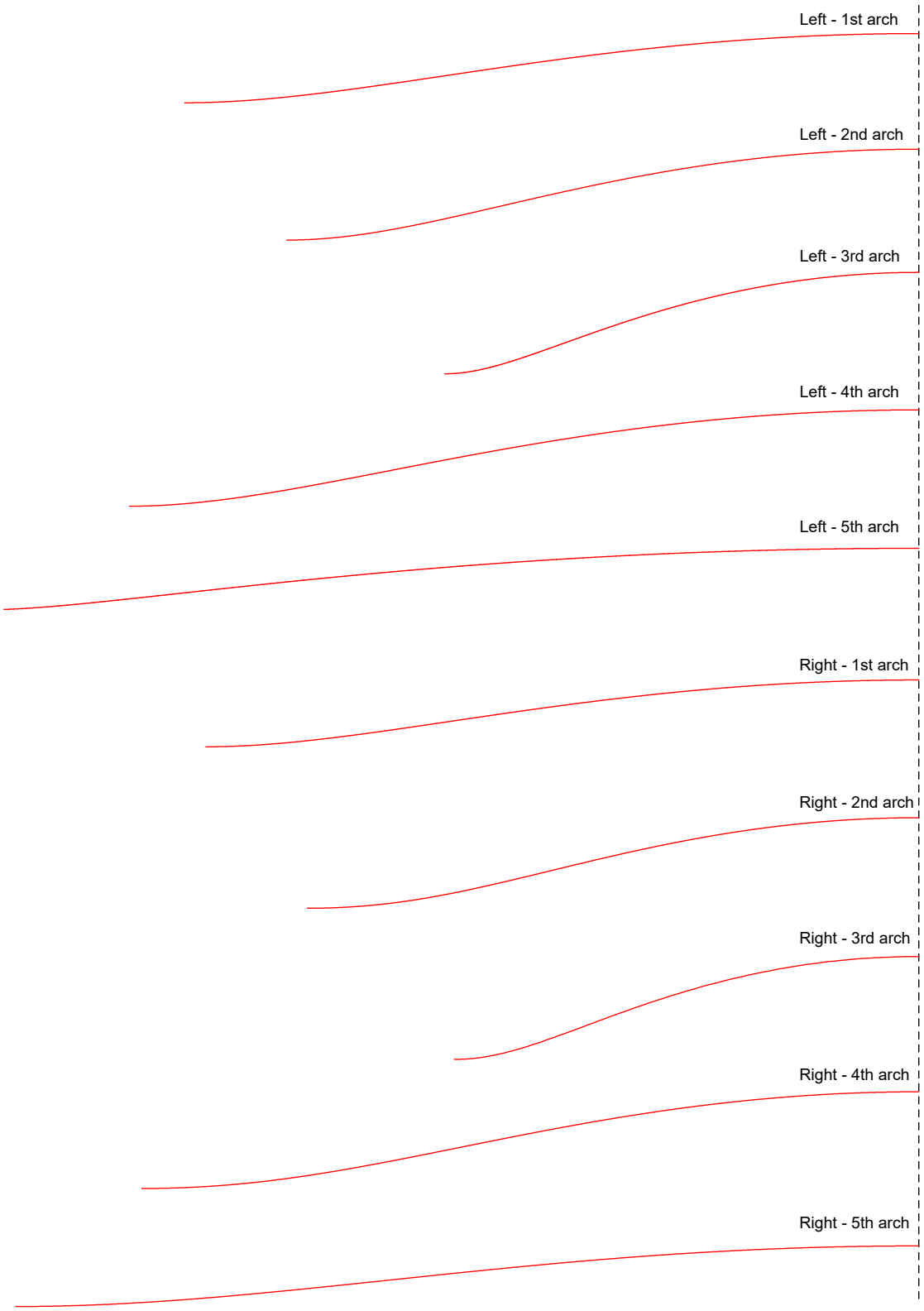

Figure 50: *Model D, Back arches no. 1-5 reconstruction results* (*Left/Right*)

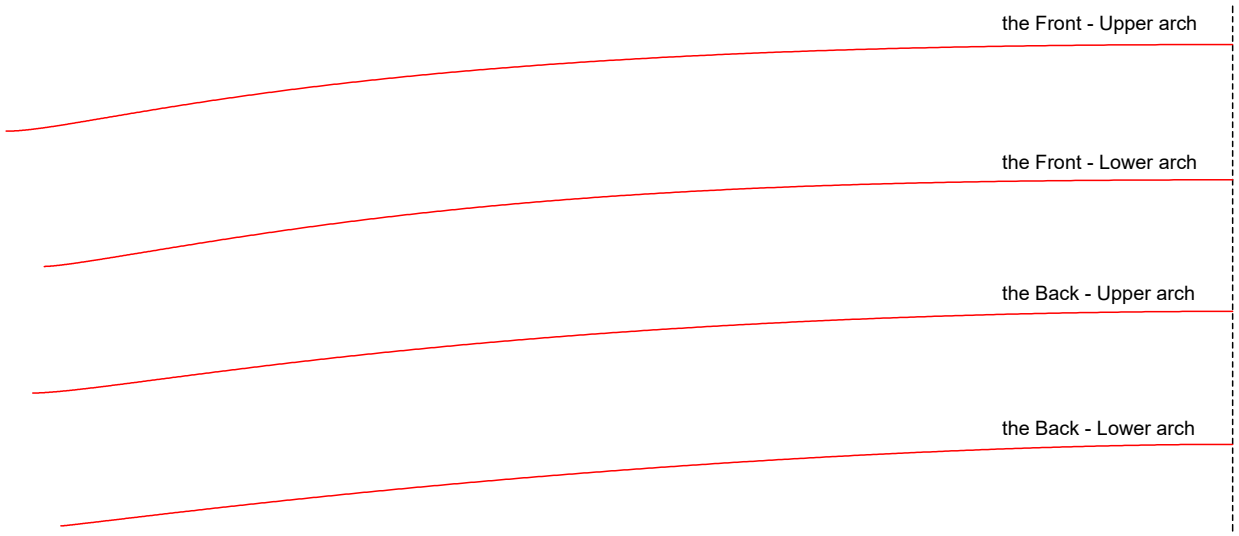

Figure 51: *Model A, 6th arch reconstruction results* (*Front/Back, Upper/Lower parts*)

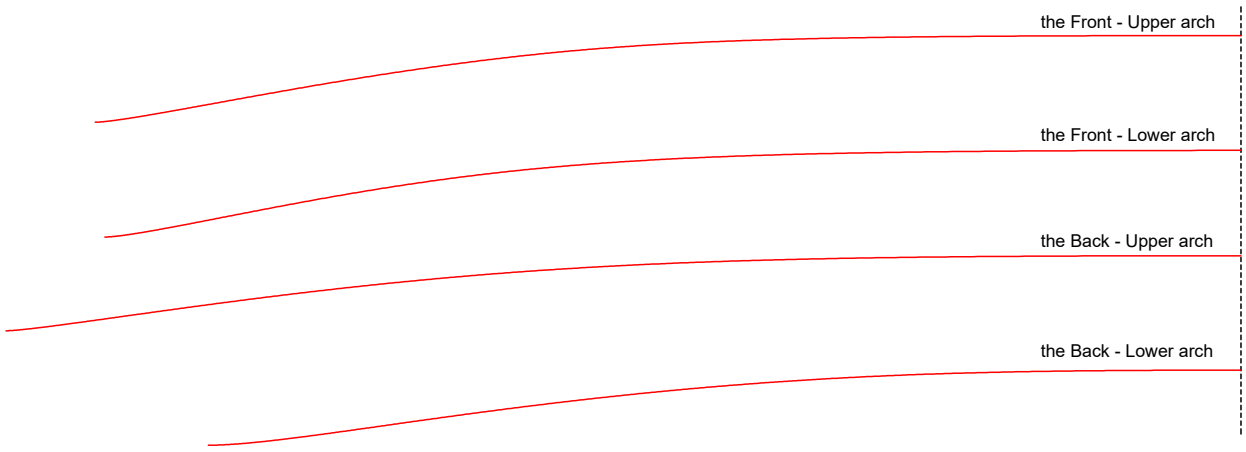

Figure 52: *Model B, 6th arch reconstruction results* (*Front/Back, Upper/Lower parts*)

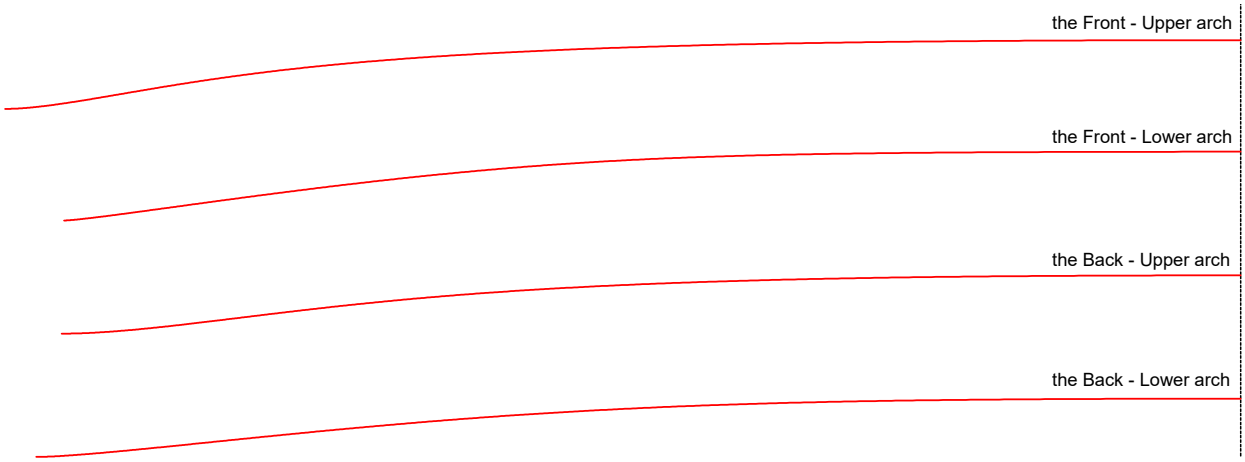

Figure 53: *Model C, 6th arch reconstruction results* (*Front/Back, Upper/Lower parts*)

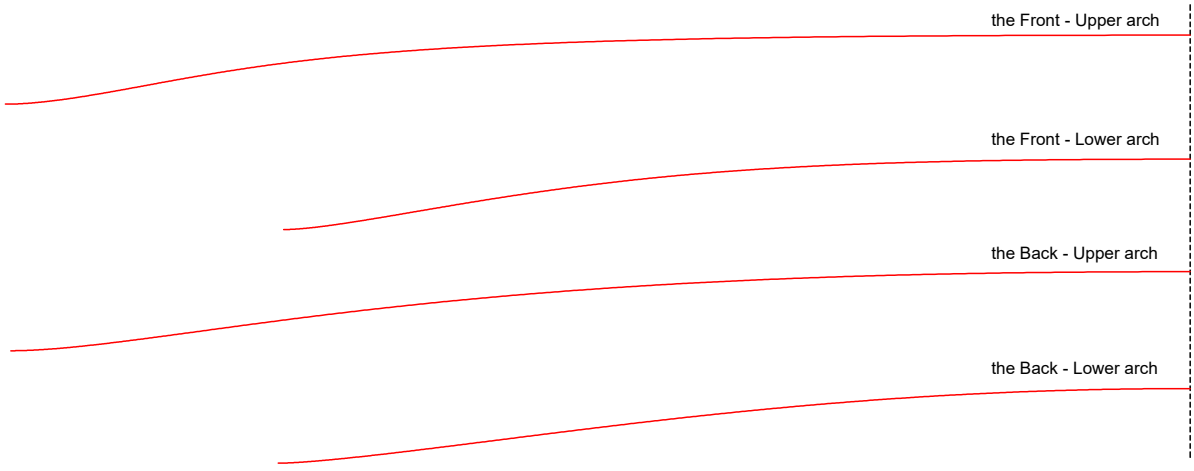

Figure 54: *Model D, 6th arch reconstruction results* (*Front/Back, Upper/Lower parts*)

8.2 Analysis of Results

This section will analyze and evaluate the reconstructed arches based on data from images, parameters, fullness, and errors. Through this analysis, this report will provide a more detailed understanding of the characteristics of the Stradivari arch and confirm the reliability of the reconstruction method.

8.2.1 Image Analysis

The figures below, from 55 to 66, show the reconstructed arches and the model arches superimposed. This report will visually compare these figures to analyze the characteristics by model and by location (e.g., 1st arch, 2nd arch). In the figures, the red line represents the reconstructed arch, and the black line represents the model arch.

By comparing the two arches, the unevenness and warping of the model arch become clearly visible, making it easy to identify the model's issues. Conversely, this also makes it easier to judge the reliability of the reconstructed arch. Most makers will likely be able to determine from this comparison alone whether the reconstruction curve can be used in actual instrument making.

* Model A - Front (Figure 55): In the model's 1st and 5th arches, the area near the first contour line is unnaturally raised, whereas the reconstructed arch shows a smooth curve. The central part of the model's 2nd arch protrudes, but the reconstructed arch is smooth. The model's 3rd arch has an issue of dropping sharply from the apex, but the reconstructed arch descends gently. For the 4th arch, the two curves are very similar, except that the central part of the model arch protrudes slightly.

* Model A - Back (Figure 56): Similar to the Front, the area near the first contour line of the model's 1st arch is unnaturally raised. The 3rd arch also shows a similar tendency to the Front. In the 2nd, 4th, and 5th arches, there are places where the model arch bulges slightly.

* Model B - Front (Figure 57): The two curves of the 1st arch are very similar. The central part of the model's 2nd arch is sharply sunken, while the reconstructed arch is smooth. In the 3rd arch, the upper part of the model protrudes and the lower part is sunken. In the 4th and 5th arches, the central part of the model sags over a wide area.

* Model B - Back (Figure 58): The central part of the model's 5th arch is unnaturally sunken. The reconstructed arch restores this part with a smooth curve. For the 3rd and 4th arches, the two curves are very similar.

* Model C - Front (Figure 59): Perhaps due to the larger size of the instrument, there are fewer irregularities compared to Models A and B. The two curves are very similar for the 1st, 2nd, 4th, and 5th arches, while the central part of the model's 3rd arch is slightly higher.

* Model C - Back (Figure 60): In all arches, the central part of the model arch is generally slightly higher. This

is noteworthy as it is not a local irregularity. This could be resolved by moving the fullness control point to the central area, but the control point location was not changed to maintain consistency in the reconstruction. This might be a unique characteristic of this instrument.

* Model D - Front (Figure 61): The error appears larger compared to other models, which is presumed to be due to plate warping caused by the sound post. Indeed, the upper parts of the left (bass bar side) arches are mostly lower, while the upper parts of the right (sound post side) arches are mostly higher. The shape at the time of making would have been an intermediate form of these two. If the reconstruction were based on the average curve of the left and right arches, the error would be much smaller.

* Model D - Back (Figure 62): The back also shows distortion due to the sound post, but the 1st and 2nd arches are exceptions where the two curves almost coincide. This seems to be because the corresponding area of the Back is stiffer and less affected by structural forces than the Front. In other models as well, the 1st and 2nd arches of the Back tend to show more similarity between the model and the reconstruction curve compared to other areas.

* 6th Arch (Figure 63∼66): Models A, B, and C have many irregularities in the original, but the reconstructed arch smoothly corrects them. In contrast, for Model D, which was created from a CT scan, the original and reconstructed arches are very similar. This indicates that if the original data is accurate, this reconstruction method demonstrates very high accuracy. Particularly for Model A, as seen in Figure 39, it can be confirmed that the 1st and 5th arches of the model are noticeably raised.

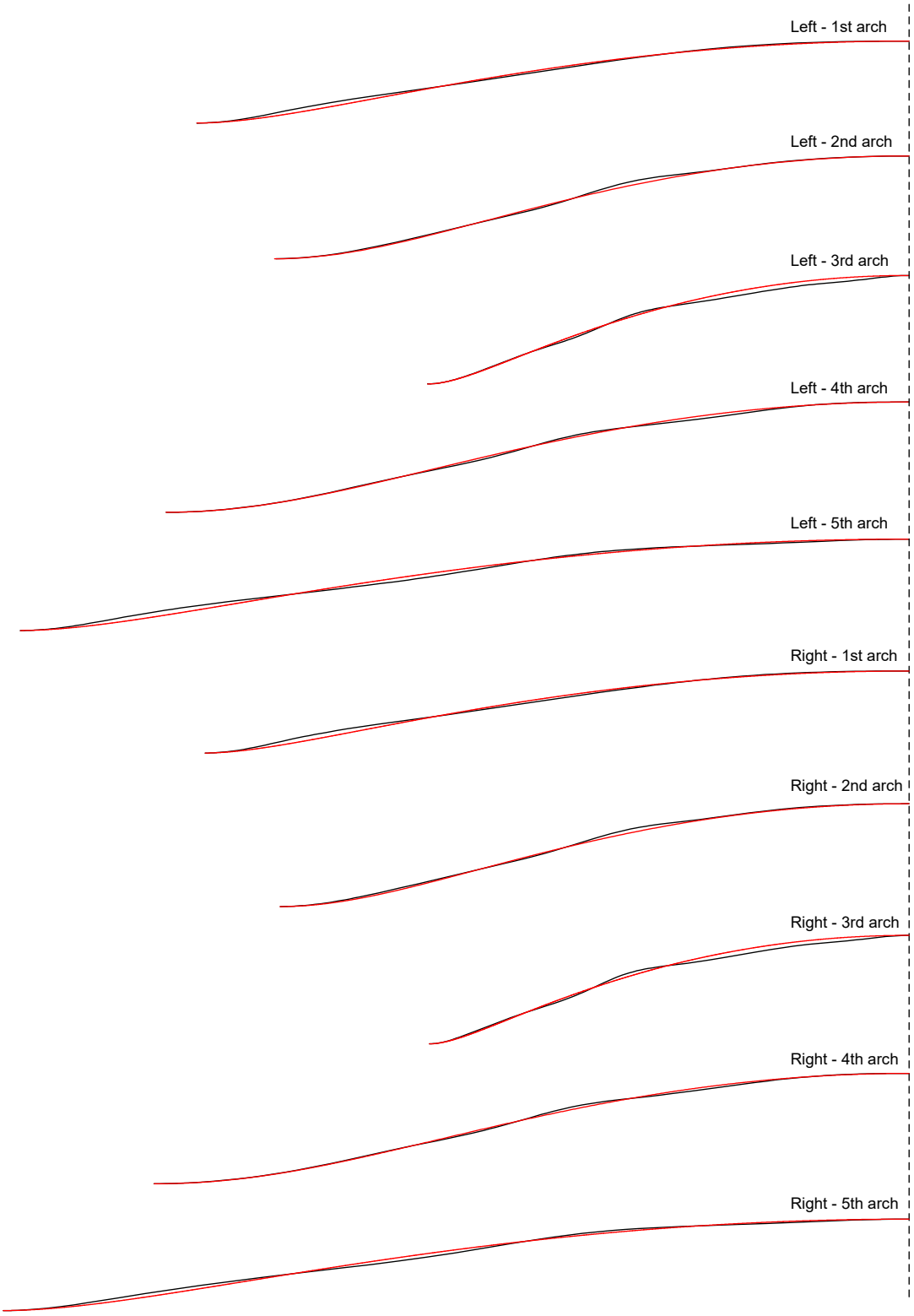

Figure 55: *Model A, Front arches no. 1-5: Comparison of reconstruction curve(red) and model curve(black), (Left/Right)*

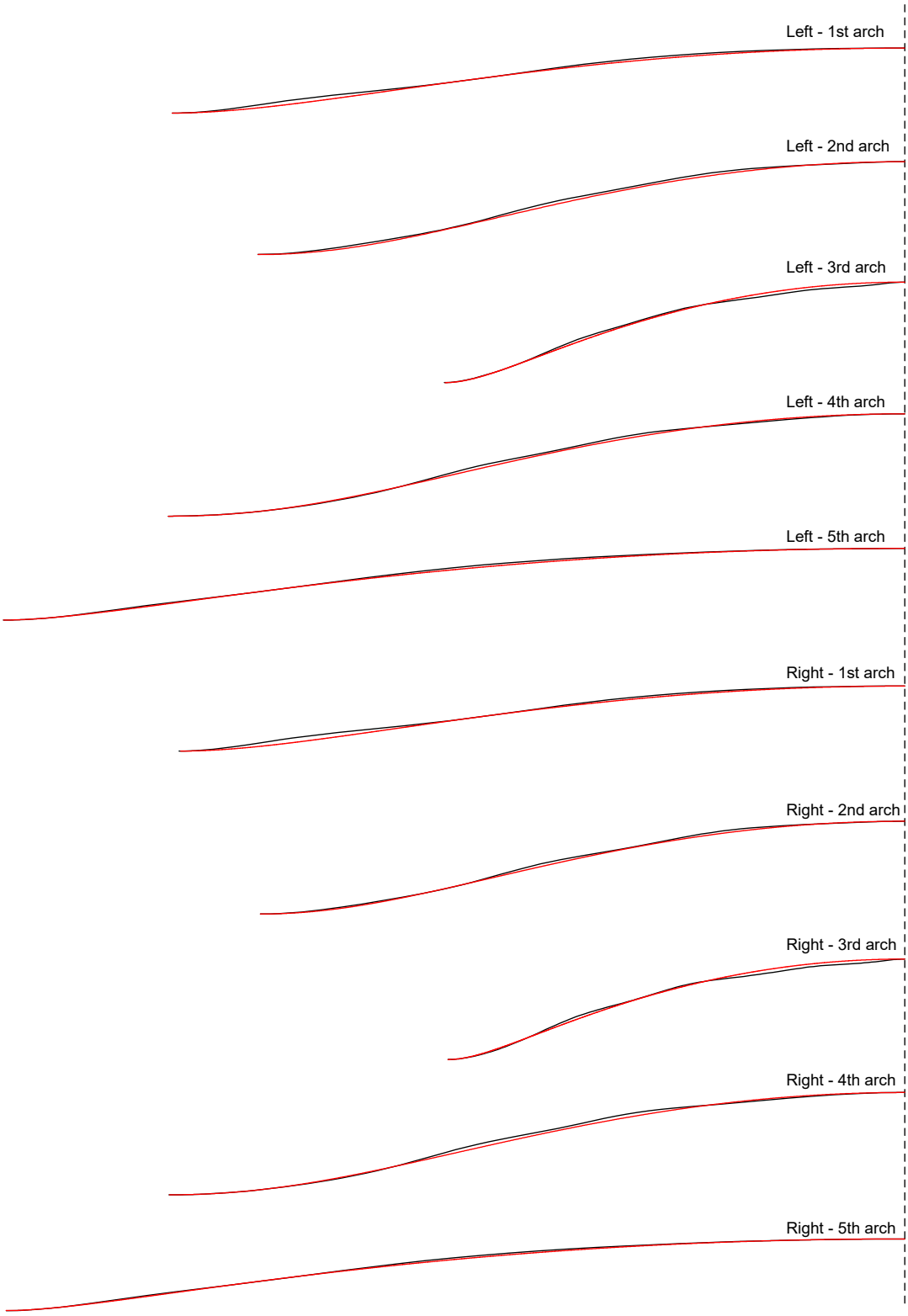

Figure 56: *Model A, Back arches no. 1-5: Comparison of reconstruction curve(red) and model curve(black), (Left/Right)*

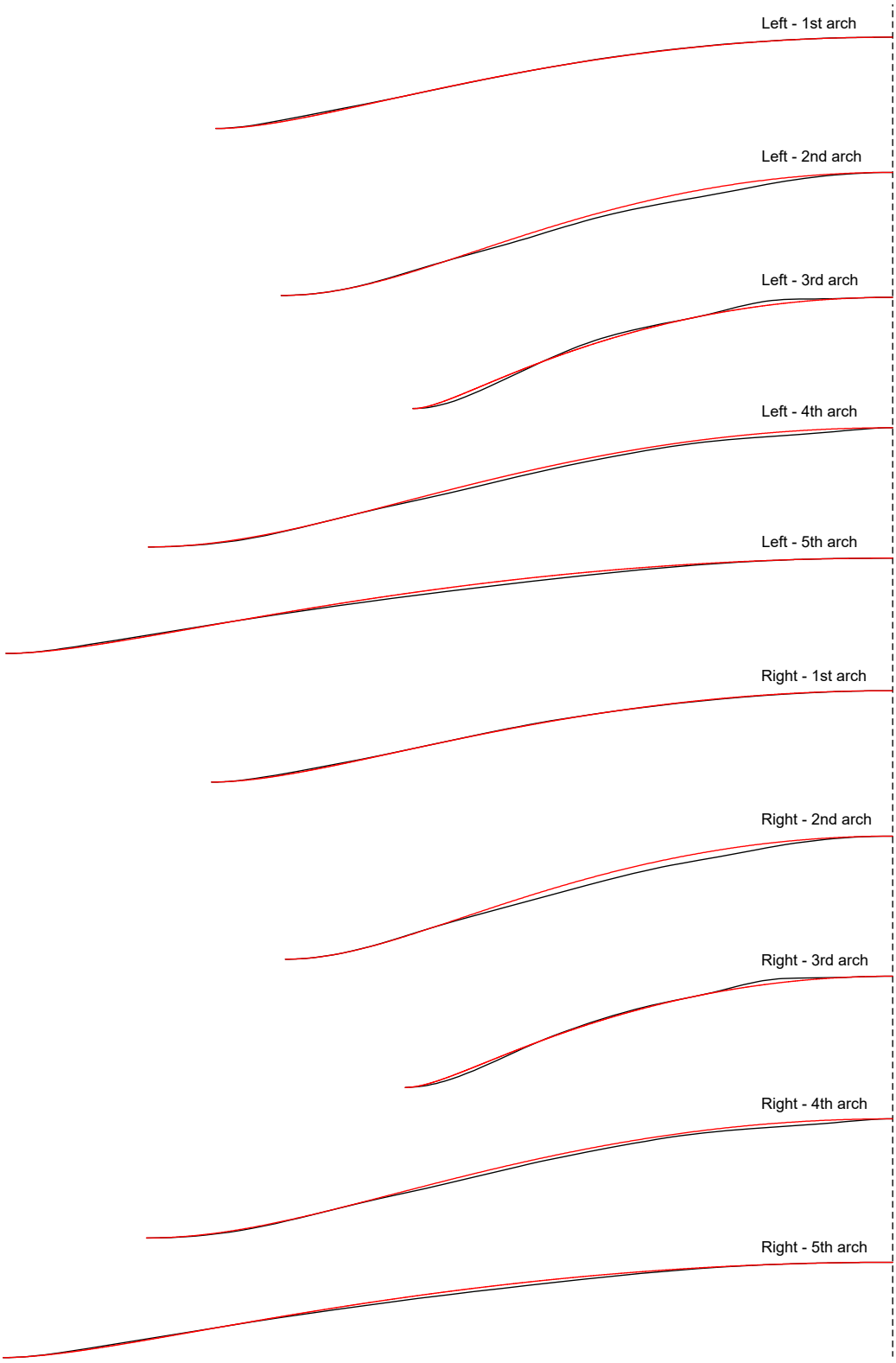

Figure 57: *Model B, Front arches no. 1-5: Comparison of reconstruction curve(red) and model curve(black), (Left/Right)*

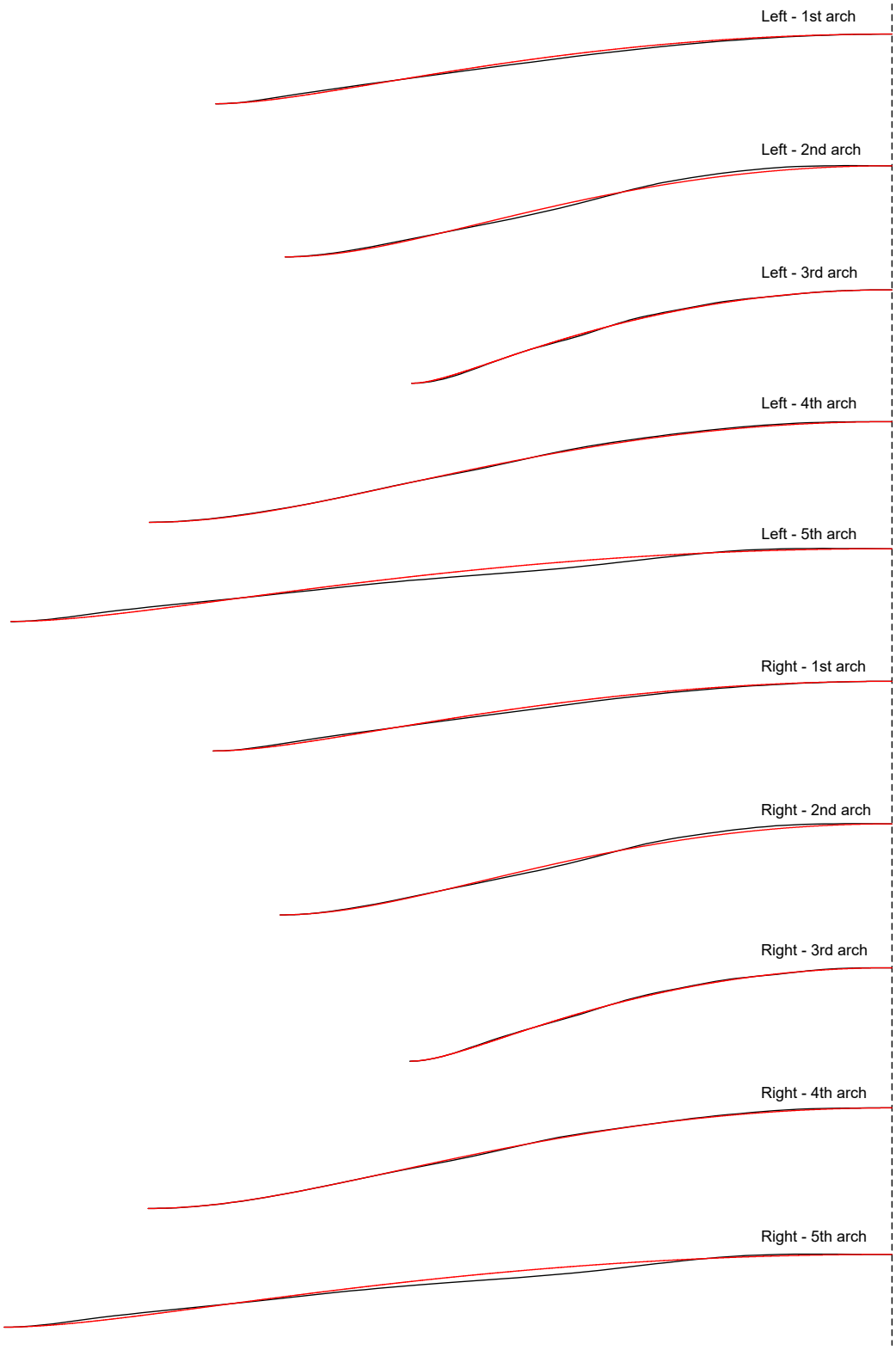

Figure 58: *Model B, Back arches no. 1-5: Comparison of reconstruction curve(red) and model curve(black), (Left/Right)*

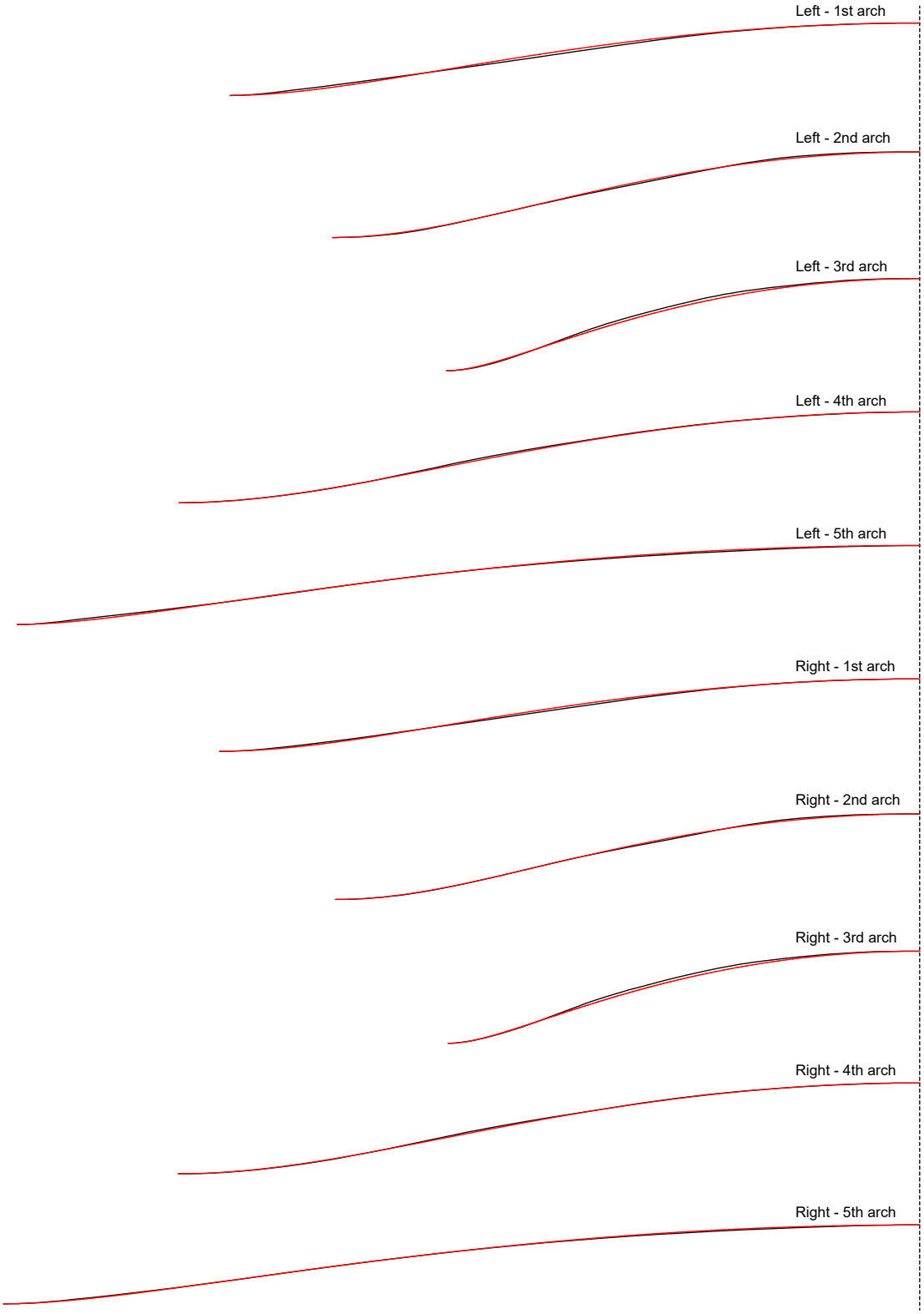

Figure 59: *Model C, Front arches no. 1-5: Comparison of reconstruction curve(red) and model curve(black), (Left/Right)*

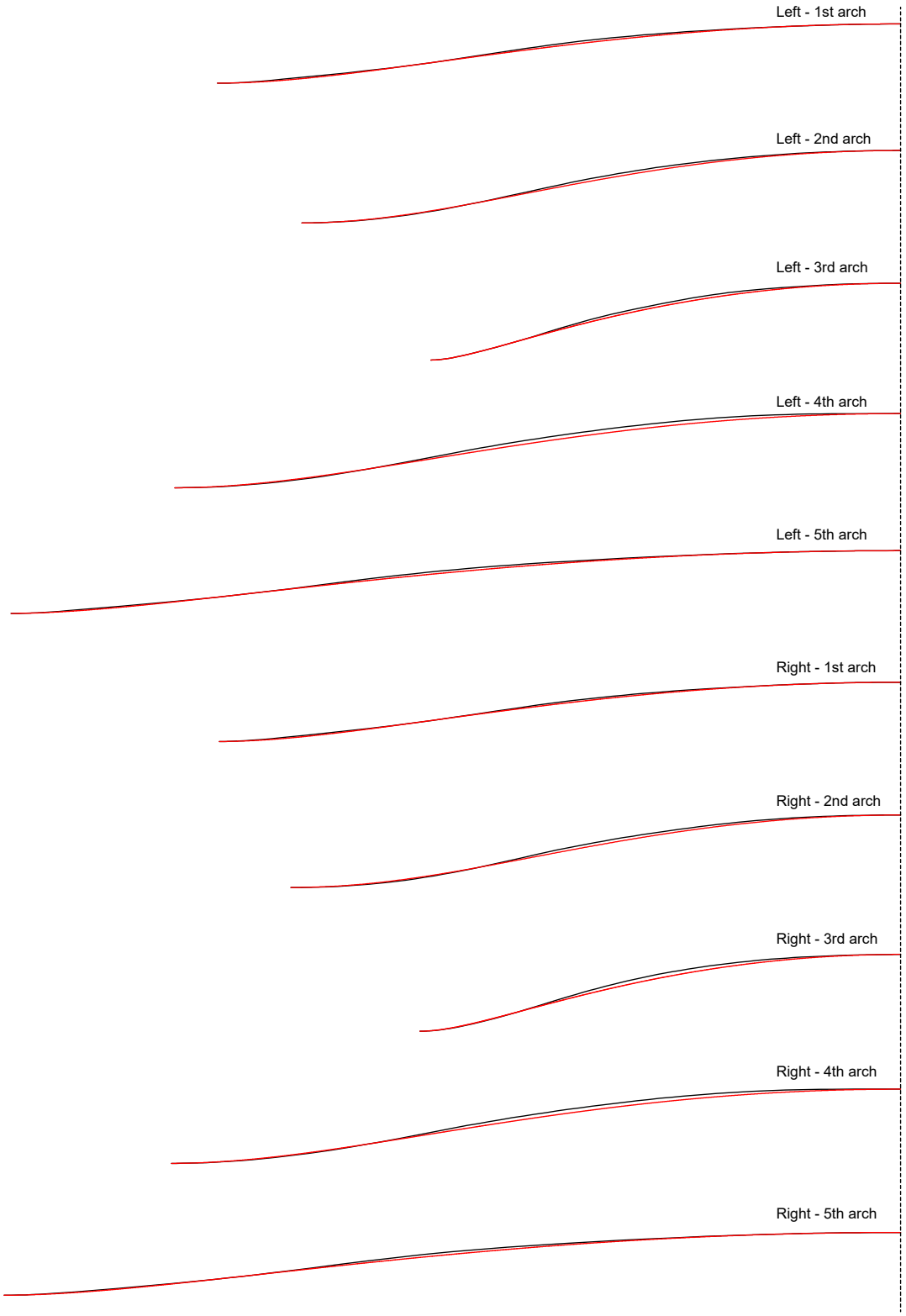

Figure 60: *Model C, Back arches no. 1-5: Comparison of reconstruction curve(red) and model curve(black), (Left/Right)*

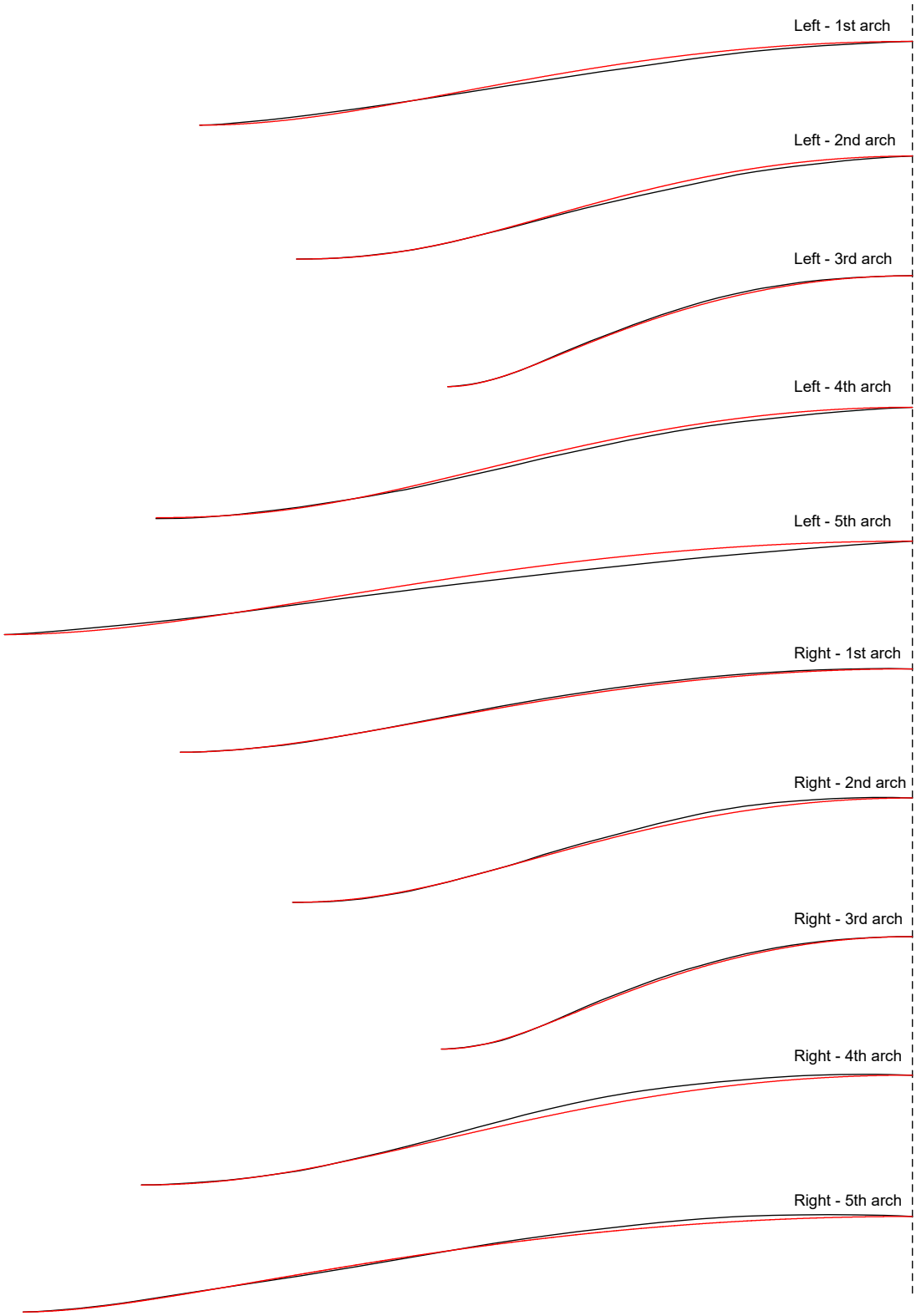

Figure 61: *Model D, Front arches no. 1-5: Comparison of reconstruction curve(red) and model curve(black), (Left/Right)*

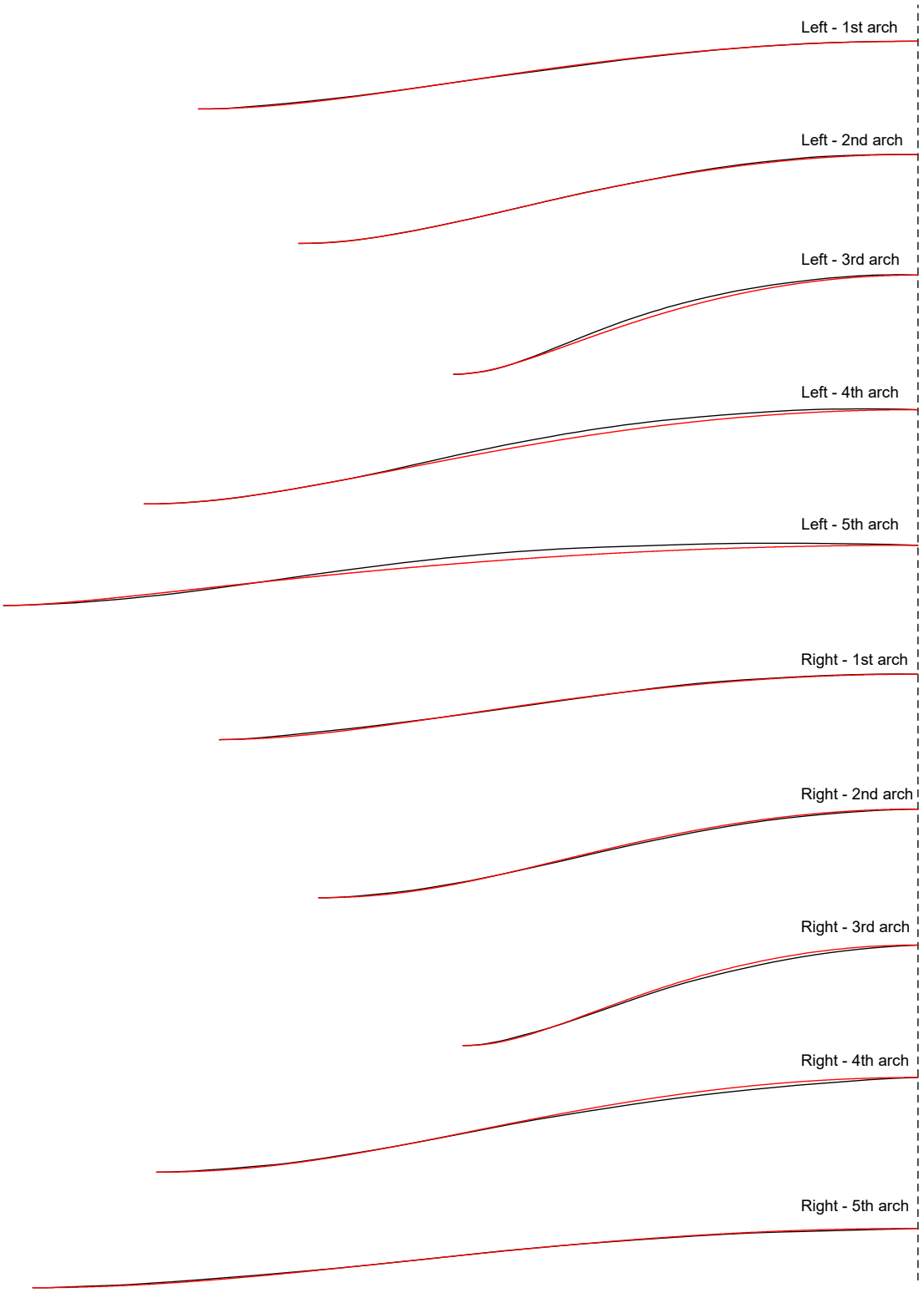

Figure 62: *Model D, Back arches no. 1-5: Comparison of reconstruction curve(red) and model curve(black), (Left/Right)*

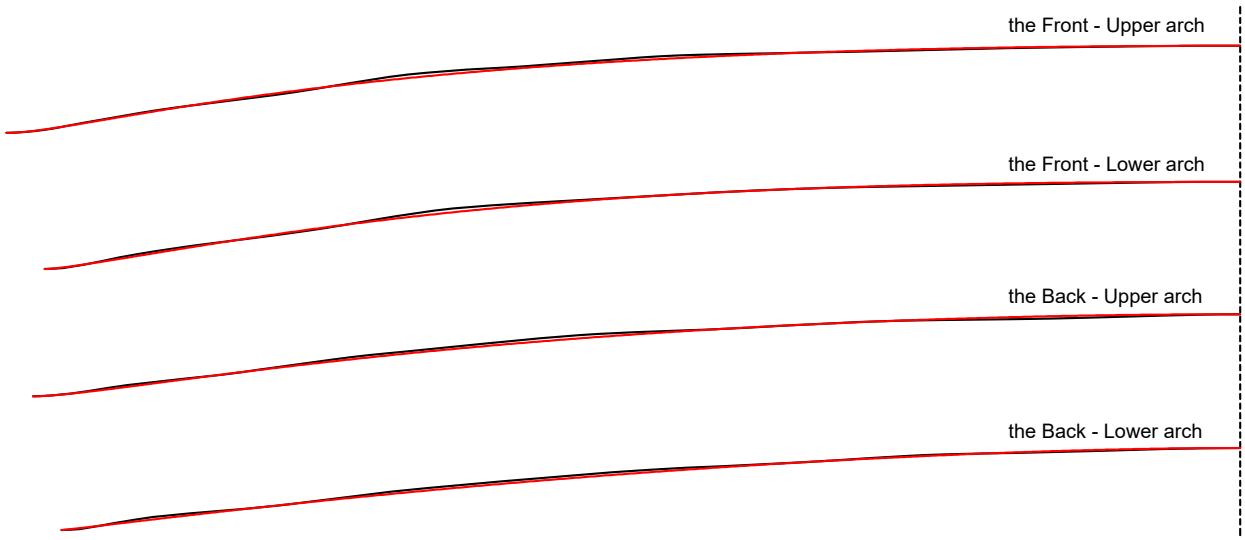

Figure 63: *Model A, 6th arch: Comparison of reconstruction curve(red) and model curve(black), (Front/Back, Upper/Lower parts)*

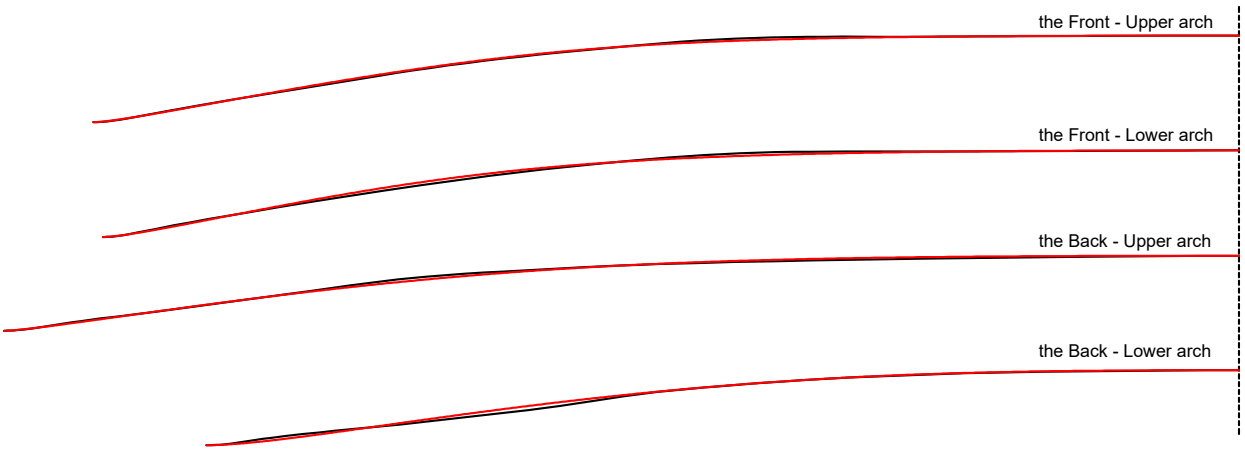

Figure 64: *Model B, 6th arch: Comparison of reconstruction curve(red) and model curve(black), (Front/Back, Upper/Lower parts)*

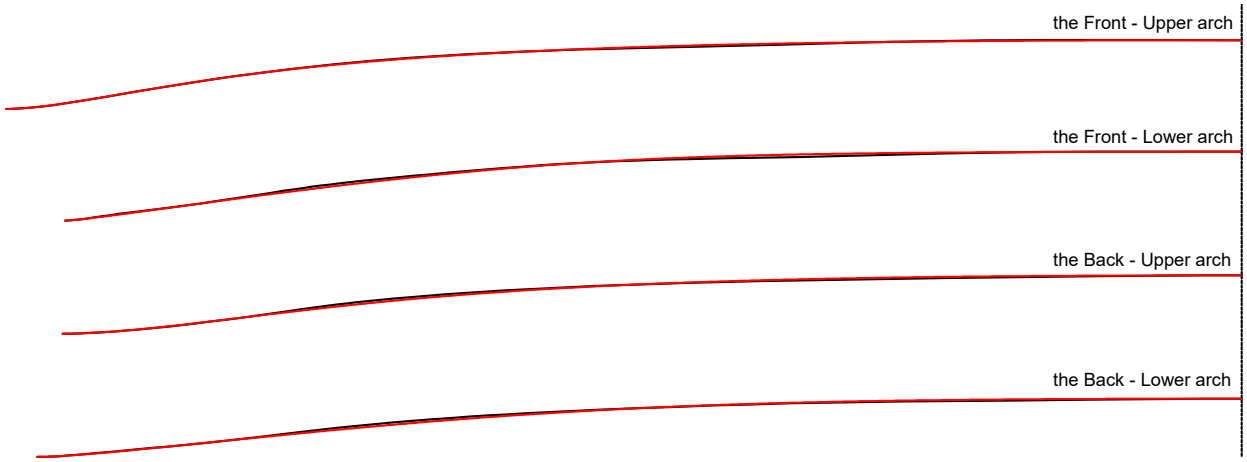

Figure 65: *Model C, 6th arch: Comparison of reconstruction curve(red) and model curve(black), (Front/Back, Upper/Lower parts)*

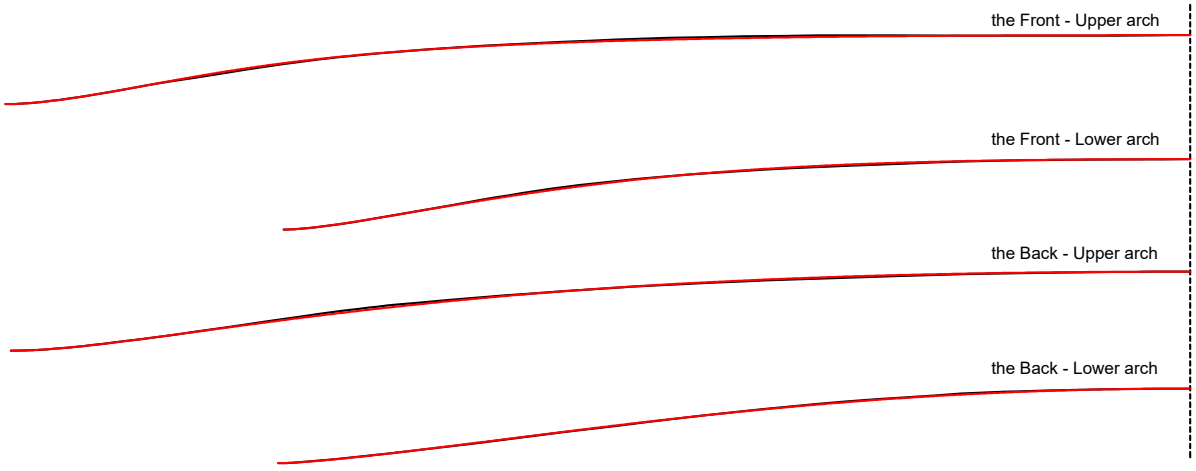

Figure 66: *Model D, 6th arch: Comparison of reconstruction curve(red) and model curve(black), (Front/Back, Upper/Lower parts)*

8.2.2 Parameter Analysis

The parameters of the reconstructed arch are indicators of its shape and character. By analyzing these parameters, we can identify the characteristics of the Stradivari arch and even classify and systematize the arches by shape.

Table 5 shows the parameter values for the 6th arches. Since all 6th arches are of the CTDAcec type, the Type column has been omitted. The meaning of each parameter is as follows.

expo is the exponent value that concentrates the cubic polynomial curve to the left or right. A positive value $+$ concentrates it to the left (towards the arch endpoint), while a negative value $-$ concentrates it to the right (towards the arch apex). The table shows that most values are positive $+$, indicating that the cubic polynomial curve is mainly concentrated to the left. This means the slope becomes steeper towards the arch endpoint, and a larger absolute value indicates a more pronounced effect. However, the effect of expo is proportional to the amplitude of the cubic polynomial curve (bamp), so if the amplitude is close to 0, the influence of the expo value is also negligible.

bamp indicates the amplitude and handle direction of the cubic polynomial curve. The symbol $-$ means the handle is on the left (towards the arch endpoint), while no symbol means it is on the right. The number itself always represents the magnitude of the (negative) amplitude. For example, bamp $= -7.313$ means the handle is on the left with an amplitude of -7.313, and bamp $= 25.272$ means the handle is on the right with an amplitude of -25.272. The table shows that most have a $-$ sign, indicating that the handle is mainly located on the left.

camp and *pamp* represent the amplitude of the catenary curve and the final pattern curve (sum of the two curves), respectively. Unlike bamp, the sign here indicates the actual sign of the value. For example, camp $= -31.683$ means the amplitude is negative (convex downwards), while camp $= 2.123$ means the amplitude is positive (convex upwards). Since camp and pamp do not have the concept of a handle, the minus sign $(-)$ indicates the actual amplitude, and the values for both are almost always negative (convex downwards). Generally, the absolute values of these amplitudes tend to be proportional to the size of the instrument.

d-diff and *u-diff* represent the error with the bottom and top shape control points, respectively. They have a maximum value of ± 0.001, and 0.000 in the table means the error is less than 0.0005.

The tolerance was set to reduce calculation time and increase the success rate. It refers to the error in the arch's width (from one endpoint to the apex), height, and the distance to the fullness control point Z. Since the approximation curves CTDAce and CTDAice allow for very precise calculations, the tolerance was set to 1e-9, which can be considered almost no error.

Among the shape control points, the bottom control point was based on CP1 (first contour point), but its y-

coordinate was partially modified if curve generation was impossible. The top control point was selected from the most suitable points among CP4 to CP7. The table shows that the coordinates of the bottom shape control point were modified for a significant number of arches, which suggests that the data for the first contour line of the original models might be inaccurate.

Model	Plate	Side	expo	bamp	camp	pamp	d-diff	u-diff	tolerance	Shape control point
A	Front	Upper	-0.613	-7.313	-31.683	-38.720	0.001	0.000	0.001	CP1, CP6
		Lower	1.400	-5.450	-34.108	-37.083	0.000	0.000	0.001	CP1 (y:-0.2), CP6
	Back	Upper	0.613	14.781	-14.435	-28.922	0.001	0.001	0.001	CP1 (y:-0.2), CP6
		Lower	0.114	25.272	-0.095	-25.358	0.001	0.001	0.001	CP1 (y:-0.2), CP6
B	Front	Upper	2.259	-28.288	-40.044	-55.495	-0.001	-0.001	0.001	CP1, CP6
		Lower	1.725	-26.375	-39.475	-56.240	0.000	-0.001	0.001	CP1 (y:-0.1), CP6
	Back	Upper	2.113	-20.238	-44.137	-53.806	-0.001	-0.001	0.001	CP1 (y:-0.1), CP7
		Lower	2.881	-8.822	-28.292	-30.537	-0.001	0.000	0.001	CP1 (y:-0.4), CP7
C	Front	Upper	0.472	-53.484	-68.319	-114.736	0.000	-0.001	0.001	CP1, CP5
		Lower	2.395	-47.717	-75.858	-99.146	-0.001	-0.001	0.001	CP1 (y:-0.1), CP5
	Back	Upper	0.556	-39.756	-55.440	-89.199	-0.001	0.001	0.001	CP1, CP5
		Lower	1.875	-27.800	-67.709	-82.027	-0.001	0.000	0.001	CP1 (y:-0.1), CP5
D	Front	Upper	0.750	-33.550	-33.083	-61.701	0.000	0.000	0.001	CP1, CP4
		Lower	1.300	-9.850	-25.149	-31.493	0.000	0.000	0.001	CP1, CP4
	Back	Upper	0.038	-5.913	-29.014	-34.157	0.001	0.000	0.001	CP1, CP4
		Lower	-0.888	6.745	-9.072	-14.478	0.001	0.000	0.001	CP1, CP4

Table 5: *Detailed parameters by model for the 6th arch. Type:CTDAcec, expo:Exponent of distorted cubic polynomial curve (+:left, −:right), bamp:Cubic polynomial curve amplitude and handle direction, camp:Catenary curve amplitude, pamp:Final pattern curve amplitude, d-diff/u-diff:Error with bottom/top shape control point, tolerance:Calculation tolerance for distance to shape and fullness control points, Shape control point:Information on top/bottom shape control points.*

For arches no. 1-5, most are of the CHTA type, which has greater fullness than a CTDA. Only a few arches were reconstructed as CETA or CTDAice types, which have less fullness than a CTDA. Approximation curves that do not have an R value, such as nCHTAce or nCETAice, have pattern curve parameters like amplitude (camp) and exponent value (expo).

Tables 6 and 7 summarize the parameters for arches no. 1-5. A noteworthy point here is that the CETA and CTDAice types (marked with *), which have less fullness than a CTDA, are mostly concentrated in the 2nd and 4th arches. Even for the 2nd and 4th arches that are CHTA types, their R values are exceptionally large compared to other arches. A large R value means the curve is close to a CTDA, i.e., its fullness is only slightly greater than that of a CTDA. In conclusion, the parameters clearly show a tendency for the 2nd and 4th arches to have less fullness compared to other arches.

On the other hand, the approximation curves that exceed the limits of trochoids (nCHTAce) are concentrated in

the 5th arch. The 5th arches that are CHTA types, not nCHTAce, also tend to have smaller R values compared to other arches. This means that the 5th arch has greater fullness compared to other arches.

The analysis so far can be summarized as the 2nd and 4th arches have less fullness, and the 5th arch has greater fullness. However, there is one problem with this: it is not logical to directly compare the fullness of arches with different widths and heights. The next section will address this problem and explain a method for objectively comparing the fullness of arches with different widths and heights.

Model	Plate	Side	Arch N.	Type	R	r	d	camp	expo	tolerance
A	Front	BB(L)	1	CHTA	176.447	30.845	15.192	-	-	0.010
			2	CHTA	10688.846	21.496	5.560	-	-	0.010
			3	CHTA	159.219	18.082	10.368	-	-	0.010
			4	*CTDAice	-	25.086	5.850	0.155	-2.034	1E-09
			5	CHTA	184.145	39.783	21.924	-	-	0.010
		SP(R)	1	CHTA	138.488	30.733	18.188	-	-	0.010
			2	CHTA	886.691	22.525	6.785	-	-	0.010
			3	CHTA	129.913	18.195	11.458	-	-	0.010
			4	*CETA	1939.080	24.277	5.065	-	-	0.010
			5	CHTA	217.751	40.452	19.656	-	-	0.010
	Back	SP(L)	1	CHTA	215.423	32.714	12.978	-	-	0.010
			2	*CETA	3644.551	21.072	4.548	-	-	0.010
			3	CHTA	178.081	16.934	8.878	-	-	0.010
			4	*CTDAice	-	24.513	5.350	1.326	-2.667	1E-09
			5	nCHTAce	167.144	42.118	24.265	-2.663	-0.811	0.010
		BB(R)	1	CHTA	202.089	32.382	13.420	-	-	0.010
			2	*CTDAice	-	21.451	4.850	0.015	-2.270	1E-09
			3	CHTA	160.507	16.909	9.252	-	-	0.010
			4	*CETA	1511.957	22.912	4.433	-	-	0.010
			5	nCHTAce	166.468	41.972	24.214	-3.600	-0.817	0.010
B	Front	BB(L)	1	CHTA	212.206	33.539	16.695	-	-	0.012
			2	*CETA	3239.278	24.081	7.296	-	-	0.012
			3	CHTA	136.848	21.652	14.691	-	-	0.012
			4	CTDAce	-	29.835	7.500	-0.198	-1.083	1E-09
			5	CHTA	189.793	46.840	29.330	-	-	0.012
		SP(R)	1	CHTA	267.250	33.225	14.322	-	-	0.012
			2	CHTA	2051.964	24.931	8.476	-	-	0.012
			3	CHTA	161.254	21.893	13.667	-	-	0.012
			4	CHTA	3322.583	30.652	8.176	-	-	0.012
			5	CHTA	185.660	47.028	30.081	-	-	0.012
	Back	SP(L)	1	CHTA	161.819	36.062	20.395	-	-	0.012
			2	CHTA	820.860	26.379	7.691	-	-	0.012
			3	CHTA	128.945	22.464	14.458	-	-	0.012
			4	CHTA	1431.019	31.890	7.995	-	-	0.012
			5	nCHTAce	192.764	49.308	29.156	-0.139	-0.889	0.012
		BB(R)	1	CHTA	167.752	36.198	19.911	-	-	0.012
			2	CHTA	991.802	26.340	7.360	-	-	0.012
			3	CHTA	151.718	22.338	13.093	-	-	0.012
			4	CHTA	1060.475	32.554	8.616	-	-	0.012
			5	nCHTAce	196.804	49.781	29.058	-0.849	-0.959	0.012

Table 6: *Detailed Parameters by Model for Arches No. 1-5 (1/2). Type:Type of reconstruction curve, R/r/d:Trochoid parameters, camp:Catenary curve amplitude, expo:Exponent of exponentially distorted catenary, tolerance:Calculation tolerance for arch width, height, and distance to fullness control point, *:Curve with less fullness than a CTDA.*

Model	Plate	Side	Arch N.	Type	R	r	d	camp	expo	tolerance
C	Front	SP(L)	1	CHTA	627.959	62.470	20.796	-	-	0.020
			2	CHTA	4318.054	43.962	10.818	-	-	0.020
			3	CHTA	316.263	39.224	21.179	-	-	0.020
			4	CHTA	2945.004	57.413	12.935	-	-	0.020
			5	nCHTAce	353.728	90.060	54.001	-0.796	-1.031	0.020
		BB(R)	1	CHTA	841.556	61.674	17.558	-	-	0.020
			2	CHTA	5781.621	43.373	10.536	-	-	0.020
			3	CHTA	314.605	39.085	21.169	-	-	0.020
			4	CHTA	3217.281	57.201	12.712	-	-	0.020
			5	CHTA	383.803	91.717	51.661	-	-	0.020
	Back	BB(L)	1	CHTA	643.186	64.150	19.267	-	-	0.020
			2	CHTA	4887.919	44.934	9.231	-	-	0.020
			3	CHTA	204.809	41.106	26.342	-	-	0.020
			4	CHTA	1442.634	60.568	13.923	-	-	0.020
			5	nCHTAce	380.492	93.017	50.206	-0.186	-0.877	0.020
		SP(R)	1	CHTA	516.159	65.516	22.815	-	-	0.020
			2	*CETA	5764.898	42.643	7.444	-	-	0.020
			3	CHTA	265.716	41.726	22.650	-	-	0.020
			4	CHTA	1375.980	61.202	14.278	-	-	0.020
			5	CHTA	428.348	93.818	45.638	-	-	0.020
D	Front	BB(L)	1	CHTA	1661.465	25.504	5.362	-	-	0.010
			2	*CETA	487.376	17.645	3.628	-	-	0.010
			3	CHTA	813.161	16.167	6.660	-	-	0.010
			4	*nCETAice	687.004	21.594	3.899	0.037	-1.901	0.010
			5	CHTA	886.179	35.128	7.975	-	-	0.010
		SP(R)	1	CHTA	601.170	28.397	7.329	-	-	0.010
			2	*CETA	738.275	19.014	4.213	-	-	0.010
			3	*CETA	1018.819	15.473	5.377	-	-	0.010
			4	*CETA	1527.610	24.364	4.809	-	-	0.010
			5	CHTA	216.966	39.200	19.164	-	-	0.010
	Back	SP(L)	1	CHTA	598.251	28.653	6.487	-	-	0.010
			2	CHTA	1499.270	21.831	5.474	-	-	0.010
			3	CHTA	414.510	16.643	6.825	-	-	0.010
			4	CHTA	635.787	29.673	8.026	-	-	0.010
			5	nCHTAce	186.319	45.242	23.778	-3.622	-0.963	0.010
		BB(R)	1	CHTA	456.513	28.642	7.165	-	-	0.010
			2	*CETA	767.208	18.183	3.521	-	-	0.010
			3	CHTA	7156.057	15.358	5.418	-	-	0.010
			4	*CETA	1446.391	23.617	3.987	-	-	0.010
			5	CHTA	2840.146	32.331	3.988	-	-	0.010

Table 7: *Detailed Parameters by Model for Arches No. 1-5 (2/2). Type:Type of reconstruction curve, R/r/d:Trochoid parameters, camp:Catenary curve amplitude, expo:Exponent of exponentially distorted catenary, tolerance:Calculation tolerance for arch width, height, and distance to fullness control point, *:Curve with less fullness than a CTDA.*

8.2.3 Fullness Analysis

The term volume is often used in relation to arches, but strictly speaking, it is not a suitable expression for an individual arch, which is a 2D cross-section. Volume refers to a three-dimensional quantity, whereas a 2D arch cross-section has no volume. Of course, an expression like the volume of a violin's front is greater than its back is possible, as it refers to the volume of the entire three-dimensional front plate. However, since this report deals with the degree to which an arch is swollen on a 2D plane, the term volume is not appropriate.

Therefore, a suitable term and an objective index are needed to represent the degree to which an arch is swollen in a 2D plane. In particular, a common standard is required to compare arches with different widths and heights. As there is currently no official term or index to describe the 2D shape of a stringed instrument's arch, this report will define and use new ones.

This report will use the term *Fullness* to represent the degree to which a 2D arch is swollen[6]. This term is already a concept used in other fields, such as naval architecture, to describe the plumpness of a hull or how much a specific cross-section fills a reference shape. Therefore, it was judged to be the most suitable for expressing the shape of a 2D arch.

To quantify this fullness, this report has introduced the *Absolute Fullness Index* (*AFI*) and the *Relative Fullness Index* (*RFI*). This report will first define these two indices and then use them to analyze the arches.

Since fullness is a concept proportional to area, we will first define the area of an arch.
(※ Hereinafter, all references to arch area and width refer to the area and width of half an arch to account for symmetry.)

> **Definition 8.1.** ***Area of the arch***
> *The area of the closed shape enclosed by the arch curve, the horizontal line passing through the arch's endpoint, and the vertical line passing through its apex.*

This corresponds to the gray area in Figure 67.(a).

Based on this, the Absolute Fullness Index is defined as follows.

> **Definition 8.2.** ***Absolute Fullness Index*** (***AFI, unit:***[%])
> *The ratio of the arch area to the area of the minimum bounding rectangle* (*width: arch width, height: arch height*)*. Expressed as a percentage* (%)*. Also abbreviated as Absolute Fullness.*

According to the definition above, the AFI is calculated with the following formula:

[6] As a term to denote the degree of swelling, several candidates such as Curvature, Convexity, and Bulginess were considered. However, after comprehensively considering the usage, nuance, and suitability as a physics term, fullness was ultimately chosen.

$$\text{AFI}[\%] = \frac{\text{Arch Area}}{\text{Arch Width} \times \text{Arch Height}} \times 100$$

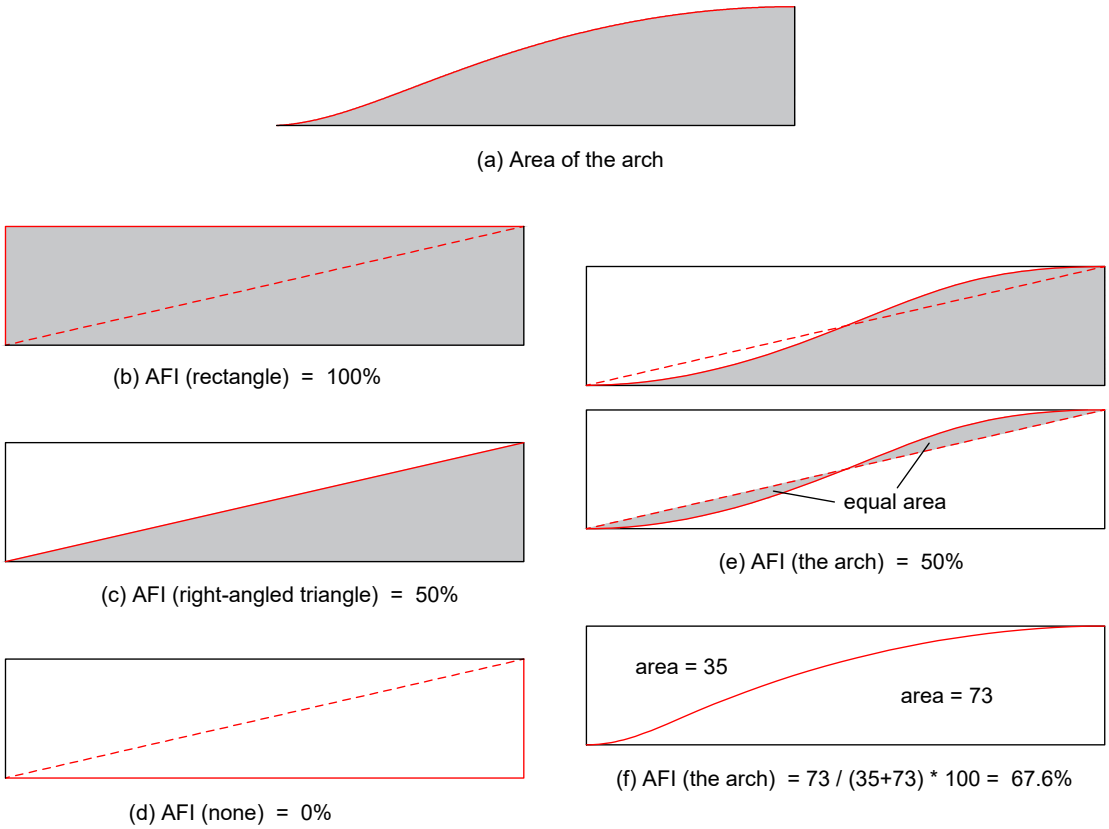

Figure 67: *Arch area and Absolute Fullness Index (AFI)*

This method of dividing the area of a specific shape by its minimum bounding rectangle is commonly used for analyzing and normalizing shape.

According to this definition, for two arches A (AFI= 85%) and B (AFI= 77%) with the same width and height, one can state that Arch A is about 8% fuller than Arch B in terms of AFI.

(Note: If an arch is symmetrical, the AFI calculated based on the whole arch is always the same as the value calculated based on half the arch.)

Figure 67.(b) shows an AFI of 100%, which can be thought of as the state where the arch curve (red solid line) has swollen to become infinitely close to a rectangle. (c) shows an AFI of 50%, which is like the state where the arch curve has been flattened into a straight line. However, since a real arch is not a straight line, when the area between the straight line connecting the endpoint and apex and the arch curve is equal above and below the line (e), the area of that arch is the same as the area of a right triangle, resulting in an AFI of 50%. An AFI of 0% is a

case where the arch area does not exist at all, as in (d).

According to the above definition, for an arch with an area of 73 and a rectangular area of 108 (=35+73) as in Figure 67.(f), the AFI can be calculated with the following formula:

$$\begin{aligned} \text{AFI} &= \frac{\text{Arch Area}}{\text{Rectangular Area}} \times 100 \\ &= \frac{73}{35+73} \times 100 \\ &\approx 67.6\% \end{aligned}$$

Next, the Relative Fullness Index is defined as follows.

Definition 8.3. ***Relative Fullness Index*** **(*RFI, unit:*** $[\%]$**)**
For a given width and height, considering a maxCHTA, a CTDA, and a minCETA, the scale is defined such that the arch area corresponds to $+100\%$ *when it equals the maxCHTA area,* 0% *when it equals the CTDA area, and* -100% *when it equals the minCETA area. It is the percentage value of the arch's area converted according to this scale. Also abbreviated as Relative Fullness.*

In other words, while the AFI uses the bounding rectangle as its reference, the RFI uses the arches with the maximum (maxCHTA), standard (CTDA), and minimum (minCETA) fullness achievable with a trochoid as its scale.

The RFI was introduced to easily grasp the following information:

- The level of the arch's fullness within the trochoid range.
- How much more the fullness can be increased or decreased.
- Whether the arch is a standard trochoid curve or an approximation curve that exceeds its limits.

For example, if an arch has an RFI of 83%, it means this arch has greater fullness than the standard (CTDA type) and still has room before reaching the maximum fullness (100%). An RFI of 112% means it has surpassed the maximum fullness (100%), indicating it is an approximation curve beyond the limits of a CHTA (nCHTAce). Similarly, an RFI of -35% indicates a CETA type with less fullness, and an RFI of -101% indicates an approximation curve beyond the limits of a CETA (nCETAice).

According to the above definition, the RFI can be calculated with the following formulas:

a. If the arch area is greater than or equal to the CTDA area (RFI$\geq$0[%]) :

$$\text{RFI}[\%] = \frac{\text{Arch Area} - \text{CTDA Area}}{\text{CHTA Area} - \text{CTDA Area}} \times 100$$

b. If the arch area is less than the CTDA area (RFI$<$0[%]) :

$$\text{RFI}[\%] = \frac{\text{Arch Area} - \text{CTDA Area}}{\text{CTDA Area} - \text{CETA Area}} \times 100$$

Figure 68 illustrates the concept of RFI. RFI uses the areas of the maxCHTA, CTDA, and minCETA as its scale, not the bounding rectangle.

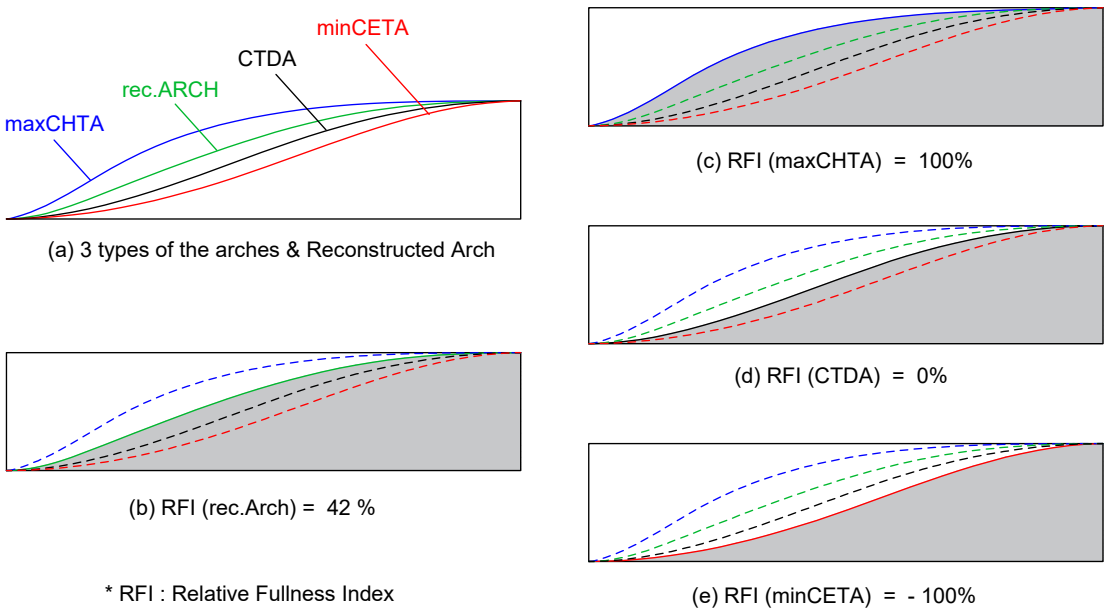

Figure 68: *Arch area and Relative Fullness Index (RFI)*

One point to note about RFI is that the amount of area change in the $+100 \sim 0\%$ range is different from that in the $0 \sim -100\%$ range. This stems from the characteristics of trochoid curves, as the variable range of a CHTA is generally wider than that of a CETA.

Based on the two newly defined indices, this report will now analyze the fullness of the reconstructed arches and examine their characteristics.

Tables 8 through 10 show the fullness of all reconstructed arches. They present the areas of the maxCHTA, CTDA, and minCETA with the same width and height as each reconstructed arch (rec.Arch), along with the AFI and RFI values calculated from them.

First, let's look at the 6th arch. In Table 8, the range of fullness expressible by a trochoid (AFI from about 47% for minCETA to about 58% for maxCHTA) is relatively narrow and has a relatively uniform distribution. The RFI of the reconstructed 6th arches is distributed over a very wide range, from 117% to 405%, all of which greatly exceed the maximum fullness of a trochoid (RFI 100%). This means the fullness of the 6th arch is very large. There is also a tendency for the fullness of the Front to be greater than that of the Back. In particular, Model D shows a very large difference in fullness between the upper part of the Front (RFI over 400%) and the lower part of the Back (RFI under 120%).

The 6th arch has a shape where the area near the apex of a CTDA curve is elongated, which causes an explosive increase in the RFI. The extreme RFI value for Model D is presumed to be due to the inaccurate apex position, as pointed out during the modeling process. In fact, the length of the upper part of Model D's 6th arch is much longer than that of other models, which appears to be the cause of the maximized fullness difference between the upper and lower parts.

(Note: For the fullness analysis of the 6th arch, the tolerance was set to double that of the other arches.)

M.	P.	S.	Area $[mm^2]$				AFI [%]				RFI [%]	T.
			maxCHTA	CTDA	minCETA	rec.Arch	maxCHTA	CTDA	minCETA	rec.Arch	rec.Arch	
A	F	U	1244.01	1112.16	977.04	1491.15	59.03	52.77	46.36	70.75	287.46	0.020
		L	1207.87	1079.41	996.54	1449.82	59.15	52.86	48.80	71.00	288.34	0.020
	B	U	1142.91	1023.63	909.64	1286.29	58.81	52.67	46.81	66.19	220.21	0.020
		L	1118.26	1000.86	948.03	1210.53	58.92	52.73	49.95	63.78	178.60	0.020
B	F	U	1768.14	1575.83	1407.11	2213.83	59.43	52.97	47.30	74.41	331.76	0.024
		L	1756.12	1563.08	1382.83	2211.13	59.54	52.99	46.88	74.97	335.71	0.024
	B	U	1625.04	1456.00	1294.11	2023.47	58.47	52.39	46.56	72.80	335.70	0.024
		L	1378.13	1228.24	1085.01	1560.59	59.30	52.85	46.69	67.16	221.74	0.024
C	F	U	4607.17	4136.30	3754.20	5985.72	58.12	52.18	47.36	75.52	392.77	0.040
		L	4399.86	3947.20	3559.57	5591.38	58.29	52.29	47.16	74.07	363.23	0.040
	B	U	3697.77	3330.29	3054.43	4558.16	57.67	51.94	47.64	71.09	334.13	0.040
		L	3774.78	3399.36	3289.01	4589.39	57.63	51.90	50.21	70.07	316.98	0.040
D	F	U	1267.91	1140.08	1007.28	1657.88	58.15	52.29	46.20	76.03	405.08	0.020
		L	1011.50	902.28	796.18	1191.74	59.47	53.05	46.81	70.06	265.02	0.020
	B	U	1460.76	1308.62	1171.55	1664.11	58.75	52.63	47.12	66.93	233.67	0.020
		L	1084.50	965.06	858.30	1105.91	59.80	53.21	47.32	60.98	117.92	0.020

Table 8: *Arch Area and Fullness by Model for the 6th Arch. M.:Model, P.:Front(F)/Back(B), S.:Upper(U)/Lower(L), Type:CTDAcec, rec.Arch:Recreated Arch, T.:Tolerance (calculation tolerance for distance to arch width, height, and fullness control point).*

Next, let's examine arches no. 1-5. In Tables 9 and 10, almost all arches with a negative RFI (CETA, CTDAice, etc.) are either the 2nd or 4th arch. Consistent with the parameter analysis, this shows the characteristic that the 2nd and 4th arches have less fullness compared to other arches. As these arches are located near the corners of the plate and have an elongated shape at their ends, their fullness seems to decrease. Even in cases where their RFI is positive, the value is significantly lower compared to other arches.

Another characteristic is that the RFI of the 5th arch is larger compared to other arches. There are many cases where the RFI exceeds 100 and was reconstructed as an approximation curve, which is consistent with the parameter analysis results.

Looking at the arch types, all arches reconstructed as nCHTAce have an RFI exceeding 100%. This means that a theoretically non-existent arch beyond the limits of a trochoid was implemented as an approximation curve. In contrast, the nCETAice arch of Model D has an RFI of -56.81%, which does not reach the limit of -100%. This corresponds to a case where it theoretically exists but could not be reconstructed due to computational issues. It would likely be possible to reconstruct it as a standard CETA by increasing the calculation precision.

Additionally, the Model A-F-B-4 arch has an RFI of -3.16% but is of the CTDAice type, not CETA. This means that since the target curve was extremely similar to a CTDA, requiring a very large R value for a CETA, an approximation curve was created instead. However, for the Model A-B-S-4 arch, it can be inferred that the calculation failed, leading to the creation of an approximation curve.

(Note: Although not in the table, the AFI of the reference CTDA and maxCHTA seems to be influenced by the arch's width/height ratio. Generally, a higher height relative to the width tends to result in a larger AFI.)

M.	P.	S.	N.	Type	Area $[mm^2]$				AFI [%]				RFI [%]	T.
					maxCHTA	CTDA	minCETA	rec.Arch	maxCHTA	CTDA	minCETA	rec.Arch	rec.Arch	
A	F	B	1	CHTA	438.41	358.32	333.05	392.56	66.71	54.52	50.68	59.73	42.76	0.010
			2	CHTA	491.11	412.68	372.66	417.85	67.08	56.37	50.90	57.08	6.59	0.010
			3	CHTA	397.35	345.53	308.31	368.65	67.67	58.84	52.50	62.78	44.61	0.010
			4	CTDAice	619.02	514.80	472.00	513.44	67.13	55.83	51.19	55.68	-3.16	1E-09
			5	CHTA	562.90	494.16	456.61	549.70	61.56	54.04	49.93	60.11	80.80	0.010
		S	1	CHTA	433.54	354.45	313.96	395.93	66.75	54.58	48.34	60.96	52.45	0.010
			2	CHTA	487.98	410.23	363.44	419.56	67.11	56.41	49.98	57.70	12.01	0.010
			3	CHTA	395.82	344.44	307.84	371.94	67.66	58.88	52.62	63.58	53.53	0.010
			4	CETA	628.53	522.23	510.58	513.28	67.08	55.74	54.49	54.78	-76.77	0.010
			5	CHTA	572.09	502.94	452.45	553.33	61.38	53.96	48.55	59.37	72.86	0.010
	B	S	1	CHTA	314.46	278.60	246.86	302.66	60.37	53.48	47.39	58.10	67.10	0.010
			2	CETA	440.23	365.05	331.73	362.06	67.08	55.63	50.55	55.17	-8.98	0.010
			3	CHTA	341.93	295.66	266.04	312.88	67.74	58.58	52.71	61.99	37.20	0.010
			4	CTDAice	553.27	456.96	420.23	447.18	67.14	55.45	51.00	54.27	-26.62	1E-09
			5	nCHTAce	421.79	375.45	336.56	437.57	59.68	53.12	47.62	61.91	134.05	0.010
		B	1	CHTA	311.22	275.57	246.63	300.40	60.45	53.53	47.90	58.35	69.65	0.010
			2	CTDAice	438.54	363.79	326.70	363.69	67.08	55.65	49.98	55.63	-0.29	1E-09
			3	CHTA	339.83	294.09	267.57	312.68	67.75	58.63	53.34	62.34	40.65	0.010
			4	CETA	552.70	456.27	404.97	446.20	67.19	55.46	49.23	54.24	-19.63	0.010
			5	nCHTAce	420.57	374.44	335.60	441.89	59.68	53.13	47.62	62.70	146.21	0.010
B	F	B	1	CHTA	657.20	542.12	489.52	590.90	67.03	55.30	49.93	60.27	42.39	0.012
			2	CETA	806.32	691.02	625.85	685.86	67.57	57.90	52.44	57.47	-7.91	0.012
			3	CHTA	569.58	499.91	443.22	544.19	67.33	59.10	52.40	64.33	63.57	0.012
			4	CTDAce	946.67	791.33	727.81	793.72	67.33	56.28	51.77	56.45	1.54	1E-09
			5	CHTA	831.36	726.57	704.83	819.39	62.04	54.22	52.60	61.14	88.58	0.012
		S	1	CHTA	660.86	545.17	524.07	586.30	66.99	55.26	53.12	59.43	35.55	0.012
			2	CHTA	801.62	687.14	630.27	693.67	67.61	57.96	53.16	58.51	5.70	0.012
			3	CHTA	578.41	506.63	452.45	545.83	67.31	58.96	52.65	63.52	54.61	0.012
			4	CHTA	948.94	792.76	730.34	800.68	67.36	56.27	51.84	56.83	5.07	0.012
			5	CHTA	833.67	728.67	667.01	823.77	62.02	54.21	49.62	61.28	90.58	0.012
	B	S	1	CHTA	462.98	406.17	366.75	452.99	61.60	54.04	48.80	60.27	82.41	0.012
			2	CHTA	593.16	492.56	453.88	506.47	67.31	55.89	51.50	57.47	13.83	0.012
			3	CHTA	482.01	412.57	371.82	452.63	67.34	57.64	51.94	63.23	57.69	0.012
			4	CHTA	801.57	658.84	633.13	673.44	67.30	55.32	53.16	56.54	10.23	0.012
			5	nCHTAce	613.56	544.99	491.23	614.57	59.94	53.25	47.99	60.04	101.48	0.012
		B	1	CHTA	464.43	407.62	373.33	453.54	61.56	54.03	49.48	60.11	80.82	0.012
			2	CHTA	597.77	496.29	476.69	507.53	67.26	55.84	53.64	57.11	11.07	0.012
			3	CHTA	482.84	413.46	367.74	447.98	67.29	57.62	51.25	62.43	49.76	0.012
			4	CHTA	803.26	659.86	605.37	677.63	67.33	55.31	50.74	56.80	12.39	0.012
			5	nCHTAce	617.28	548.99	512.77	623.45	59.84	53.22	49.71	60.44	109.03	0.012

Table 9: *Arch Area and Fullness by Model for Arches No. 1-5 (1/2). M.:Model, P.:Front/Back, S.:Left/Right, N.:Arch Number, Type:Type of reconstruction curve, rec.Arch:Recreated Arch, T.:Tolerance (for arch width, height, and distance to fullness control point).*

M.	P.	S.	N.	Type	Area $[mm^2]$				AFI [%]				RFI [%]	T.
					maxCHTA	CTDA	minCETA	rec.Arch	maxCHTA	CTDA	minCETA	rec.Arch	rec.Arch	
C	F	S	1	CHTA	1601.13	1403.81	1290.47	1495.07	61.73	54.12	49.75	57.64	46.25	0.020
			2	CHTA	1751.12	1454.56	1306.96	1468.41	67.08	55.72	50.06	56.25	4.67	0.020
			3	CHTA	1529.66	1305.71	1153.25	1398.67	67.53	57.64	50.91	61.75	41.51	0.020
			4	CHTA	2283.76	1915.45	1693.04	1953.72	65.35	54.81	48.45	55.91	10.39	0.020
			5	nCHTAce	2228.60	1978.54	1791.83	2240.74	60.19	53.43	48.39	60.52	104.85	0.020
		B	1	CHTA	1623.55	1423.53	1282.79	1500.40	61.65	54.06	48.71	56.98	38.43	0.020
			2	CHTA	1742.57	1447.54	1311.77	1461.02	67.11	55.75	50.52	56.27	4.57	0.020
			3	CHTA	1523.98	1302.14	1149.38	1395.19	67.49	57.67	50.90	61.79	41.95	0.020
			4	CHTA	2285.07	1917.31	1710.34	1953.84	65.32	54.81	48.89	55.85	9.93	0.020
			5	CHTA	2259.07	2006.80	1857.80	2247.26	60.09	53.38	49.42	59.78	95.32	0.020
	B	B	1	CHTA	1264.33	1121.80	1065.03	1197.11	60.19	53.41	50.70	56.99	52.83	0.020
			2	CHTA	1511.29	1231.80	1195.99	1243.91	67.17	54.75	53.16	55.29	4.33	0.020
			3	CHTA	1261.20	1056.34	982.03	1172.06	67.36	56.42	52.45	62.60	56.49	0.020
			4	CHTA	1717.17	1508.94	1447.62	1566.08	61.47	54.01	51.82	56.06	27.44	0.020
			5	nCHTAce	1709.82	1528.82	1494.61	1711.93	59.02	52.77	51.59	59.09	101.17	0.020
		S	1	CHTA	1261.65	1118.90	1026.17	1205.85	60.23	53.42	48.99	57.57	60.91	0.020
			2	CETA	1538.47	1252.59	1142.26	1237.70	67.14	54.66	49.85	54.01	-13.50	0.020
			3	CHTA	1290.88	1078.21	978.35	1174.37	67.38	56.28	51.06	61.29	45.22	0.020
			4	CHTA	1723.51	1515.20	1390.93	1574.91	61.42	54.00	49.57	56.12	28.67	0.020
			5	CHTA	1722.60	1540.19	1468.92	1708.31	59.00	52.75	50.31	58.51	92.17	0.020
D	F	B	1	CHTA	451.65	367.52	328.91	374.40	67.11	54.61	48.87	55.63	8.17	0.010
			2	CETA	483.63	405.21	360.98	378.82	67.52	56.57	50.40	52.89	-59.67	0.010
			3	CHTA	395.24	344.83	303.73	350.43	68.04	59.36	52.29	60.33	11.10	0.010
			4	nCETAice	635.58	525.72	466.51	492.08	67.38	55.74	49.46	52.17	-56.81	0.010
			5	CHTA	588.83	516.99	466.95	535.93	61.55	54.04	48.81	56.02	26.37	0.010
		S	1	CHTA	462.01	375.35	337.06	390.37	67.05	54.47	48.92	56.65	17.33	0.010
			2	CETA	492.63	412.91	373.60	398.44	67.54	56.61	51.22	54.62	-36.81	0.010
			3	CETA	406.70	355.01	321.32	350.25	68.02	59.38	53.74	58.58	-14.11	0.010
			4	CETA	643.71	530.87	483.33	519.53	67.40	55.59	50.61	54.40	-23.84	0.010
			5	CHTA	594.97	519.89	459.73	571.06	62.05	54.22	47.94	59.55	68.15	0.010
	B	S	1	CHTA	333.72	294.67	261.36	307.40	60.81	53.70	47.63	56.02	32.61	0.010
			2	CHTA	417.73	345.45	312.43	350.65	67.29	55.65	50.33	56.48	7.18	0.010
			3	CHTA	352.07	302.90	275.33	311.84	67.87	58.39	53.08	60.12	18.20	0.010
			4	CHTA	552.46	450.16	411.22	467.57	67.24	54.79	50.05	56.91	17.02	0.010
			5	nCHTAce	364.28	326.52	307.78	382.66	58.67	52.59	49.57	61.63	148.69	0.010
		B	1	CHTA	313.10	276.50	250.79	290.28	60.79	53.68	48.69	56.36	37.66	0.010
			2	CETA	402.63	333.53	307.95	321.49	67.37	55.80	51.52	53.79	-47.07	0.010
			3	CHTA	349.46	302.07	278.52	302.97	67.89	58.68	54.11	58.86	1.90	0.010
			4	CETA	545.03	445.20	403.43	432.90	67.18	54.88	49.73	53.36	-29.46	0.010
			5	CHTA	346.93	310.82	286.68	317.10	58.74	52.63	48.54	53.69	17.39	0.010

Table 10: *Arch Area and Fullness by Model for Arches No. 1-5 (2/2). M.:Model, P.:Front/Back, S.:Left/Right, N.:Arch Number, Type:Type of reconstruction curve, rec.Arch:Recreated Arch, T.:Tolerance (for arch width, height, and distance to fullness control point).*

8.2.4 Error Analysis

The error between the reconstructed arch and the model arch is defined as follows. First, the two arches are superimposed by aligning their apexes, and the area between the two curves, the error area(mm^2), is calculated. Then, this error area is divided by the length of the model arch(mm) to calculate the *error per unit length*(mm^2/mm). The smaller this value, the more similar the two curves are considered, with 0 indicating identical curves. The error per unit length is calculated for all arches, and based on this, the group and overall error averages(mm) and standard deviations(mm) are determined.

The error area is found by integrating the closed curve formed by the two arches. During this process, due to the tolerance set in the reconstruction process, slight differences in the width and height of the two arches occur, causing a minor misalignment at the arch ends. Since a closed curve is not formed in this misaligned part, the integration was performed after creating a closed shape by drawing a perpendicular line from the end of the shorter width. A custom program was used for the calculation.

Figure 69 shows the closed curve formed by the two arches, i.e., the error area. When the black curve is the model arch and the red is the reconstructed arch, the green hatched area is the error area.

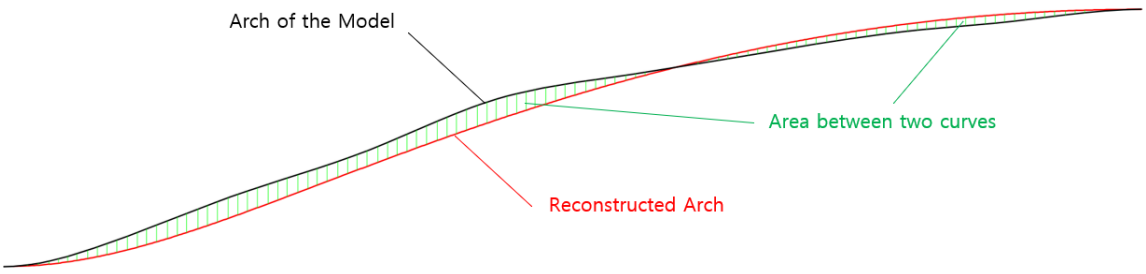

Figure 69: *Area between the two curves (error area)*

After finding the error for individual arches, they are grouped by position (1st, 2nd, 3rd, etc.) to calculate the average error for each group. This is because the character of the arch differs by position. By checking the group and overall error averages, a primary assessment of the reconstruction method's reliability can be made.

Next, the standard deviation is checked, as the average value alone does not reveal the distribution of the data. For example, the two sets [-5, -3, 3, 5] and [-1, 0, 0, 1] both have an average of 0, but the data in the first set is much more scattered from the mean than in the second. Standard deviation is a measure of how spread out the data is around the mean. A smaller standard deviation means the data is clustered around the average value. Therefore, by also checking the standard deviation, the reliability of the reconstruction method can be evaluated more deeply.
(※ The sample standard deviation is used, with the population standard deviation also noted in parentheses.)

Table 11 shows the error per unit length and the standard deviation, while Table 12 organizes the original data (Raw Data) for each arch pair by group. The most prominent feature here is that the 1st arch has the smallest error. Excluding the 6th arch, the error increases in the order of 1st<2nd<4th<3rd<5th arch. The standard deviation shows a similar trend, indicating that the 1st and 2nd arches have the least variation.

Comparing the Front and the Back, the error for the Back is smaller overall. This seems to be because the Back has less deformation than the Front. Meanwhile, despite the complex reconstruction method for the 6th arch, its error was surprisingly smaller than that of the other arches. The overall error average is less than 0.2, and the 6th arch, in particular, showed a satisfactory result of 0.161. The standard deviation is also small, less than 0.1, indicating that the reconstruction results are relatively uniform.

Considering the irregular surface of the original models, plate deformation, and computational tolerances, this level of error average and standard deviation demonstrates that this reconstruction method has a sufficiently high degree of reliability.

Group	Arch	Error per unit length [mm^2/mm]						Std. Dev. SD (PSD)			
		Min.	Max.	Avg.							
1	Front-1st	0.044	0.261	0.147	0.141			0.083	0.066		
2	Back-1st	0.043	0.177	0.134				0.050			
3	Front-2nd	0.089	0.391	0.199	0.183			0.111	0.096		
4	Back-2nd	0.043	0.293	0.167				0.082			
5	Front-3rd	0.107	0.325	0.213	0.201	0.184		0.083	0.094	0.102	
6	Back-3rd	0.062	0.385	0.190				0.108		(0.101)	
7	Front-4th	0.086	0.326	0.181	0.194		0.180	0.098	0.122		0.097
8	Back-4th	0.062	0.429	0.207				0.148			(0.096)
9	Front-5th	0.088	0.495	0.206	0.203			0.122	0.121		
10	Back-5th	0.055	0.379	0.199				0.129			
11	Front-6th-U	0.111	0.159	0.127	0.154	0.161		0.021	0.052	0.065	
12	Back-6th-U	0.104	0.257	0.181				0.063		(0.063)	
13	Front-6th-L	0.084	0.296	0.178	0.168			0.093	0.079		
14	Back-6th-L	0.060	0.236	0.157				0.074			

Table 11: *Error data per unit length by group*

Group	Arch	Error Area [mm^2]	Original Arch Length [mm]	Error per unit length [mm^2/m]	Group	Arch	Error Area [mm^2]	Original Arch Length [mm]	Error per unit length [mm^2/m]
1	A-F-1-B	10.226	76.149	0.134	7	A-F-4-B	7.460	79.890	0.093
	A-F-1-S	11.505	75.283	0.153		A-F-4-S	6.994	81.163	0.086
	B-F-1-B	3.812	86.202	0.044		B-F-4-B	23.782	95.154	0.250
	B-F-1-S	3.973	86.723	0.046		B-F-4-S	24.189	95.354	0.254
	C-F-1-B	28.723	160.600	0.179		C-F-4-B	14.760	170.583	0.087
	C-F-1-S	40.152	158.215	0.254		C-F-4-S	17.417	170.388	0.102
	D-F-1-B	19.892	76.275	0.261		D-F-4-B	20.146	81.371	0.248
	D-F-1-S	8.581	78.424	0.109		D-F-4-S	27.047	83.068	0.326
2	A-B-1-B	11.821	76.272	0.155	8	A-B-4-B	10.492	77.900	0.135
	A-B-1-S	11.069	76.988	0.144		A-B-4-S	8.251	77.976	0.106
	B-B-1-B	14.352	86.266	0.166		B-B-4-B	5.905	95.017	0.062
	B-B-1-S	15.008	85.928	0.175		B-B-4-S	7.156	94.863	0.075
	C-B-1-B	27.631	156.323	0.177		C-B-4-B	70.837	166.484	0.425
	C-B-1-S	22.145	155.892	0.142		C-B-4-S	71.665	167.218	0.429
	D-B-1-B	5.033	74.509	0.068		D-B-4-B	13.998	81.420	0.172
	D-B-1-S	3.327	76.730	0.043		D-B-4-S	20.894	82.923	0.252
3	A-F-2-B	6.084	68.299	0.089	9	A-F-5-B	18.311	94.900	0.193
	A-F-2-S	7.458	67.836	0.110		A-F-5-S	16.584	96.689	0.172
	B-F-2-B	26.978	78.806	0.342		B-F-5-B	21.105	112.430	0.188
	B-F-2-S	30.649	78.291	0.391		B-F-5-S	18.924	112.799	0.168
	C-F-2-B	15.051	134.954	0.112		C-F-5-B	18.517	209.786	0.088
	C-F-2-S	21.449	135.660	0.158		C-F-5-S	30.302	206.642	0.147
	D-F-2-B	13.124	66.496	0.197		D-F-5-B	47.980	96.976	0.495
	D-F-2-S	12.714	67.096	0.189		D-F-5-S	19.133	95.194	0.201
4	A-B-2-B	7.055	68.277	0.103	10	A-B-5-B	6.117	94.354	0.065
	A-B-2-S	10.504	68.531	0.153		A-B-5-S	7.377	94.640	0.078
	B-B-2-B	14.923	78.396	0.190		B-B-5-B	37.108	112.574	0.330
	B-B-2-S	16.478	77.747	0.212		B-B-5-S	35.063	111.712	0.314
	C-B-2-B	33.017	137.652	0.240		C-B-5-B	36.802	203.237	0.181
	C-B-2-S	41.008	140.188	0.293		C-B-5-S	38.955	204.817	0.190
	D-B-2-B	6.784	64.402	0.105		D-B-5-B	5.144	94.144	0.055
	D-B-2-S	2.874	66.540	0.043		D-B-5-S	36.946	97.361	0.379
5	A-F-3-B	11.216	52.666	0.213	11	A-F-6-U	27.506	173.469	0.159
	A-F-3-S	12.161	52.520	0.232		B-F-6-U	23.877	199.364	0.120
	B-F-3-B	14.061	62.691	0.224		C-F-6-U	45.537	378.590	0.120
	B-F-3-S	10.806	63.564	0.170		D-F-6-U	21.605	194.149	0.111
	C-F-3-B	35.778	110.249	0.325	12	A-B-6-U	32.973	169.548	0.194
	C-F-3-S	35.522	110.583	0.321		B-B-6-U	36.110	214.484	0.168
	D-F-3-B	5.465	51.155	0.107		C-B-6-U	92.649	360.992	0.257
	D-F-3-S	5.879	51.870	0.113		D-B-6-U	20.094	193.230	0.104
6	A-B-3-B	8.207	49.235	0.167	13	A-F-6-L	21.401	168.116	0.127
	A-B-3-S	7.904	49.584	0.159		B-F-6-L	40.678	197.677	0.206
	B-B-3-B	3.866	62.371	0.062		C-F-6-L	106.601	360.537	0.296
	B-B-3-S	4.458	62.167	0.072		D-F-6-L	12.551	148.740	0.084
	C-B-3-B	30.750	108.894	0.282	14	A-B-6-L	24.118	165.571	0.146
	C-B-3-S	42.876	111.394	0.385		B-B-6-L	33.268	179.422	0.185
	D-B-3-B	7.628	49.617	0.154		C-B-6-L	86.874	368.659	0.236
	D-B-3-S	12.091	50.768	0.238		D-B-6-L	9.020	149.513	0.060

Table 12: *Raw data of error per unit length by group. Abbreviation:Model(A/B/C/D)-Plate(Front/Back)-Arch N.(1/2/3/4/5/6)-Side(Bass bar/Sound post or Upper/Lower))*

9 Application in Instrument Making

So far, this report has examined the process of reconstructing the arches of four models. The ultimate goal of this research is to find a method for applying the Stradivari arch to instruments of different sizes from the models used in the study. Therefore, this chapter will explore how to apply this method when the arch's width and height are different. As before, this report will discuss arches no. 1-5 and arch no. 6 separately.

9.1 Arches No. 1-5

The parameters needed to create an arch are its width, height, and the position of the fullness control point. The width is determined by the maker based on the plate's dimensions and edge width. The height is automatically determined once the 6th arch is created. Therefore, the arch can be created if only the position of the fullness control point is known.

Since the goal is to reconstruct the shape of the Stradivari arch, a standard model is needed as a reference. This standard model serves as a scale for calculating the position of the fullness control point for a new instrument. That is, the relative distance from the arch endpoint is applied proportionally.

For example, let's assume we have chosen the left side of the Front of Model A's 1st arch as the standard model for the 1st arch. In this standard model, the fullness control point is located 25.91 horizontally (x-axis) and 3.9 vertically (y-axis) from the arch endpoint. If we are making a new arch that is 1.1 times the width and 0.9 times the height of the standard model, the position of the fullness control point is calculated as follows:

Horizontal position: $25.91 \times 1.1 = 28.50$, Vertical position: $3.9 \times 0.9 = 3.51$

We then need to create a trochoid curve that passes through this calculated position. In practice, one can pre-calculate the position ratio of the fullness control point relative to the width and height of the standard model, and then multiply this ratio by the width and height of the new instrument. For example, assume the position ratio of the standard model's fullness control point is as follows:

$$\begin{aligned}\text{Position Ratio in x-axis direction (Rate\_Zx)} &= \frac{\text{(x-axis distance from arch endpoint to fullness control point)}}{\text{(half arch width)}} \\ &= \frac{25.91}{75.53} \\ &= 0.3430\end{aligned}$$

$$\begin{aligned}\text{Position Ratio in y-axis direction (Rate\_Zy)} &= \frac{\text{(y-axis distance from arch endpoint to fullness control point)}}{\text{(arch height)}} \\ &= \frac{7.2-3.3}{12.0-3.3} = \frac{3.9}{8.7} \\ &= 0.3793\end{aligned}$$

Using this ratio, the position of the fullness control point for the arch to be created (width 81.0mm, height 7.8mm) can be calculated as follows:

$$\begin{aligned}\text{x-axis distance from arch endpoint to fullness control point} &= \text{Arch width} \times \text{Rate\_Zx} \\ &= 81.0 \times 0.3430 \\ &= 27.783\end{aligned}$$

$$\begin{aligned}\text{y-axis distance from arch endpoint to fullness control point} &= \text{Arch height} \times \text{Rate\_Zy} \\ &= 7.8 \times 0.3793 \\ &= 2.9585\end{aligned}$$

Thus, by knowing the position ratio of the fullness control point for each arch, one can create an arch with the same fullness ratio as the standard model, even if the instrument's width and height are different.

9.2 The 6th Arch

Since the 6th arch has additional shape control points, information that determines the shape of the arch itself is also needed. For arches no. 1-5, there is only one trochoid curve that passes through the three points (apex, endpoint, fullness control point). However, for the 6th arch, there are infinitely many curves that can pass through these three points, so the following additional variables are needed to specify the shape:

- Amplitude of the cubic polynomial curve: Proportional to the arch height. Similar to the fullness control point, the *ratio* of the amplitude to the arch height of the standard model is calculated and applied.

- Handle direction and exponent value: These are intrinsic values that determine the shape regardless of the arch's width or height, so the values from the standard model are used directly.

For example, the amplitude ratio of the cubic polynomial curve for the standard model (Model A, Front, 6th arch upper part, height 15.1, amplitude -9.1) is as follows:

$$\begin{aligned}\text{Amplitude Ratio of Cubic Polynomial Curve (Rate\_bamp)} &= \frac{\text{(Amplitude of cubic polynomial curve)}}{\text{(Arch height)}} \\ &= \frac{-7.313}{(15.5-3.3)} \\ &= -0.5946\end{aligned}$$

If the height of the new arch is 11.9, the amplitude of the cubic polynomial curve to be used is as follows:

$$\begin{aligned}\text{Amplitude of Cubic Polynomial Curve} &= \text{(Arch height)} \times \text{(Rate\_bamp)} \\ &= 11.9 \times (-0.5946) = -7.0757\end{aligned}$$

(※ The amplitude of the cubic polynomial curve is always negative, and the minus sign $(-)$ in front of the number indicates the handle direction.)

In conclusion, by knowing the amplitude and handle direction (-7.0757), exponent value (-0.613), and the position of the fullness control point (calculation method is the same as for arches no. 1-5) of the standard model's cubic polynomial curve, one can create an arch with the same fullness and shape ratio as the standard model, even if the arch width and height change.

10 Conclusion and Discussion

Stradivari arches exhibit varying degrees of swell, or Fullness, depending on the location. This analysis revealed that the 2nd and 4th arches have low Fullness, whereas the 5th arch is characterized by high Fullness, and the 6th arch by very high Fullness. To implement such diverse Fullness, it is necessary to be able to control the Fullness while maintaining the arch's width and height.

The Curtate Trochoid curve, previously considered a prominent model, cannot be used for Stradivari arches because its Fullness cannot be adjusted. However, We have confirmed that the Curtate Hypotrochoid and Curtate Epitrochoid curves—generated by a circle rolling on the interior or exterior of another circle—allow for Fullness adjustment and can be used to reproduce Stradivari arches.

However, these two curves have limitations in adjusting Fullness. In cases that fall beyond these limits, the arches can be reproduced using an approximation curve created from a pattern curve. For this purpose, this report used an exponentially distorted catenary curve as the pattern. The approximation curve is obtained by deforming a trochoid curve according to the coordinate values of this pattern curve. This research reproduced the uniquely shaped 6th arch by deforming a Curtate Trochoid, using an exponentially distorted cubic polynomial curve and a catenary curve as patterns.

Through analysis of their images, parameters, Fullness, and error margins, we confirmed that the arches reproduced using these methods are highly similar to the original ones.

To compare the Fullness of arches with different widths and heights more objectively and quantitatively, I have introduced new metrics: the Absolute Fullness Index and the Relative Fullness Index. These indices allowed us to quantify the reconstructed arches' Fullness characteristics, and the results can be said to represent the unique properties of the original Stradivari arches.

The average error per unit length for all reconstructed arches was approximately $0.180(mm^2/mm)$, with a sample standard deviation of 0.097. Considering the irregular surfaces and warping of the source arches, this suggests that this reconstruction technique has a very high degree of accuracy and reliability. I expect the error would be significantly lower if the target were a smooth, symmetrical average curve without any warping.

To apply this reconstruction method to actual instrument making, a standard model to serve as a reference is required. Luthiers can use the proportional positions of the Fullness control points and the parameter ratios of the pattern curves from this standard model to create arches with identical proportional Fullness on instruments of any desired size. Therefore, securing an ideal standard model with minimal warping, from which sufficient data can be extracted, is of paramount importance for the successful application of this method.

This report has several limitations. First, the number of samples is small. This is a significant issue that could

affect not only the reliability of the reproduction process but also the determination of the edge width, which will be discussed in the appendix. Second, the reproduction method for 6th arch is somewhat complex and not intuitive. Follow-up research is needed to find a more concise and intuitive method. Third, this method is difficult to implement using only simple hand tools. However, I expect this issue will be resolved by a dedicated software application that will be distributed in the future.

We cannot know the exact intentions or methods Stradivari used to create these arches in Cremona over 300 years ago. However, this report clearly demonstrates that by utilizing Curtate Hypotrochoid, Curtate Epitrochoid, and approximation curves, it is possible to reconstruct arches that are remarkably similar to his work.

The fact that Stradivari arch—crafted solely by experience in an age without computers—almost perfectly matches modern mathematical calculations was a profound shock to me. I hope that through this research, this beautiful gift, the Stradivari arch, can be passed on to many more people.

11 Appendix

11.1 Arch Pattern Analysis

(※ Please note that the content of this section may be inaccurate due to the small number of samples and the inclusion of the author's speculation.)

Once the arch to be reconstructed is defined, its shape must be analyzed for a more in-depth reconstruction. This analysis involves understanding the pattern of the contour line data. For this purpose, this chapter introduces a new tool called the *Contour map*. Through contour map analysis, the characteristics of the Stradivari arch can be understood in more detail, which will be of great help in designing arches for actual instrument making.

The ultimate goal of this research is not to simply replicate existing Stradivari arches as they are today. It is to reconstruct their appearance before they were warped, that is, their initial state at the time of making. This is ultimately a process of understanding Stradivari's design intentions, and it requires logical speculation and imagination. This chapter presents several methods to aid in such a reasoning process.

There are two main points to consider in arch reconstruction. The first is how faithfully each individual arch is reconstructed, and the second is how well the relationships between the arches are reflected. The reconstructed arch will inevitably have slight differences from the original. This difference may not be apparent when looking at an individual arch alone, but it can become more distinct in the context of its relationship with other arches. Therefore, a proper reconstruction must faithfully reproduce the interrelationships between the arches.

The most common way to understand the interrelationships between arches is to check the overall contour lines. However, this can be difficult to draw and inefficient for comparing relationships. To overcome these shortcomings, a new analysis tool called the Contour map has been introduced. The contour map consists of a simplified skeleton of the overall contour lines and a diagram where these are aligned in a row.

Figure 70 Contour map-A shows the skeleton of the overall contour lines.

- Composition: The left side represents the Front, and the right side represents the Back. Red dots indicate the endpoints and apex of the arch, while black dots indicate the positions of the contour lines.
- Central connecting lines: By connecting contour points of the same number on the Front and back with straight lines, the shape difference of the 6th arch can be compared at a glance. (Contour points of different heights are connected by dotted lines, while the plate edges of the same height are connected by solid lines.)
- Usage: The slope of the arch can be determined from the spacing of the dots. It is also useful for quickly identifying the differences and characteristics of the 6th arches of the Front and back through the pattern of the connecting lines (slope, direction, etc.).

Analyzing the 6th arch through Contour map-A, the central part of the Front is flat and the slope becomes steeper

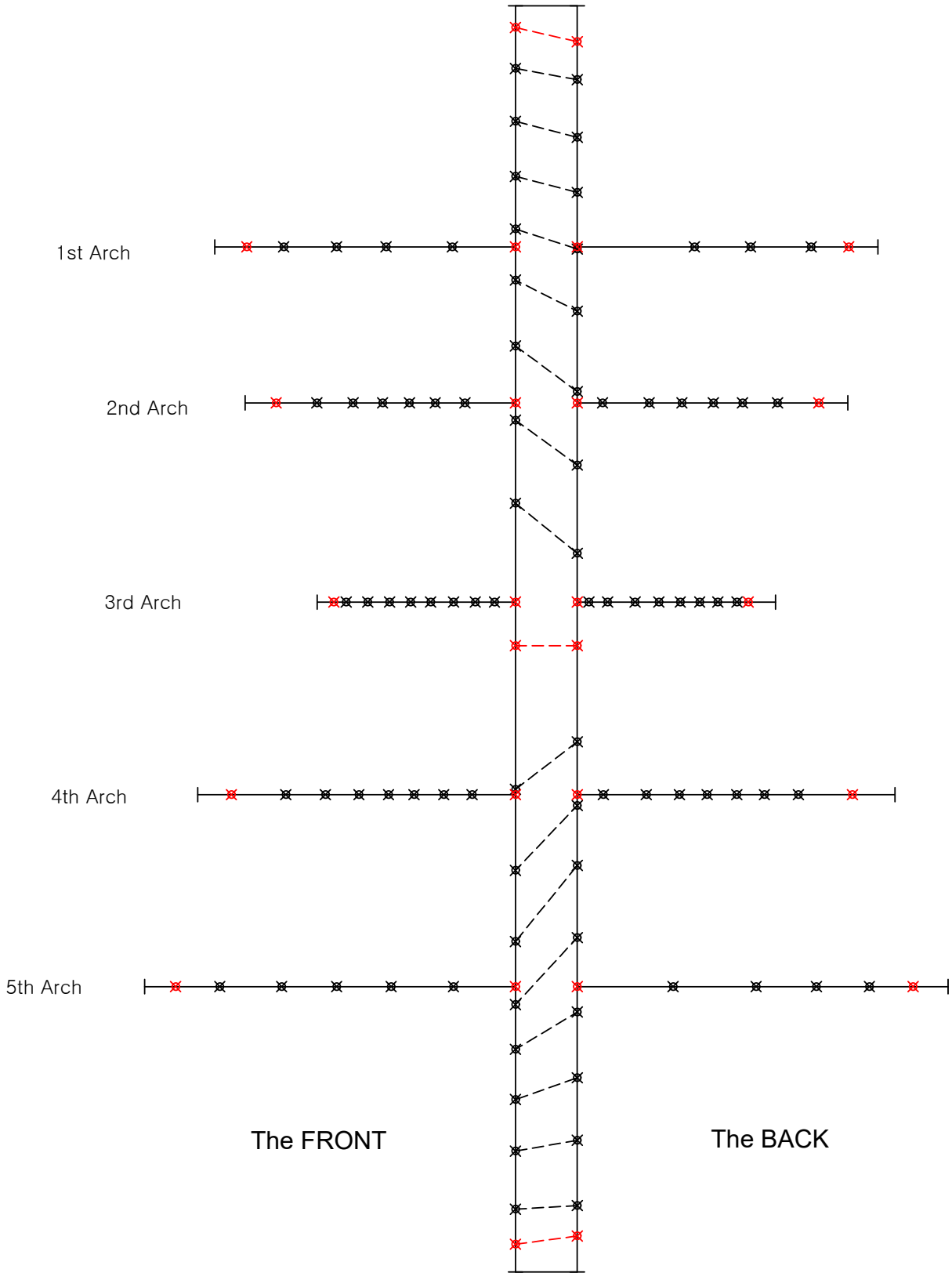

Figure 70: *Contour map(A) of the Model A*

towards the ends, whereas the Back forms a gentle curve overall. On the other hand, some parts suspected of measurement error are observed, such as the unusually narrow edge width of the upper part of the 6th arch on the Front. In an ideal arch, the slope of the central connecting lines should change gradually, but in the lower part of the 6th arch, there is a section where the slope changes somewhat irregularly, suggesting that the arch is not smooth.

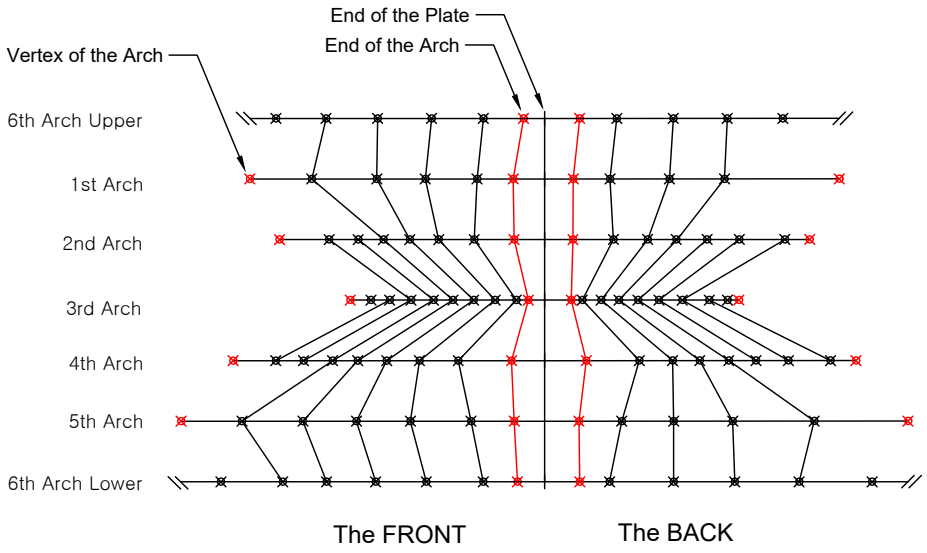

Figure 71: *Contour map(B) of the Model A*

Figure 71 Contour map-B is a diagram where the contour skeletons of the six arches are aligned side-by-side based on the plate endpoint.

- Composition: The left side is the Front, and the right side is the Back. Unlike Map-A, contour points of the same height within the same plate are connected by solid lines.
- Usage: It is useful for comparing the patterns of arches no. 1-5 with each other, and especially for understanding the relationship between the 6th arch and the 1st (upper part) and 5th (lower part) arches. Through this, the pattern differences between the Front and back can also be clearly seen.

Analyzing Contour map-B, the 1st arch of the Front has a total of four contour points, while the Back has only three. The 5th arch on the Back also has one fewer. This means that the height of the Back arch decreased more quickly than the Front. Looking at the relationship between the 6th upper and 1st arches, and the 6th lower and 5th arches, the 6th arch is generally steeper than the 1st and 5th arches for the Front. In contrast, for the Back, they are similar, or the 6th is very slightly gentler than the 1st and 5th.

A particularly noteworthy part of this diagram is the position of the arch endpoints, indicated by red solid lines. Since the arch endpoints determine the length of the arch, it is very important to accurately identify their positions.

The irregularity in the positions of the arch endpoints shown on the map could be due to errors in the data extraction process or measurement errors in the original source material itself. This is because the boundary of the arch ends is not distinct in handmade instruments, making precise measurement difficult.

The irregular slope of the connecting lines on the lower part of the Back is a sign that the measurement points are inaccurate or the curve is not smooth. Also, the edge width of the 3rd arch on the Back is unusually wide, which means the fullness of the 3rd arch is abnormally small. This seems to be a unique characteristic of that instrument.

Finally, the edge widths of Models A, B, and C vary by location. While many modern makers make the upper and lower bouts the same width and the C-bout narrower, the source material shows that this was not the case.

While Stradivari's exact design intentions are unknown, the following rules can be inferred from Models A, B, and C.

La: distance from the plate end to the arch endpoint
Lc: distance from the plate end to the first contour point

- Rule 1. (Front/Back) For arches no. 1-5, the magnitude of Lc is in the order of 3rd<1st<5th<2nd <4th.
- Rule 2. (Front) The slope of the upper part of the 6th arch is steeper than that of the 1st arch.
- Rule 3. (Front) The slope of the lower part of the 6th arch is steeper than that of the 5th arch.
- Rule 4. (Front) The La andLc of the 6th arch are narrower than those of the 1st and 5th arches.
- Rule 5. (Back) The slope of the upper part of the 6th arch is gentler than or similar to that of the 1st arch.
- Rule 6. (Back) The slope of the lower part of the 6th arch is gentler than or similar to that of the 5th arch.
- Rule 7. (Back) The La and Lc of the 6th arch are wider than those of the 1st and 5th arches.
- Rule 8. (Front/Back) Overall, La and Lc are wider on the Back than on the Front.

By synthesizing the above rules, the order of La (edge width) for the entire front arch can be inferred as follows.

- Rule 9. (Front) The magnitude of La is in the order of 3rd<6th(upper)<6th(lower)<1st<5th<2nd<4th.

For the Back, it is difficult to be certain due to the lack of samples, but based on the above rules, the following can be speculated.

- Rule 10. (Back) The magnitude of La is in the order of 3rd<1st<6th(upper)<5th<2nd<6th(lower)<4th.

Finally, summarizing Rules 9 and 10 in a table gives Table 13.

Referring to this order of edge widths will be helpful in reconstructing the Stradivari arch more faithfully.

Arch	the FRONT	the BACK
6th Arch-Upper	2	3
1st Arch	4	2
2nd Arch	6	5
3rd Arch	1	1
4th Arch	7	7
5th Arch	5	4
6th Arch-Lower	3	6

Table 13: *Order of Edge Width*

11.2 Speculation on the Original Arch of Model A

The arches reconstructed in this report are based on their current, deformed state after many years. However, what we truly wish to know is the original form from 300 years ago, before any deformation occurred, as intended by the maker.

In this chapter, this report attempts to reconstruct the appearance at the time of making by correcting for these deformations and modifying the questionable positions of the arch endpoints through logical reasoning. To do this, this report first reduced warping and measurement errors by using the average of the left and right side data of the plate, and then corrected the edge widths according to the method described earlier.

(※ Even if Model A's data were from the Messiah, it would be incorrect to compare these reconstruction results with the actual Messiah's data. This is because the present results are estimations based on data from uneven curves. In fact, the heights of some arches have errors of up to 0.5(mm) compared to the source data.)

The reconstruction results are attached in PDF and DXF file formats, and the descriptions for each attached file are as follows.

- Front/Back_All_Arches.pdf: All arches and related data (bamp: amplitude and handle direction of the cubic polynomial curve, camp: amplitude of the catenary curve, pamp: amplitude of the final pattern curve, expo: exponent value, tc: tolerance)
- Front/Back_All_Arches_Plate.pdf: All arches including the plate and related data
- Front/Back_Contour_Map.pdf: Contour map
- Contour_Map_Comparison_A/B.pdf: Comparison of Front and Back contour maps
- Front/Back_All_Arches.dxf: All arches (universal CAD file for output)

(※ The attached files above were created with Violin Arch Designer - ver. 1.0.0, a program developed by the author.)

11.3 Abbreviations and Fullness Zones

Notation	Description
TD	(Trochoid) General term for Trochoid curves
CTD	(Curtate Trochoid) A Curtate Trochoid curve with a continuous repeating pattern
CHT	(Curtate Hypotrochoid) A Curtate Hypotrochoid curve with a continuous repeating pattern
CET	(Curtate Epitrochoid) A Curtate Epitrochoid curve with a continuous repeating pattern
CTDA	(Curtate Trochoid Arch) An arch curve extracted from a CTD
CHTA	(Curtate Hypotrochoid Arch) An arch curve extracted from a CHT. (Greater fullness than a CTDA.)
CETA	(Curtate Epitrochoid Arch) An arch curve extracted from a CET. (Less fullness than a CTDA.)
nCHTA	(near.CHTA) A CHTA near the target CHTA. (Greater fullness than a CTDA.)
nCETA	(near.CETA) A CETA near the target CHTA. (Less fullness than a CTDA.)
maxCHTA	(maximum.CHTA) The CHTA with the maximum possible fullness for a fixed arch width and height.
minCETA	(minimum.CETA) The CETA with the minimum possible fullness for a fixed arch width and height.
nCHTAce	(near.CHTA.catenary.exponential) An approximated arch curve created by transforming a nearby CHTA using a catenary curve and an exponential function, used when the target CHTA cannot be created by normal methods. (Greater fullness than a CTDA.)
nCETAice	(near.CETA.inverted catenary.exponential) An approximated arch curve created by transforming a nearby CETA using an inverted catenary curve and an exponential function, used when the target CETA cannot be created by normal methods. (Less fullness than a CTDA.)
CTDAce	(CTDA.catenary.exponential) An approximated arch curve created by transforming a CTDA using a catenary curve and an exponential function, used when the target CHTA or CETA cannot be created by normal methods. (Greater fullness than a CTDA.)
CTDAice	(CTDA.inverted catenary.exponential) An approximated arch curve created by transforming a CTDA using an inverted catenary curve and an exponential function, used when the target CHTA or CETA cannot be created by normal methods. (Less fullness than a CTDA.)
CTDAcec	(CTDA.cubic polynomial.exponential.catenary) An arch curve created by transforming a CTDA using a catenary curve, a cubic polynomial function, and an exponential function. (Used only for the 6th arch, not an approximation curve.)

Table 14: *Abbreviations*

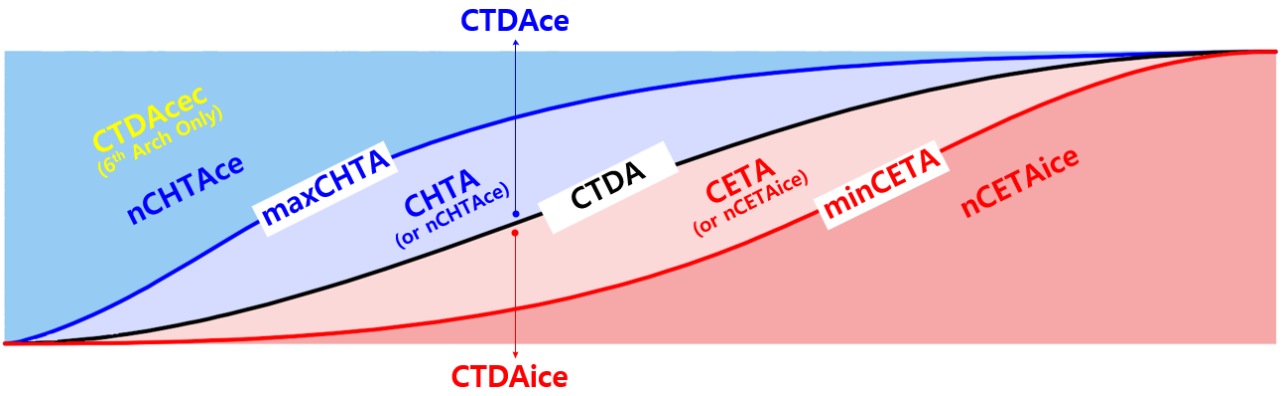

Figure 72: *Fullness Zones by Type of Curve*

References

[1] S. F. Sacconi, *I 'segreti' di Stradivari*. Cremona: Libreria del Convegno, 1972, pp. 63–83.

[2] The Strad, *Antonio Stradivari 'Titian' Violin, 1715*, Poster, London, UK, n.d.

[3] R. M. Mottola, "Comparison of Arching Profiles of Golden Age Cremonese Violins and Some Mathematically Generated Curves," *Savart Journal*, vol. 1, no. 3, pp. 172–191, 2011.

Websites

- H.I.S. Violin Atelier (Arch creation program) – https://www.hisviolins.com